Cladding Protection of Reinforced Concrete Structural Members against Blast Loading

Ye Xia
Bachelor of Engineering (Architectural) (Hons)

Thesis submitted for the degree of Doctor of Philosophy at the University of Adelaide, Australia

The School of Civil, Environmental and Mining Engineering

May 2017

Table of Contents

Abstract 1
Statement of Originality 2
List of publications 3
Acknowledgements 4
Chapter 1 - Introduction 5
Introductory background 5
Research gaps and objectives 8
Chapter 2 – Numerical Analysis of Foam-Protected RC Members under Blast Loads 14
Abstract 17
1. Introduction 17
2. Material Models in *LS-DYNA* 21
   2.1 Aluminium foam 21
   2.2 Concrete 24
   2.3 Steel 25
3. Experimental Validations of the Numerical Model 25
   3.1 Blast test 25
   3.2 Blast Loading 27
   3.3 LS-DYNA model 29
4. Generation of P-I Diagram 33
5. Sensitivity Study 35
   5.1 Influence of foam thickness 35
   5.2 Influence of Foam Density 38
   5.3 Influence of slab thickness 42
   5.4 Thicker unprotected slab vs. foam-protected slab 43
6. Conclusion 45
Acknowledgements 45
Chapter 3 - Optimised Design of Foam Cladding for Protection of Reinforced Concrete Members under Blast Loading 49
Abstract 51
1. Introduction 51
2. Load-cladding-structure model 53
3. Experiments and Validation 55
4. Optimisation 60
   4.1 Non-dimensional parameters $\boldsymbol{\kappa}$ 60
   4.2 Non-dimensional parameter $\boldsymbol{\tau}$ 61
   4.3 Normalised pressure $\boldsymbol{p}$ and impulse $\boldsymbol{i}$ 64
5. Parametric study 65
6. Conclusion 67
Chapter 4 – Protective Effect of Graded Density Aluminium Foam on RC Slab under Blast Loading – An Experimental Study 70
Abstract 73
1. Introduction 74
2. Quasi-Static Compressive Test of Aluminium Foams 75
   2.1 Uniform Density Foams 76
   2.2 Linear Density Foams 78
   2.3 Unordered Density Foams 82
3. Blast Test of Foam-Protected RC Slabs 83
   3.1 Event 1 86
   3.2 Event 2-6 88
   3.3 Strain-time histories 93

4. Conclusion 95
Acknowledgements 95
Chapter 5 - An Analytical Model of Linear Density Foam Protected Structure under Blast Loading 99
Abstract 101
1. Introduction 101
2. Derivation of analytical model 103
3. Verification of analytical model 109
   3.1 Simulation of the blast load 110
   3.2 Resistance function of the RC slab 112
   3.3 Aluminium foams in the blast test 113
   3.4 Result comparisons 113
4. Case Study 116
5. Conclusion 117
Chapter 6 – Concluding Remarks and Recommendation for Future Work 120

Abstract

With the increasing threat of explosions on infrastructures across the world, the protective techniques against blast loading on existing structures have become more and more significant. As an energy absorptive material, aluminium foam has been introduced to be a sacrificial cladding on structures.

This thesis aims to discover the protective effect of aluminium foam on reinforced concrete (RC) structural members which has been a common structural type for existing buildings. Homogeneous aluminium foam was firstly studied both numerically and theoretically. Based on the investigations of homogeneous foam, graded density aluminium foam was introduced to improve the protective effectiveness and efficiency. Blast experiment and analytical model were involved in the study of graded density aluminium foam on RC slabs.

Statement of Originality

I certify that this work contains no material which has been accepted for the award of any other degree or diploma in my name, in any university or other tertiary institution and, to the best of my knowledge and belief, contains no material previously published or written by another person, except where due reference has been made in the text. In addition, I certify that no part of this work will, in the future, be used in a submission in my name, for any other degree or diploma in any university or other tertiary institution without the prior approval of the University of Adelaide and where applicable, any partner institution responsible for the joint-award of this degree.

I give consent to this copy of my thesis when deposited in the University Library, being made available for loan and photocopying, subject to the provisions of the Copyright Act 1968.

I acknowledge that copyright of published works contained within this thesis resides with the copyright holder(s) of those works.

I also give permission for the digital version of my thesis to be made available on the web, via the University's digital research repository, the Library Search and also through web search engines, unless permission has been granted by the University to restrict access for a period of time.

I acknowledge the support I have received for my research through the provision of an Australian Government Research Training Program Scholarship.

……	……	……..……
Print Name	Signature	Date

List of publications

1. Xia, Y., Wu, C., Zhang, F., Li, Z.-X. & Bennett, T. A. 2014. Numerical Analysis of Foam-Protected RC Members under Blast Loads. *International Journal of Protective Structures*, 5(4). 367-390.
   Status: Published

2. Xia, Y., Wu, C. & Li, Z.-X. 2014. Optimized design of foam cladding for protection of reinforced concrete members under blast loading. *Journal of Structural Engineering*, 141**,** 06014010.
   Status: Published

3. Xia, Y., Wu, C., Liu, Z.-X. & Yuan, Y. 2016. Protective effect of graded density aluminium foam on RC slab under blast loading–An experimental study. *Construction and Building Materials*, 111**,** 209-222.
   Status: Published

4. Xia, Y., Wu, C., & Bennett, T. An analytical model of linear density foam protected structure under blast loading.
   Status: Under preparation

Acknowledgements

My sincerest gratitude goes to Professor Chengqing Wu, whose knowledge in the field of structural responses to blast loading knows no bounds. For his willingness to provide guidance and assistance, no matter where he is, I am also extremely grateful for.

I would also like to thank Dr Terry Bennett, who is always willing to help and provide his expertise when needed. Also, Yuemin Yuan and Dr Zhong-Xian Liu deserve my thanks and much more, for their efforts and supports in the experiments. Finally, I acknowledge the support of the Australian Government's Research Training Program Scholarship.

Chapter 1 - Introduction

Introductory background

The threats of terrorist attacks and explosions on infrastructure across the world have been increasing in recent decades. They can result in catastrophic damage not only to the surrounding structures but also to the humans that occupy the area. Researchers and scientists have expressed significant concerns and hence, many protective technologies have been investigated to mitigate the impact of explosions on civilian buildings and further, prevent casualties [1-9].

New buildings constructed of advanced materials and structural forms can realise the benefits from reducing the blast influence. At the same time, protection for existing buildings is also of vital importance. Reinforced concrete (RC) is widely used for existing buildings as it combines the advantages of both concrete and steel. However, explosive incidents have still threatened the safety of RC building structures. From the previous research [10-14], sacrificial cladding has been recognised to be effective in mitigating the blast effect on the protected structures.

Among the various cladding materials, aluminium foam is known as one of the most convenient and economical sacrificial claddings used to mitigate the blast effects on existing building because it is lightweight, mobile, recyclable and inexpensive [15-21]. Also, its long range of plateau stress ensures an outstanding capacity for energy absorption during compaction. Due to various attractive properties, aluminium foams have been widely studied and can be manufactured in a significant range of densities, configurations and mechanical properties [22-25]. It is essential to appropriately design the properties or materials of the foam cladding to avoid the waste of cost or even the amplification of the blast effect on target structures.

Researchers have conducted a variety of field tests investigating the capacity of aluminium foam to protect structural members. Some results show that aluminium foam is capable of reducing blast effects [10, 11, 26]. However, contrasting experimental results on

the protection effect of metallic foams were sometimes observed and have brought researchers' attention. According to a test by Hanssen et al. [27], it was found that the foam cladding could both reduce and increase the energy transmitted onto the protected structure. This probability of the energy amplification of the foam claddings has also been agreed by some numerical models [12, 28]. Therefore, to the extent of efficient and effective protection, investigation of the optimised design of foam cladding is very imperative.

A general characteristic is that most foam properties are a function of the foam density, as illustrated in Figure 1. This means that the collapse load for blast-protective sacrificial claddings made of aluminium foam is easily specified by selection of the proper foam density. It is possible to increase the plateau stress by increasing the foam density.

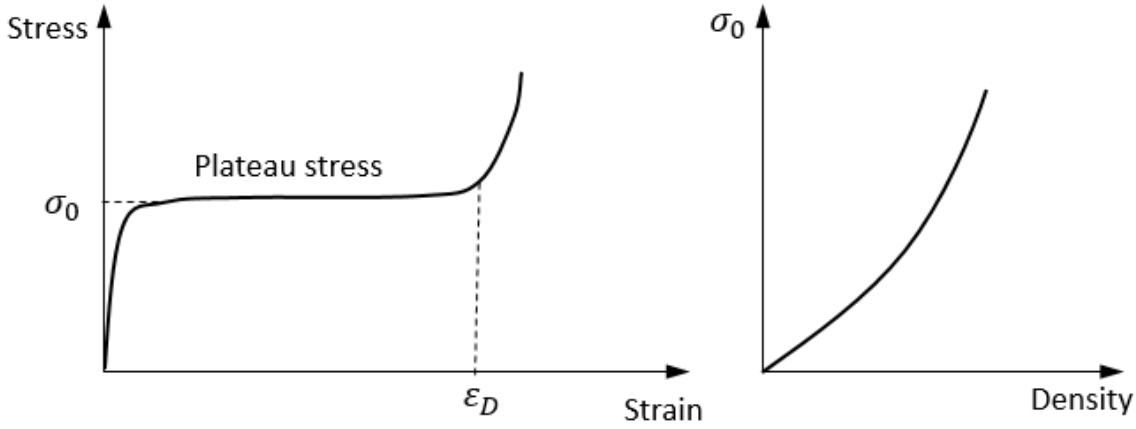

Figure 1. Compressive properties of aluminium foam and the dependency of the foam density

The potential of density-graded foam structures was demonstrated explicitly under dynamic impact with improved mass efficiency and absorbing efficiency [29-35]. Researchers have noticed that a higher plateau stress of the foam can increase the energy absorption capacity, but also increase the pressure transformed to the protected structure [12, 31]. This finding leads to the concept that graded-density foam could absorb high blast energy by incorporating a higher density of foam at the load-receiving face of the foam and transfer lower pressure to the target via the less dense foam at the foam-structure interface, as shown in Figure 2.

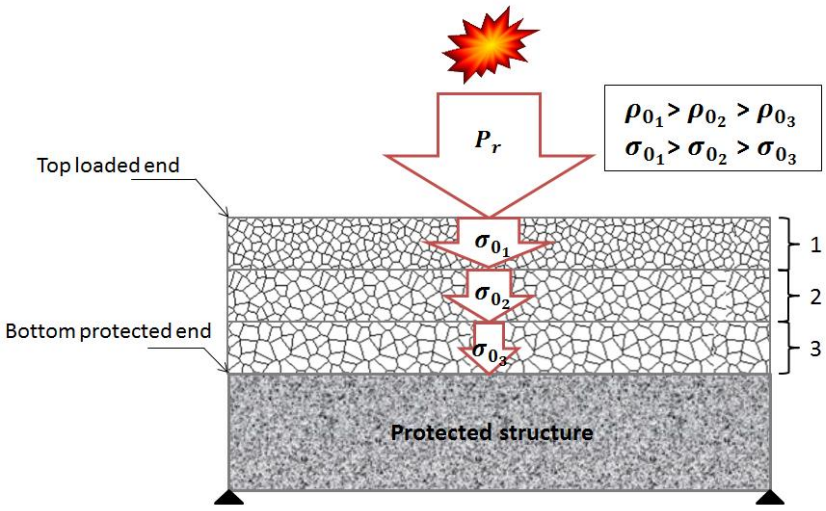

Figure 2. Mitigating mechanism of graded density foam

The study of Ma and Ye [36] shows that double-layered foam structure increases the maximum blast impulses that the claddings can withstand. In addition, they also found that foam claddings were able to absorb much more energy when they were subjected to high strain rate dynamic loading than quasi-static loading. Following that, Li [31] built a mesoscale Vornonoi tessellation model to simulate the energy absorbing ability and effectiveness of aluminium foam with three grades of densities. The results indicated that, by increasing the impact velocity, the initial stress acting upon the top of the foam was increased; however, the stress transmitted to the protected structure still remained small, which was solely determined by the plateau stress of foam at the bottom which was in direct contact with the protected structure. Moreover, functionally graded foams were studied and showed their better mitigation effect and superior blast resistance by both numerical and theoretical models [34, 35]. In addition, several methods have been developed over the last decade for processing of density-graded aluminium foams [37-41], which allows experimental research to be undertaken.

Blast trials are expensive to perform, and thus, limited events can be conducted. Numerical simulation is an alternative way to investigate the effect of foam cladding on structures. Finite element modelling (FEM) is a dominant discretisation technique in structural mechanics, which includes the use of mesh generation techniques for dividing a

complex problem into small elements, as well as the use of software program coded with FEM algorithm. LS-DYNA is an advanced general-purpose FEM simulation software package developed by the Livermore Software Technology Corporation. It is used to solve multi-physics problems including soil mechanics, heat transfer, and fluid dynamics either as separate phenomena or as coupled physics. In LS-DYNA, 3D models can be drawn and material data are filled. The output is highly accurate, detailed, and pictorial, but relatively time-consuming. With the consideration of convenience and budget, a theoretical /analytical method based on single-degree-of-freedom (SDOF) model is more suitable for the huge amount of sensitivity studies. A basic SDOF model is simply a force equilibrium relying on various transformation factors. Along with the one-dimensional shock-wave theory [42], the dynamic response of aluminium foam can be analysed theoretically. Additionally, suitable blast test data can be wisely incorporated with the numerical and analytical model to verify the predictions.

Research gaps and objectives

Based on the discussions above, several knowledge gaps in the study of the protective effect of foam cladding under blast loading can be concluded:

- A combined finite element model of foam-protected RC slab is missing to draw pressure-impulse diagrams of the protected RC slabs with different foam claddings under blast loading.
- No analytical model has been developed for non-linear structures / RC structures with aluminium foam cladding against blast loading.
- The optimisation of foam design for RC structural members is required to get the effective and efficient protection.
- Experimental investigations are limited to graded density aluminium foams as sacrificial claddings on RC structural members.

- A numerical model for graded density is missing to predict the response of protected structure under blast loading.

This thesis aims to investigate the structural response of RC slabs with aluminium foam cladding under blast loading and to fill the knowledge gaps identified previously. It contains four manuscripts which either have been published in, or to be submitted to, internationally recognised journals.

In Chapter 2, the paper focuses on the numerical investigation of the protective effect of uniform density aluminium foams on RC slabs. The numerical model developed in this paper is validated against some previously obtained experimental results. Pressure-impulse diagrams are generated to demonstrate the improvement in blast resistance of RC slab with foam protection. The results from sensitivity study indicate that the same aluminium foam can have different blast mitigation effects depending on the configuration of the target RC slab. Therefore, the third Chapter focuses on the optimisation of foam design on RC structural members.

Based on the findings from Chapter 2, optimised design of foam cladding on RC structural member is investigated in Chapter 3. The paper introduces an analytical model for foam protected RC slabs under blast loading. The optimised relationship between the foam cladding and the protected RC slab is discussed based on the analytical study and a method to achieve the optimised foam design is also proposed.

The optimisation study of homogeneous aluminium foam in Chapter 3 suggested that graded density foams could improve the mitigation efficiency when the foam thickness is specified. Therefore, in Chapter 4, a range of quasi-static and blast experiments are carried out to study graded density foams. The experiments compare the protective effects of uniform density foams, linear density foams and unordered density foams. The performance of graded density aluminium foams under both static and dynamic loading is reported in this Chapter.

The results from Chapter 4 indicate that the linear density foam outperforms the uniform density foam with the same average density. As a result, an analytical model to predict the dynamic structural response with the protection of linearly graded foam cladding is developed in in Chapter 5. The analytical model is validated against the experimental data from Chapter 4. The parametric study indicates that the linearly graded foam is capable of mitigating the blast damage more effectively.

References

[1] Zhang, F, Wu, C, Zhao, X-L, Xiang, H, Li, Z-X, Fang, Q, Liu, Z, Zhang, Y, Heidarpour, A, and Packer, JA, *Experimental study of CFDST columns infilled with UHPC under close-range blast loading.* International Journal of Impact Engineering, 2016.

[2] Zhang, F, Wu, C, Zhao, X-L, Heidarpour, A, and Li, Z, *Experimental and numerical study of blast resistance of square CFDST columns with steel-fibre reinforced concrete.* Engineering Structures, 2016.

[3] Ma, G, Huang, X, and Li, J, *Damage assessment for buried structures against internal blast load.* Structural Engineering and Mechanics, 2009. **32**(2): p. 301-320.

[4] Ma, G, Huang, X, and Li, J, *Simplified damage assessment method for buried structures against external blast load.* Journal of Structural Engineering, 2009. **136**(5): p. 603-612.

[5] Hao, H and Ma, G, *Research at the University of Western Australia on structure protections against blast and impact loads.* Australian Journal of Structural Engineering, 2012. **13**(1): p. 19-41.

[6] Liew, JR and Wang, T, *Novel steel-concrete-steel sandwich composite plates subject to impact and blast load.* Advances in Structural Engineering, 2011. **14**(4): p. 673-687.

[7] Mazek, SA and Wahab, M, *Impact of composite materials on buried structures performance against blast wave.* Structural Engineering and Mechanics, 2015. **53**(3): p. 589-605.

[8] Yu, Z, Xue, P, and Chen, Z, *Nested tube system applicable to protective structures against blast shock.* International Journal of Impact Engineering,

2017. **102**: p. 129-139.

[9] Hao, Y, Hao, H, Shi, Y, Wang, Z, and Zong, R, *Field testing of fence type blast wall for blast load mitigation.* International Journal of Structural Stability and Dynamics, 2017: p. 1750099.

[10] Schenker, A, Anteby, I, Nizri, E, Ostraich, B, Kivity, Y, Sadot, O, Haham, O, Michaelis, R, Gal, E, and Ben-Dor, G, *Foam-protected reinforced concrete structures under impact: experimental and numerical studies.* Journal of Structural Engineering, 2005. **131**(8): p. 1233-1242.

[11] Wu, C, Huang, L, and Oehlers, DJ, *Blast testing of aluminum foam–protected reinforced concrete slabs.* Journal of Performance of Constructed Facilities, 2010. **25**(5): p. 464-474.

[12] Ye, Z and Ma, G, *Effects of foam claddings for structure protection against blast loads.* Journal of Engineering Mechanics, 2007. **133**(1): p. 41-47.

[13] Wu, C and Sheikh, H, *A finite element modelling to investigate the mitigation of blast effects on reinforced concrete panel using foam cladding.* International Journal of Impact Engineering, 2013. **55**: p. 24-33.

[14] Ma, G and Ye, Z, *Analysis of foam claddings for blast alleviation.* International Journal of Impact Engineering, 2007. **34**(1): p. 60-70.

[15] Perrella, G, Faiella, D, Brandonisio, G, Fraldi, M, and Mele, E. *Design of functionally graded beam of aluminium foam for civil structural application*. in *Key Engineering Materials*. 2016. Trans Tech Publ.

[16] Merrett, R, Langdon, G, and Theobald, M, *The blast and impact loading of aluminium foam.* Materials & Design, 2013. **44**: p. 311-319.

[17] Langdon, G, Karagiozova, D, Theobald, M, Nurick, G, Lu, G, and Merrett, R, *Fracture of aluminium foam core sacrificial cladding subjected to air-blast loading.* International Journal of Impact Engineering, 2010. **37**(6): p. 638-651.

[18] Hassan, M, Guan, Z, Cantwell, W, Langdon, G, and Nurick, G, *The influence of core density on the blast resistance of foam-based sandwich structures.* International Journal of Impact Engineering, 2012. **50**: p. 9-16.

[19] Altenaiji, M, Guan, ZW, Cantwell, W, and Zhao, Y. *Characterisation of aluminium matrix syntactic foams dynamic loading*. in *Applied Mechanics and Materials*. 2014. Trans Tech Publ.

[20] Su, Y, Wu, C, and Griffith, M, *Mitigation of blast effects on aluminum foam protected masonry walls.* Transactions of Tianjin University, 2008. **14**: p. 558-562.

[21] Li, JD, Zhou, HY, and Ma, GW, *Numerical simulation of blast mitigation cladding with gradient metallic foam core.* Applied Mechanics and Materials, 2011. **82**: p. 461-466.

[22] Wei, L, Yao, G-c, Zhang, X-m, and Luo, H-j, *Preparation of foam aluminium by powder metallurgy process.* JOURNAL-NORTHEASTERN UNIVERSITY NATURAL SCIENCE, 2003. **24**: p. 1071-1074.

[23] Banhart, J, *Manufacture, characterisation and application of cellular metals and metal foams.* Progress in materials science, 2001. **46**(6): p. 559-632.

[24] Schäffler, P and Rajner, W, *Process stability in serial production of aluminium foam panels and 3D parts.* Advanced Engineering Materials, 2004. **6**(6): p. 452-453.

[25] Haidar, S, Ansary, S, and Rahman, A. *Production and compressive characterization of aluminium MMC foam manufactured using dual foaming agent*. in *IOP Conference Series: Materials Science and Engineering*. 2016. IOP Publishing.

[26] Schenker, A, Anteby, I, Gal, E, Kivity, Y, Nizri, E, Sadot, O, Michaelis, R, Levintant, O, and Ben-Dor, G, *Full-scale field tests of concrete slabs subjected to blast loads.* International Journal of Impact Engineering, 2008. **35**(3): p. 184-198.

[27] Hanssen, A, Enstock, L, and Langseth, M, *Close-range blast loading of aluminium foam panels.* International Journal of Impact Engineering, 2002. **27**(6): p. 593-618.

[28] Li, Q and Meng, H, *Attenuation or enhancement—a one-dimensional analysis on shock transmission in the solid phase of a cellular material.* International Journal of Impact Engineering, 2002. **27**(10): p. 1049-1065.

[29] Daxner, T, Rammerstorfer, FG, and Böhm, HJ, *Adaptation of density distributions for optimising aluminium foam structures.* Materials Science and technology, 2000. **16**(7-8): p. 935-939.

[30] Brothers, AH and Dunand, DC, *Mechanical properties of a density-graded replicated aluminum foam.* Materials Science and Engineering: A, 2008. **489**(1): p. 439-443.

[31] Li, J, Ma, G, Zhou, H, and Du, X, *Energy absorption analysis of density graded aluminium foam.* International Journal of Protective Structures, 2011. **2**(3): p. 333-349.

[32] Li, S, Wang, Z, Wu, G, Zhao, L, and Li, X, *Dynamic response of sandwich*

spherical shell with graded metallic foam cores subjected to blast loading. Composites Part A: Applied Science and Manufacturing, 2014. **56**: p. 262-271.

[33] Liang, M, Zhang, G, Lu, F, and Li, X, *Blast resistance and design of sandwich cylinder with graded foam cores based on the Voronoi algorithm.* Thin-Walled Structures, 2017. **112**: p. 98-106.

[34] Liu, X, Tian, X, Lu, T, and Liang, B, *Sandwich plates with functionally graded metallic foam cores subjected to air blast loading.* International Journal of Mechanical Sciences, 2014. **84**: p. 61-72.

[35] Zhou, H, Wang, Y, Wang, X, Zhao, Z, and Ma, G, *Energy absorption of graded foam subjected to blast: A theoretical approach.* Materials & Design, 2015. **84**: p. 351-358.

[36] Ma, G and Ye, Z, *Energy absorption of double-layer foam cladding for blast alleviation.* International Journal of Impact Engineering, 2007. **34**(2): p. 329-347.

[37] Brothers, AH and Dunand, DC, *Density‐graded cellular aluminum.* Advanced Engineering Materials, 2006. **8**(9): p. 805-809.

[38] Hassani, A, Habibolahzadeh, A, and Bafti, H, *Production of graded aluminum foams via powder space holder technique.* Materials & Design, 2012. **40**: p. 510-515.

[39] He, S-Y, Zhang, Y, Dai, G, and Jiang, J-Q, *Preparation of density-graded aluminum foam.* Materials Science and Engineering: A, 2014. **618**: p. 496-499.

[40] Higuchi, M, Adachi, T, Yokochi, Y, and Fujimoto, K. *Controlling of distribution of mechanical properties in functionally-graded syntactic foams for impact energy absorption*. in *Materials Science Forum*. 2012. Trans Tech Publ.

[41] Pollien, A, Conde, Y, Pambaguian, L, and Mortensen, A, *Graded open-cell aluminium foam core sandwich beams.* Materials Science and Engineering: A, 2005. **404**(1): p. 9-18.

[42] Mazor, G, Ben-Dor, G, Igra, O, and Sorek, S, *Shock wave interaction with cellular materials.* Shock Waves, 1994. **3**(3): p. 159-165.

Chapter 2 – Numerical Analysis of Foam-Protected RC Members under Blast Loads

Statement of Authorship

Title of Paper	Numerical Analysis of Foam-Protected RC Members Under Blast Loads
Publication Status	☑ Published ☐ Accepted for Publication ☐ Submitted for Publication ☐ Unpublished and Unsubmitted work written in manuscript style
Publication Details	Xia, Y., Wu, C., Zhang, F., Li, Z.-X. & Bennett, T. 2014. Numerical Analysis of Foam-Protected RC Members Under Blast Loads. *International Journal of Protective Structures,* 5(4). 367-390.

Principal Author

Name of Principal Author (Candidate)	Ye Xia		
Contribution to the Paper	Established the model, conducted parametric studies, analysed and interpreted data, and wrote manuscript.		
Overall percentage (%)	85%		
Certification:	This paper reports on original research I conducted during the period of my Higher Degree by Research candidature and is not subject to any obligations or contractual agreements with a third party that would constrain its inclusion in this thesis. I am the primary author of this paper.		
Signature		Date	

Co-Author Contributions

By signing the Statement of Authorship, each author certifies that:

i. the candidate's stated contribution to the publication is accurate (as detailed above);

ii. permission is granted for the candidate in include the publication in the thesis; and

iii. the sum of all co-author contributions is equal to 100% less the candidate's stated contribution.

Name of Co-Author	Chengqing Wu		
Contribution to the Paper	Supervised development of work, helped in manuscript evaluation and acted as corresponding author.		
Signature		Date	24/11/2016

Name of Co-Author	Fangrui Zhang		
Contribution to the Paper	Helped in model establishment and manuscript evaluation.		
Signature		Date	19/12/2016

Name of Co-Author	Zhong-Xian Li		
Contribution to the Paper	Provided comments for the manuscript.		
Signature		Date	2016.11.28

Name of Co-Author	Terry Bennett		
Contribution to the Paper	Provided comments for the manuscript.		
Signature		Date	19/12/2016

NUMERICAL ANALYSIS OF FOAM-PROTECTED RC MEMBERS UNDER BLAST LOADS

Ye Xia, Chengqing Wu, Fangrui Zhang, Zhong-Xian Li, Terry Bennett

Abstract

Due to the threat of terrorist activities worldwide, research on the protection of building structures from the effects of explosions is critical in order to avoid catastrophic damage to buildings. Protecting our infrastructures means protecting lives. Metallic foam is an economical, light-weight and recyclable material used as a sacrificial cladding to protect structures. Its efficient energy absorption enables metallic foam to mitigate the blast energy acting on the protected structure. This paper describes our numerical investigation of the protective performance of metallic foam cladding on reinforced concrete (RC) structural members using LS-DYNA. In the numerical model, Modified Honeycomb (Material 126) from the LS-DYNA material library was used to represent the aluminium foam while Continuous Surface Cap Model (Material 159) was selected to model the behaviour of concrete. The numerical model was validated by field blast testing results. Using the validated numerical model, parametric studies were conducted to assess the influence of different foam properties on the pressure-impulse (P-I) diagrams of the foam-protected RC slabs. The influence of the thickness of the RC members was also investigated. The derived P-I diagrams will prove useful in the preliminary design of the foam cladding on RC members.

1. Introduction

With the rapid development of technology, the probability of accidental explosions such as incident blasts, mine explosions and terrorist attacks, have increased in urban areas. The highly intensive pressure and impulse of these explosions result in critical damage to

the surrounding buildings and any living thing in the vicinity of the blast. In order to reduce the loss of property and lives, structural protection against blast loads has been investigated worldwide. The study of structural protection involves investigating protective cladding and the response of the protected structural member to an explosion.

The protective cladding is integral to the threatened structure, but attached either after or during construction. If designed appropriately, the cladding is able to mitigate the blast effect on a protected structure by absorbing a significant amount of blast energy through deformation. During compaction, a sacrificial cladding will sacrifice, but protect the structure from the worst of the blast pressure waves.

Aluminium foam has been recognised as an effective and efficient sacrificial cladding owing to its outstanding energy absorption capacity [1-6]. Moreover, aluminium foams can be manufactured with a large range of densities and used to meet different requirements and situations. It is a light-weight material, low in thermal conductivity, fire resistant, sound and vibration damping and absorbing, can attenuate shock waves and be recycled. Therefore, a considerable amount of research has been conducted to examine the protective ability of aluminium foam [1-14].

Experimental study has been one of the effective methods to investigate the protective ability of aluminium foam against explosions [1, 7-9]. While most experiments proved that metallic foams were able to reduce the blast effect by absorbing energy, a pendulum test that achieved unexpected results brought researchers' attention [1].

The pendulum test was carried out by Hanssen et al. in 2002 to assess the protective effect of aluminium foam panels subjected to close-range blast loading [1]. Most of the events in the pendulum test showed that adding aluminium panel increased the transferred impulse and energy experienced by the protected ballistic pendulum. Hanssen et al. attempted to explain the unexpected results using both finite element and analytical models. These models validated the shock wave theory [2]: the foam panel was able to reduce the

blast pressure to the stress level of the foam and keep the blast impulse constant. Unfortunately, Hanssen et al.'s models were unable to clarify the increased swing of the pendulum in the blast test.

Ye and Ma [5] argued that the increased response of the pendulum might be caused by the unbalanced relationship between the pendulum's blast resistant capacity and the stress level of the foam panel. However, this analytical argument was unsupported by effective validations and its accuracy proved unreliable due to various assumptions. Therefore, a more precise modelling method, finite element modelling, was commonly used to investigate the protecting performance of aluminium foams in blast events [7, 15-19].

LS-DYNA is a commercial software used for finite element modelling and has been proven effective when simulating structural damage during explosions [7, 10-16]. Mullin and O'Toole [12] built a LS-DYNA model to compare the modelling simulations against the ballistic pendulum experiments conducted by Hanssen et al. [1]. The comparing results showed similar deformation patterns compared to the experiments. However, no comparisons on the reaction angle of the pendulum or energy absorption of the foam layer were considered by Mullin and O'Toole [12]. The researchers compared two loading methods to simulate blast loads, these are (1) the ConWep air blast function (Enhanced_Load_Blast) and (2) the Arbitrary Lagrangian-Eulerian (ALE) method [12].

According to the results [12], one of the most significant parameters in LS-DYNA is the mesh size of the model, which is a key element for balancing accuracy and computational cost. Smaller mesh sizes can provide more accurate simulations, but require longer running time in most cases. As the ConWep method has no explicit air shock model, it is more often used in LS-DYNA models to reduce the computational burden of blast-related problems. The comparing results showed that the ConWep simulation could

accurately reflect the original experimental results, while the ALE method could represent blast propagation characterised by various boundary conditions [12].

The unexpected results from Hanssen et al.'s pendulum test led Schenker [14] to conduct a series of impact tests on full-scale RC structural members and field blast tests on foam-protected RC plates in order to empirically test the protective effect of aluminium foam. Both the empirical test and the LS-DYNA model (ConWep method) indicated the addition of aluminium foam reduced the energy and impulse transferred to the RC structural member. In their model, three-dimensional elements and beam elements were used to model the RC members. Although the numerical models predicted similar dynamic behaviour with those in the experiments [14], the accuracy was not very high.

It is noticed that few of the previous work generated pressure-impulse diagrams from LS-DYNA models for aluminium foam-protected RC structural members. A pressure-impulse (P-I) diagram is a safe-damage boundary of a certain structural system under a particular shape of dynamic loading [15, 20, 21]. The peak pressure and impulse of an explosion are two major parameters that determine the blast-induced damage to structures. The points on the curve represent the combinations of pressure and impulse that will result in the failure of the target structure. That is, the final structural deflection just equals to the previously specified allowable deflection. Therefore, the P-I diagram can be used to quickly and easily determine whether the structural member survives or fails under a specific explosion.

In the present study, LS-DYNA was employed to investigate the P-I diagrams for aluminium foam-protected RC slabs. With the purpose of improving the accuracy and saving computational time, the material models and blast input were simplified from the previous studies [12-14] and quarter symmetry was exploited by using one-fourth model. The numerical model in the current study was validated using field blast tests. Therefore,

P-I diagrams could be generated with considerable accuracy from the validated LS-DYNA models for the RC slab used in the tests, with and without aluminium foam.

Sensitivity analysis was carried out to test the influence of several significant properties of the aluminium foam on the corresponding P-I diagrams. Additionally, the foam cladding was tested with two different thicknesses of RC slabs in order to determine its efficiency in a variety of circumstances. The findings from this study are significant and valuable for preliminary designs of metallic foam claddings on RC structural members.

2. Material Models in *LS-DYNA*

The numerical model used in the current research was based on field blast tests carried out by [22], whose blast testing data were previously used to validate a single degree of freedom model [23] and a simplified finite element model [24]. However, the accuracy of these models is relatively low. Using LS-DYNA, the blast test scenarios can be simulated using three-dimensional models. Therefore, LS-DYNA is capable of simulating and predicting the foam performance more accurately.

2.1 Aluminium foam

The aluminium foam sheet was modelled using Modified-Honeycomb (Material 126). The Modified-Honeycomb Model has been used by many previous researchers, such as Shkolnikov [25] and Jackson [26]. This material model is able to reflect the real anisotropic behaviour of the aluminium foam whose mathematical formulation consists of two main stages – an undensified phase and a fully densified phase [27].

According to *LS-DYNA* manual [27], in Material 126, the elastic moduli E_{ii} vary from initial values E_{ii}^{un} to fully densified values E^{com} following the equation below:

$$E_{ii} = E_{ii}^{un} + \beta(E^{com} - E_{ii}^{un}) \quad (1)$$

where,

$$\beta = max\left[min\left(\frac{1-V}{1-V_f}, 1\right), 0\right] \quad (2)$$

Volume change is a significant parameter of Material 126 in LS-DYNA, which defines the densification level. The relative volume V is defined as the ratio of the current volume over the initial volume. In eqn. (2), V_f is relative volume when the foam is fully densified. Similarly to strain, the volumetric strain is the ratio of the deformed volume over the original volume and can be expressed as (1–V). The densification strain used in this paper means the volumetric strain of the foam at the fully densified condition.

The stresses in the undensified phase are updated using the input stress-strain curve and following the following equation:

$$\sigma_{ii}^{n+1} = \sigma_{ii}^{n} + E_{ii}\Delta\varepsilon_{ii} \quad (3)$$

where $\Delta\varepsilon_{ii}$ is the strain increment and *n* is the time step.

The honeycomb is assumed to be elastic to perfectly plastic in Material 126. In the fully densified phase, the stresses are updated based on the stress component s_{ij}, the pressure component p, and the kronecker delta δ_{ij} following Cauchy's first law of motion:

$$\sigma_{ij}{}^{n+1} = s_{ij}{}^{n+1} - p^{n+1}\delta_{ij} \quad (4)$$

The aluminium foam used in the blast tests had a density of 400kg/m^3. Due to limited information about the tested foam, the detailed material properties of the foam were taken from information in the *CYMAT Manual* [28] (CYMAT Technologies Ltd., producers of stabilised aluminium foam products), using the 400kg/m^3 density standard (AS35620SC 020SS) as shown in Table 1.

Table 1. Material properties of aluminium foam

Parameter	Value
Mass density (kg/m^3)	400
Young's modulus (MPa)	71000
Elastic modulus (MPa)	500
Yield stress (MPa)	322
Shear modulus (MPa)	920
Compressive strength (MPa)	4
Poisson's ratio	0.19
Densification strain	68%

Cellular metals have been found to be strain-rate sensitive [29]. Yu et al. [30] used numerical analysis to indicate that the plateau stress of cellular metals increased with strain rate which cannot be explained by now. As no reliable reference can be used for dynamic increase factor of CYMAT aluminium foams, the strain rate effect was not considered in the present study.

To validate the aluminium foam model (Material 126: Modified-Honeycomb Model), the quasi-static compression test conducted by Zhu [22] on a sample (150 mm × 150 mm × 75 mm dimension) was utilised. Figure 1 shows the compression test of a 400 kg/m^3 aluminium foam specimen. The comparison of the stress-strain relationship generated by LS-DYNA and that obtained from the experiment [22] is illustrated in Figure 2. The LS-DYNA foam model behaved well and with considerable correlation to the experimental result.

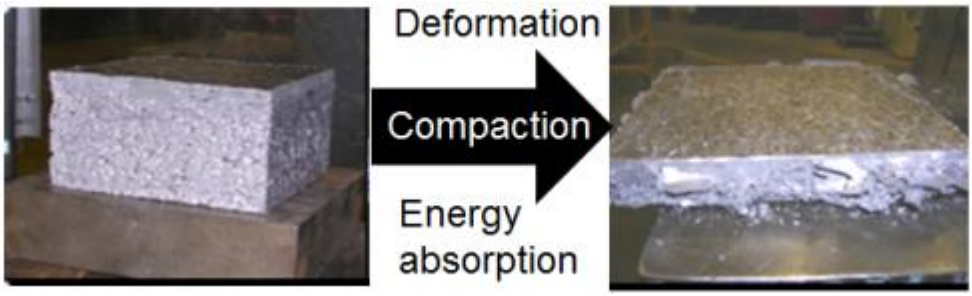

Figure 1. Compression test of Aluminium foam

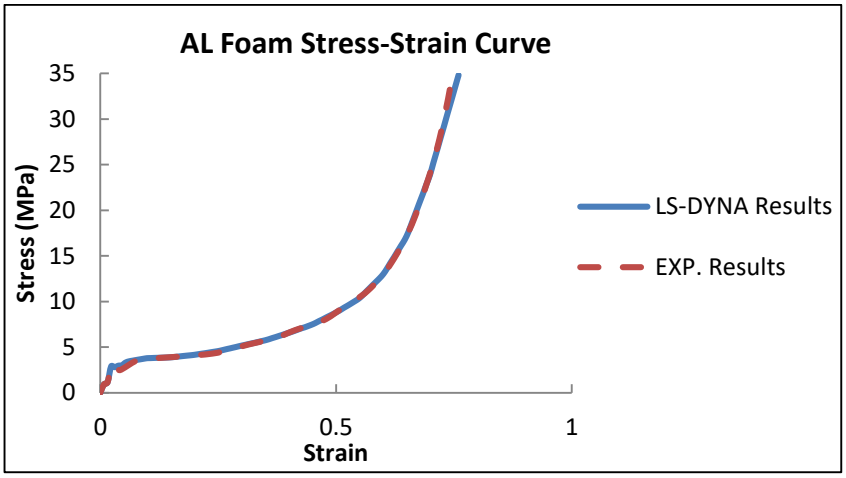

Figure 2. Stress-Strain relationship of Aluminium foam

2.2 Concrete

Concrete was modelled by Material 159-CSCM (Continuous Surface Cap Model) in LS-DYNA. The yield surface is defined by a continuous intersection between the shear yield surface and the hardening cap [27, 31]:

$$f(I_1, J_2, J_3, \kappa) = J_2 - \Re^2 F_f^2 F_c \tag{5}$$

where I_1 is the first invariant of the stress tensor, J_2 is the second invariant of the deviatoric stress, J_3 is the third invariant of the stress tensor, κ is the cap hardening parameter, $\Re$ is the Rubin three-invariant factor, F_f is the shear failure surface, and F_c is the cap hardening surface. Strain rate effect is modelled by viscoplastic algorithm [27, 31].

Due to a lack of the detailed concrete properties, CSCM_Concrete, which is able to self-generate material properties based on simple inputs, was used in the present study. The unconfined compressive strength of concrete used in the test was 32 MPa. With the given unconfined compressive strength, the program can find all required aspects from the

default library, including stiffness, three-dimensional yield strength, hardening, and damage. Research conducted by Murray [31] showed that Material 159 is able to account for structural response and failure criteria using limited input data. Table 2 summarises the input data for the CSCM _Concrete model used in the present study.

Table 2. Material properties of concrete

Parameter	Value
Mass density (kg/m^3)	2400
Unconfined compressive strength (MPa)	32
Aggregate size (mm)	19
Poisson's ratio	0.19

2.3 Steel

Steel reinforcing bars was modelled by Material 3-Mat_Plastic_Knematic in the numerical model. The yield stress of the steel bar used in the RC slabs was 500 MPa and was idealised to be isotropic. Table 3 shows the basic inputs for the steel bars (Material 3).

Table 3. Material properties of steel bar

Parameter	Value
Mass density (kg/m^3)	7830
Yield stress (MPa)	500
Young's modulus (GPa)	200
Poisson's ratio	0.28
Fracture strain	0.08

3. Experimental Validations of the Numerical Model

3.1 Blast test

The numerical model using above material models was validated against the blast test program conducted by Zhu et al. in 2009 [22-24]. Four blast events with different standoff distances were carried out in the blast test [22]. The experimental setup is shown in Figure 3. Timber frame was used as the support structure and the explosive charge was suspended by strings over the slab in the desired orientation and at the specified height. 7.5

kg spherical charges (composition B) were used for all four events. It is important to note that the composition B explosive (60% RDX and 40% TNT) was converted to TNT equivalence from eqn. (6) given by Zhu [22], and weight (TNT) was taken as 8.195 kg for a 7.5 kg charge.

$$Weight_{(TNT)} = (2.15/1.97) \times Weight_{(composition\ B)} \quad (6)$$

The distance between the explosive and the slab was altered to examine the reflected pressure at different standoff distances, as well as the structural response under different blast loads.

Normal strength concrete specimens were designed with both tension and compression reinforcement using a 12 mm diameter mesh, with a 15 mm concrete cover (Figure 4). The mesh bars were spaced at 326 mm centres in the major bending plane and 89.5 mm in the minor plane, and its reinforcement ratio in Section A–A is 1.4%. Tables 2 and 3 summarise the material properties of the RC slab used for the blast program.

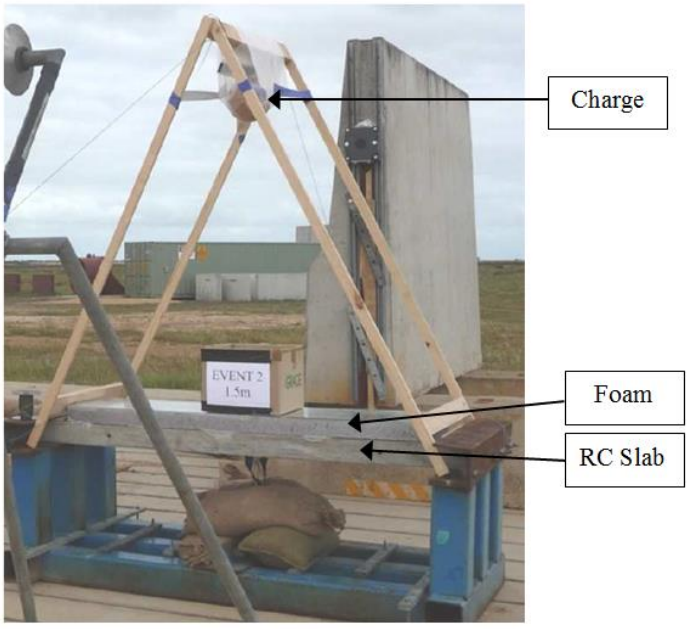

Figure 3. Experiment setup

Aluminium foams were cladded on the RC slabs by epoxy adhesive in Events 2–4. The employed foams were identical with a thickness of 75 mm and a density of 400 kg/m3. Table 1 lists the material properties of the aluminium foam used for the blast program.

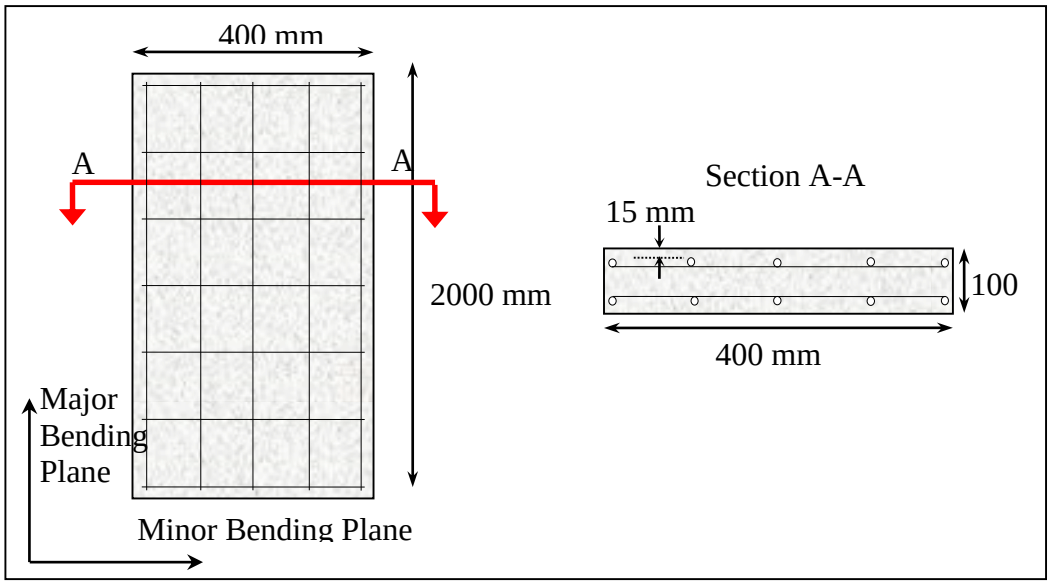

Figure 4. RC slab configuration

3.2 Blast Loading

The ConWep blast function in LS-DYNA is based on the Unified Facilities Criteria (UFC) guidelines [32]. When compared to the previous reports of the blast experiment by Zhu [22], the UFC guidelines over-predicted the impulses by a significant amount when checked against the experimental measurements shown in Table 4. The narrow nature of the clearing distance, which is taken as half of the width of the target structure (roughly 200 mm), suggests blast wave clearing occurred. During the clearing period, the peak reflected pressure remained unchanged, but the impulse for finite width targets was lower than that of infinite width. Both factors were observed in the test results, suggesting that clearing phenomena did affect the impulse. In addition, Ballantyne et al. [33] reported a 50% decrease in impulse for scaled distances greater than 2 m/kg1/3. This suggests 34.27% and 29% for scaled distance $1.488\mathrm{m/kg}^{1/3}$ and $1\mathrm{m/kg}^{1/3}$ is acceptable.

Table 4. Impulse comparison between UFC predicted and experimental

Charge Distance (m)	Scaled Distance ($\mathrm{m/kg}^{1/3}$)	Predicted Impulse (UFC) (kPa.s)	Mean Test Impulse (kPa.s)	Difference %
3	1.488	0.723	0.476	-34.27
2	1	1.103	0.783	-29

The large error in predicted impulse will significantly affect the predicting accuracy of the structural response. Therefore, with the purpose of validating the numerical model

against the blast test, the blast load in the current model was manually exerted on the structural surface based on the testing results. The exerted loading was idealised as a linearly decaying triangular shape by keeping the peak pressure and the positive impulse unchanged [33]. With the idealised triangular load, the peak pressure and the impulse of the blast were easily calculated and used in the generation of P-I diagrams [5, 15, 20, 33].

According to Wu and Sheikh [24], Eqn. (7) was used to curve fit impulses following the test data points of the 8.195kg TNT charge for varying scaled distances Z.

$$I_{r\ (8.195kg)} = 0.7823 \times Z^{-1.276} \quad (7)$$

Figure 5 shows the test predicted impulse curve against UFC, the impulse curve for the 8.195 kg charge. The test prediction curve under-predicts the impulse by an average of 35.04%. However, it follows the shape of the expected UFC curve well for the given scaled distances. Table 5 summarises the predicted pressures and impulses for all events which were implemented in the validation of the LS-DYNA model. Figure 6 shows the final idealised reflected pressure-time histories for each scaled distance. The positive durations of explosives were calculated from eqn. (8) due to the triangular idealisation of pressure-time histories.

$$t_d = 2 \times \frac{I_r}{P_r} \quad (8)$$

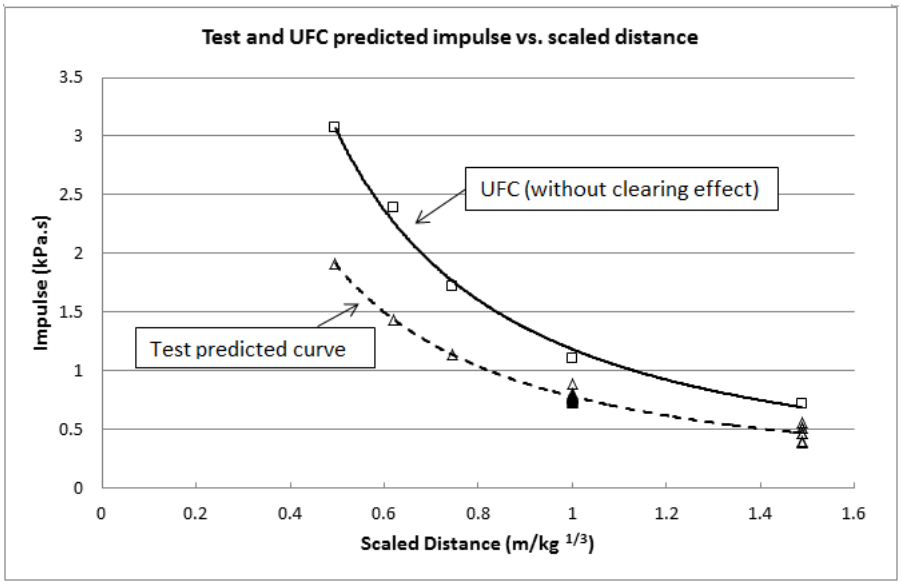

Figure 5. Impulse comparison of UFC prediction and test predictions

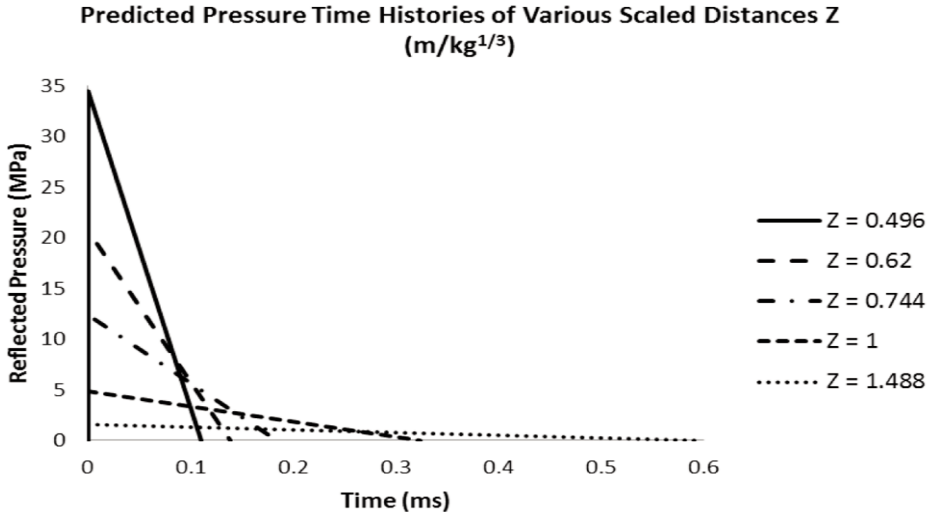

Figure 6. Predicted pressure-time histories for various scaled distances

Table 5. Blast loading prediction

Event No.	Standoff Distance (m)	Scaled Distance ($m/kg^{1/3}$)	Pressure (kPa)	Impulse (kPa. s)	Foam Thickness (mm)
1	1.50	0.744	12420	1.141	0
2	1.50	0.744	12420	1.141	75
3	1.25	0.62	20700	1.440	75
4	1.00	0.496	34500	1.914	75

3.3 LS-DYNA model

A model was constructed in LS-DYNA (Figures 7 and 8) with a slab 2000 mm long, 100 mm thick and 400 mm wide and fully covered by 75 mm thick foam. The concrete

slab was reinforced on both faces with five 12 mm diameter steel bars. The clamps on both ends were included in the model which are close to simply supported.

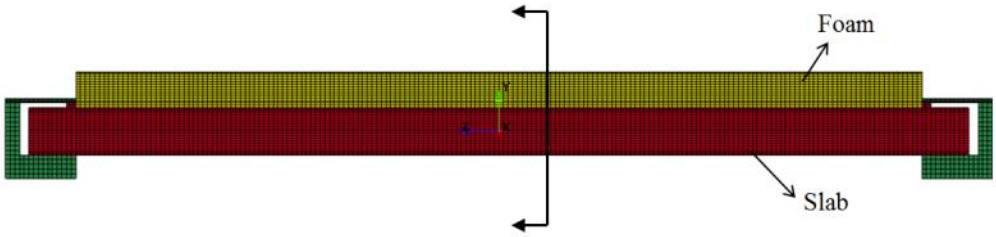

Figure 7. Model setup (front view)

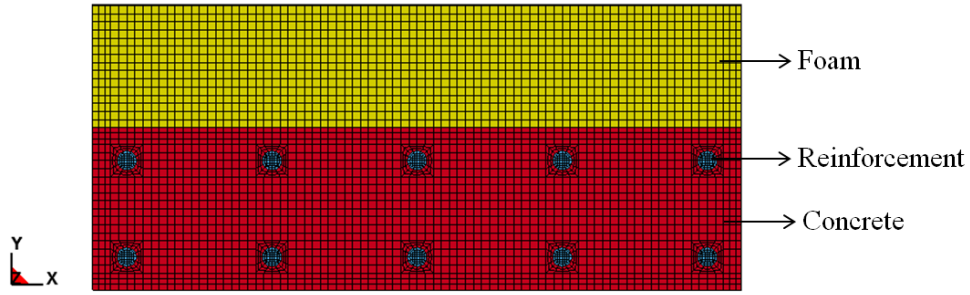

Figure 8. Model setup (cross-section)

A mesh convergence study was also carried out to determine the suitable mesh size. It was found that when mesh size of concrete and foam was around 5 mm in X/Y direction and 10 mm in Z direction, the model yielded the good results in terms of accuracy and efficiency. Steel reinforcement was merged with concrete. The mesh size of reinforcement was about 1.5 mm in X/Y direction and 10 mm in Z direction as shown in Figure 8.

Figures 9–12 present the comparisons of the deflection-time history for each event. In Event 1, the RC slab was unprotected and the LS-DYNA simulation resulted in a close peak deflection of the RC slab, but with an unmatched period. In Event 2 and Event 3 of the blast tests, the RC slabs survived with some minor cracks under the protection of aluminium foam layers. Compared with the experimental results, the LS-DYNA model accurately predicted the peak deflection and period of the foam-protected RC slabs before failure. In Event 4, the blast load was more intensive as the standoff distance of explosive was smaller. This caused the RC slab failed by exceeding the allowable deflection of 50 mm (calculated from ultimate rotation [34]). From Figure 12, it was noticed that the

accuracy of the current LS-DYNA model decreased after the slab failed, which might be caused by the inaccurate default parameters of the concrete model in LS-DYNA program.

Since the failure criterion of RC slabs under blast loading is mainly displacement-controlled, the maximum displacement of each event was compared. Table 6 summarises the recorded peak deflections for each event along with the simulation results. It can be seen that the LS-DYNA model accurately predicted the peak deflections of foam-protected RC slabs, giving an average error of 3.3% compared with the experimental data [22]. Furthermore, the period of structural response, such as the time at which peak deflection occurs, can also be correctly estimated.

Table 6. Summary of validation results

Event No.	**1**	**2**	**3**	**4**
Experimental deflection (mm)	33.7	23.1	31.5	65.2
LS-DYNA deflection (mm)	32.8	23.5	31.8	60.2
Difference	2.7%	1.8%	0.7%	7.8%

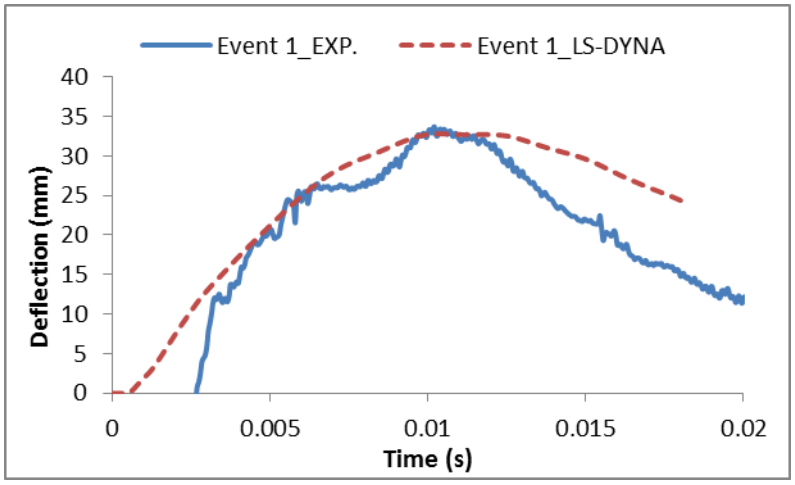

Figure 9: Validation of Event 1

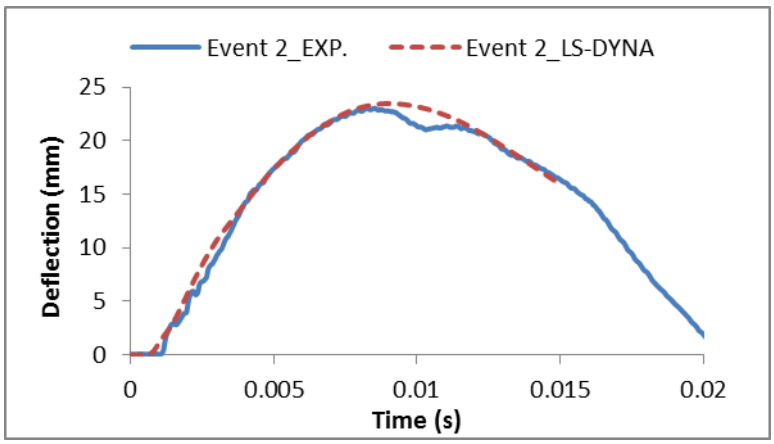

Figure 10: Validation of Event 2

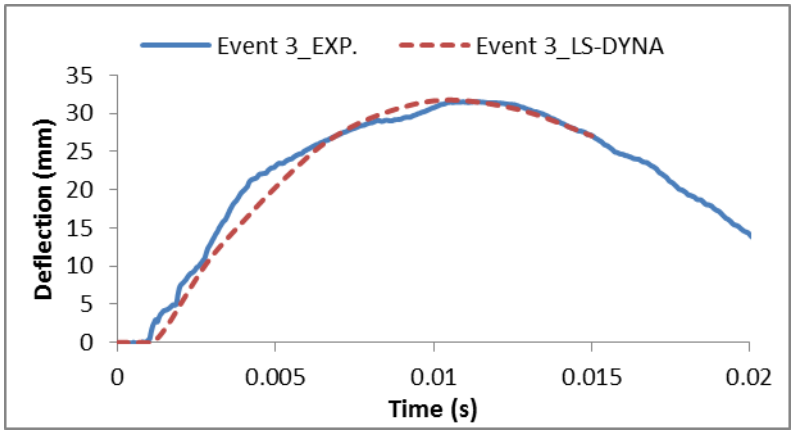

Figure 11: Validation of Event 3

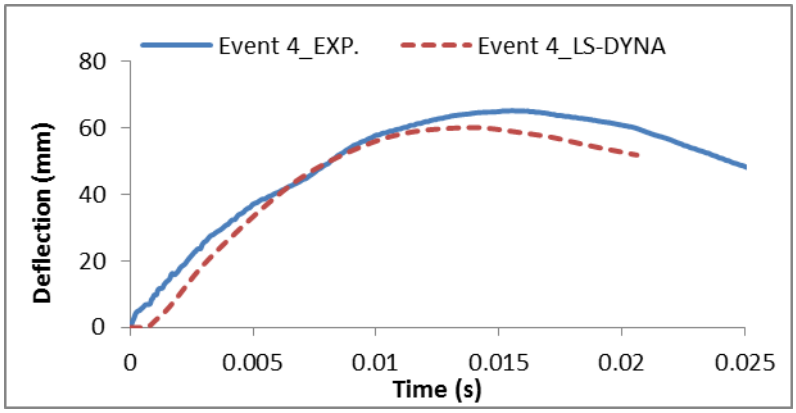

Figure 12: Validation of Event 4

As the RC slab in Event 4 failed, the failure patterns in the experiment were compared with the plastic strain diagrams output from the numerical models. Since the mesh size of concrete is relatively too big to represent the cracks by erosion, the level of plastic strain of concrete was adopted to show the damage potential of the finite element model. Figure 13 shows an obvious flexural crack formed at mid-span of the RC slab in

Event 4 which was captured by the numerical model. In Event 4, the compressive face (top) of the slab crushed under the intensive blast, and as shown in Figure 14 the numerical model caught the compressive failure of the slab.

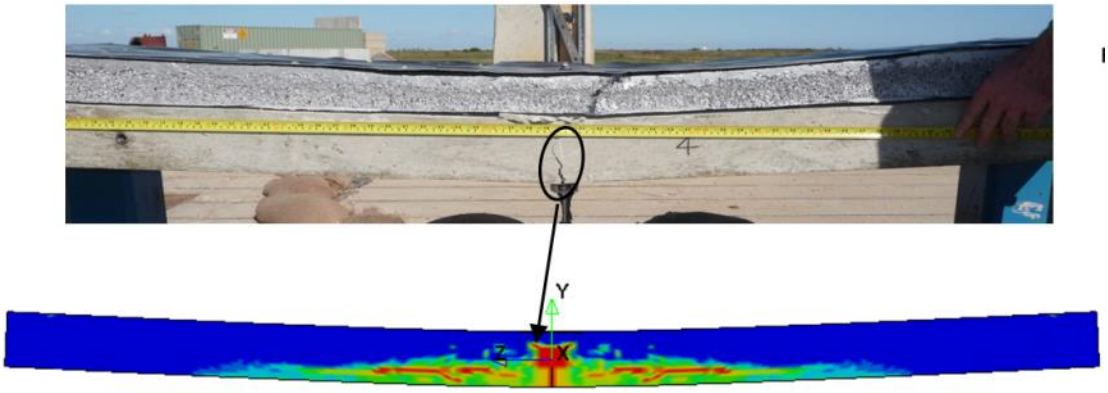

Figure 13. Tensile failure of the RC slab in Event 4

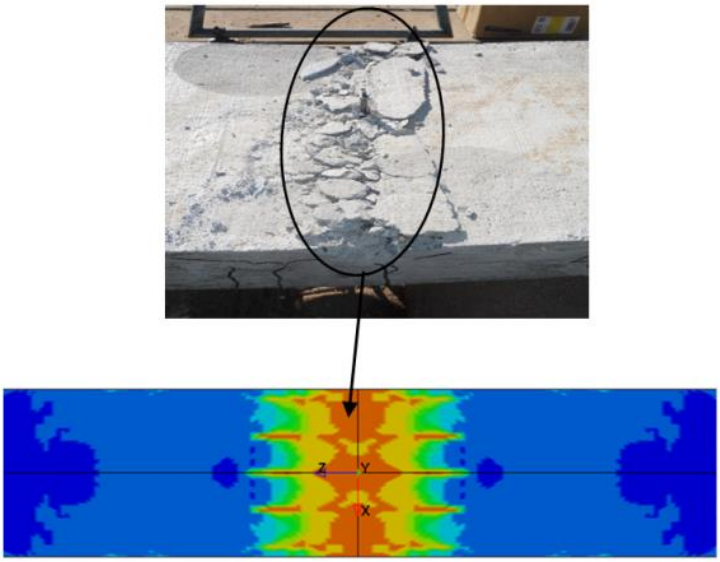

Figure 14. Compressive failure of the RC slab in Event 4

4. Generation of P-I Diagram

With the validated model, parametric studies can be conducted to derive P-I diagrams of foam protected RC slabs under blast loads. A typical P-I diagram can be divided into three regimes based on two asymptotes as shown in Figure 15 [15, 20, 21]. An impulsive loading regime is the part that is close to the impulsive asymptote. In this regime, the peak pressure is extremely high with short blast duration. The structural deflection, in

this case, is controlled by the blast impulse. The dynamic loading regime is the transitional state where the damage level is determined by both peak pressure and impulse. The quasi-static loading regime is near the pressure asymptote. When the peak pressure is relatively low, but with a longer duration, the impact will be close to the quasi- static loading on the structure. Thus, in this regime, the structural damage is dominated by peak pressure.

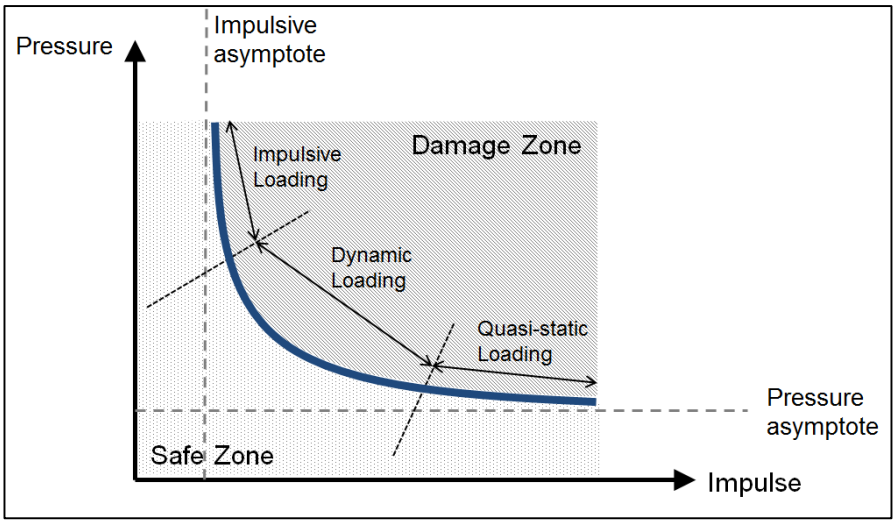

Figure 14. A typical pressure-impulse diagram

The steps used to generate a P-I diagram in LS-DYNA are as follows:

Define a maximum allowable deflection (called critical deflection) for the structural member deflection [34].

Fix a pressure (e.g. 20MPa), gradually increase the impulse (which is achieved by increasing the loading time) until the structural deflection output reaches the critical deflection with a difference below 1%.

Record the valid P-I combination. (This is going to be one point of the P-I curve.)

Reduce the pressure (e.g. 1MPa), and repeat steps 2-3 to get the valid impulse corresponding to P = 15MPa.

Once a number of P-I points are achieved (typically 10 points), a smooth line can be drawn through all valid points, representing the required P-I curve.

Figure 16 shows the P-I curve for the 100 mm thick slab, with and without 75 mm thick aluminium foam protection, which was used in the field experiment.

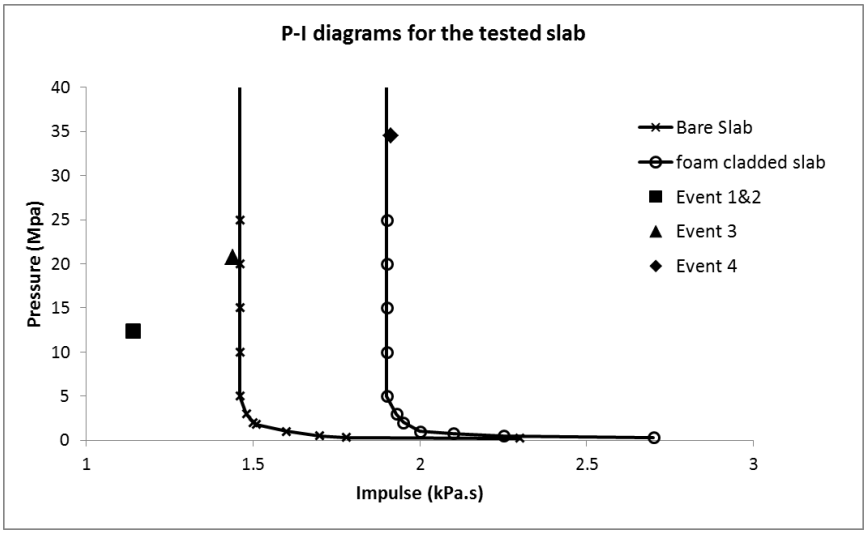

Figure 16: P-I diagram for the tested slab

As shown in Figure 16 within the impulse controlled region (where the pressure is greater than 5 MPa), the presence of the aluminium foam is very effective and provides a 30% increase in blast resistant capacity of the RC slab. However, when the pressure drops to about 1MPa, the mitigation of a blast effect can hardly be achieved because when the pressure is too low, the aluminium foam becomes too strong to be compressed and unable to absorb energy. In such cases, the minor increase in strength comes from the additional mass of foam which slightly increases the overall structural weight.

5. Sensitivity Study

In the current research, the properties of the aluminium foam and the RC slab were varied to determine the influence of each component on the corresponding P-I diagrams. Three different aluminium foams chosen from CYMAT [28] and two thicknesses of RC slab were used to conduct the sensitivity study.

5.1 Influence of foam thickness

In order to determine the influence of foam thickness in mitigating blast effects, the foam of 400 kg/m^3 was used with three different thicknesses of RC slab: 50 mm, 75 mm and 100 mm. Using LS-DYNA to simulate Zhu et al.'s field tests, we observed the protective behaviour of the foam on the RC slabs under three different blast loads (the same loads as Event 2-4 given in the previous section). The predicted deflection-time diagrams of each case are shown in Figures 17–19.

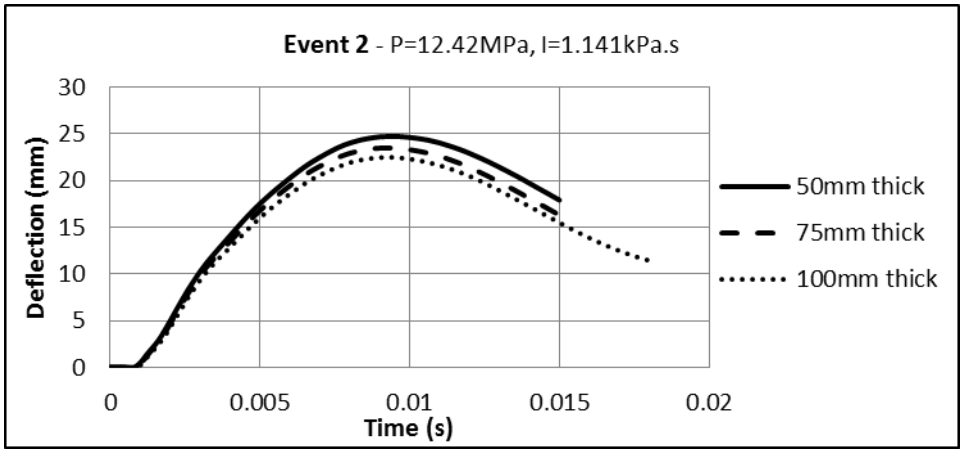

Figure 17. The predicted deflection times of RC slabs covered with different thicknesses of aluminium foam (Event 2)

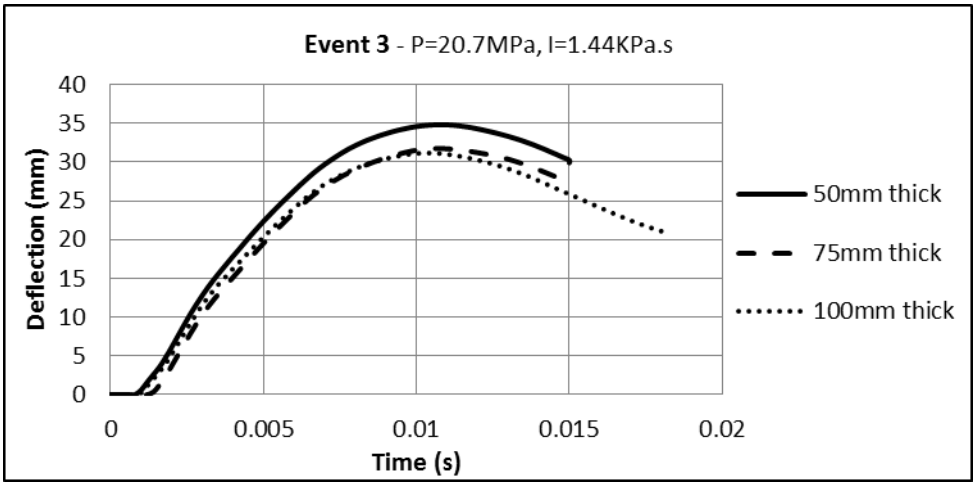

Figure 18. The predicted deflection times of RC slabs covered with different thicknesses of aluminium foam (Event 3)

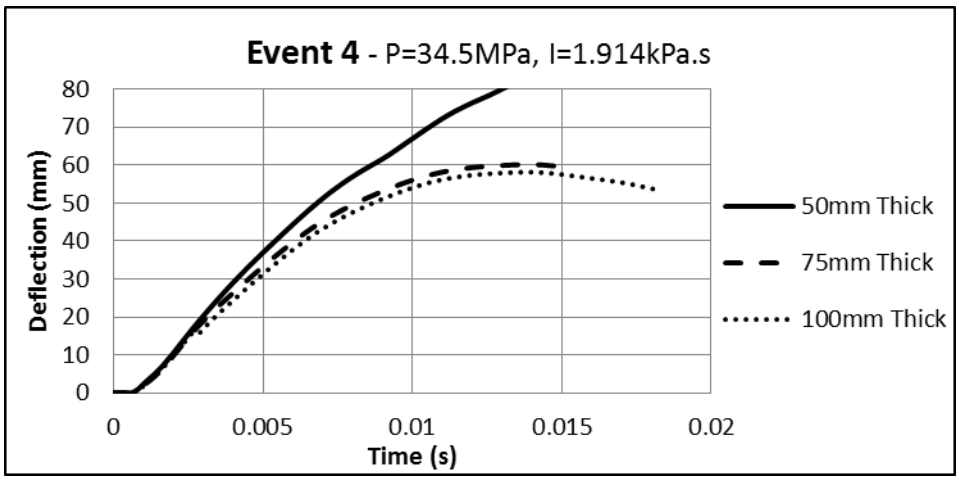

Figure 19. The predicted deflection times of RC slabs covered with different thicknesses of aluminium foam (Event 4)

As shown, for Events 2 and 3 (blast loads are relatively low), the difference in foam thickness does not have a huge impact on the energy absorbing capacity. Specifically, when peak pressure is relatively low, none of these foams is fully densified. The slight difference in peak deflection mainly comes from the extra structural resistance resulting from the different weights of foams (thicker foams have larger self-weight).

However, when the blast load is further increased (Event 4), the peak deflection experienced by the test specimen with 50 mm thick foam layer is significantly greater than the deflection of the specimen with 75 mm and 100 mm thick foam layers. Under large blast loads, the 50 mm thick layer is likely to be fully densified whereas the thicker foam layers have more compressible volume. Once a foam layer is fully densified, it behaves like a solid aluminium sheet with no further energy absorbing capacity. It is thus evident that under the blast load of Event 4, the 50 mm thick foam will become fully densified and unable to further absorb blast energy. On the other hand, both the 75 mm and 100 mm thick foam layers are still serviceable under such loads.

Figure 20 shows the P-I diagrams of RC slabs protected with different foam thicknesses. The figure indicates that the 75 mm thick foam layer is almost as effective as the 100 mm thick foam layer in terms of absorbed energy. However, the 50 mm layer shows less increase in the impulsive asymptote, although it has the same material properties.

As mentioned previously, the lack of increase in the asymptote is because the 50 mm thick foam layer compacts completely when used as a protective layer for a 100 mm thick RC slab. Conversely, 75 mm and 100 mm thick foams remain undensified when the RC slab fails. In this case, the undensified part of the foam is redundant and has no influence on the absorption of energy during compaction. Ideally, the foam would be densified fully just at the time when the RC slab fails. However, once the foam is fully densified, it will completely lose its ability to mitigate the effects of the blast.

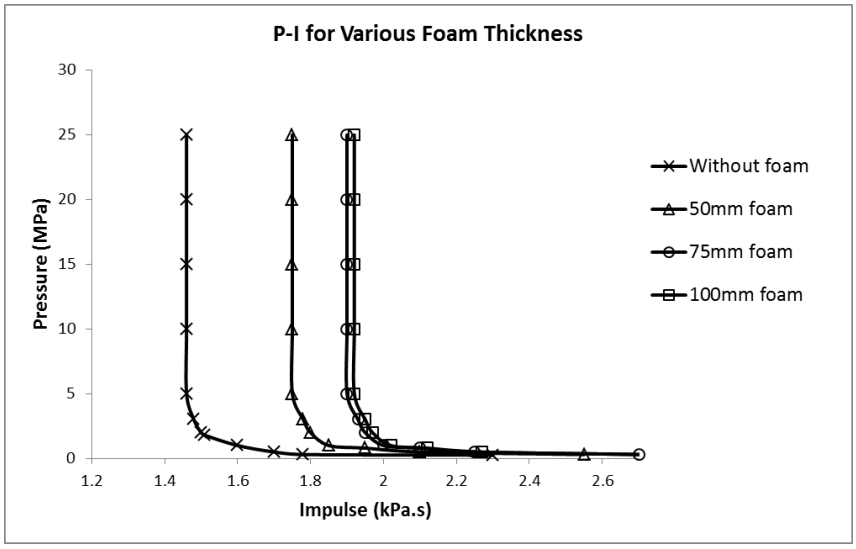

Figure 20: Influence of foam thickness on P-I diagrams

5.2 Influence of Foam Density

When the density of the foam is altered, its stress-strain relationship also changes. With the increase of the density, the compressive strength of the foam is increased [1, 27, 35]. In the current study, the foam thickness was fixed at 75 mm and three different densities were studied: 200 kg/m3, 300 kg/m3, 400 kg/m3. Their stress-strain curves are shown in Figure 21.

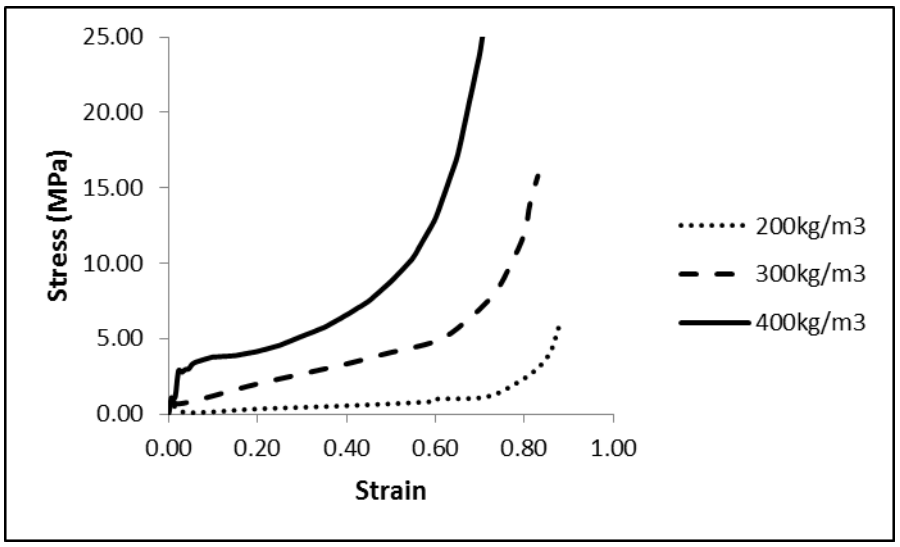

Figure 21. Stress-strain curves of foams with different densities

As seen, lower density results in lower plateau stress in the foam. However, densification strain decreases with the increase of density: 80% for 200 kg/m^3 density foam, 72% for 300 kg/m^3 density foam, and 68% for 200 kg/m^3 density foam [28].

Three blast loads were applied (Events 2–4) to these foam layers and the results are presented in Figures 22–24 and Tables 7–9. It was expected that under identical blast loads, the less dense foam layers would result in a larger peak deflection than denser foam layers. However, for Events 2 and 3, all three foam layers reduced the blast effect to the same level. In Event 4, only the 400 kg/m^3 foam layer successfully prevented the RC slab from failure.

Data in Tables 7–9 indicate that under the same blast load, the foams with smaller densities deform more than denser foams when dissipating the same amount of energy. This result corresponds with the experiments conducted by CYMAT [28]. It was suggested by CYMAT that the energy absorbed by the 200 kg/m^3 foam at 50% strain (2.3 kJ/kg) is larger than the energy absorbed by the 400 kg/m^3 foam at 20% strain (1.8 kJ/kg). It can be concluded therefore that weaker foams can absorb the same amount of energy as long as the blast is within a zone of tolerance that allows them to deform without completely compacting. The stronger foams can, of course, absorb the energy equally as well.

Furthermore, until the RC slab failed in Event 4, the maximum volumetric strain of the 400 kg/m^3 foam was just 40%, whereas its densification strain was 68%. This suggests that the foam used in the field experiment utilised at most only 60% of its capacity which indicated that it was over-designed.

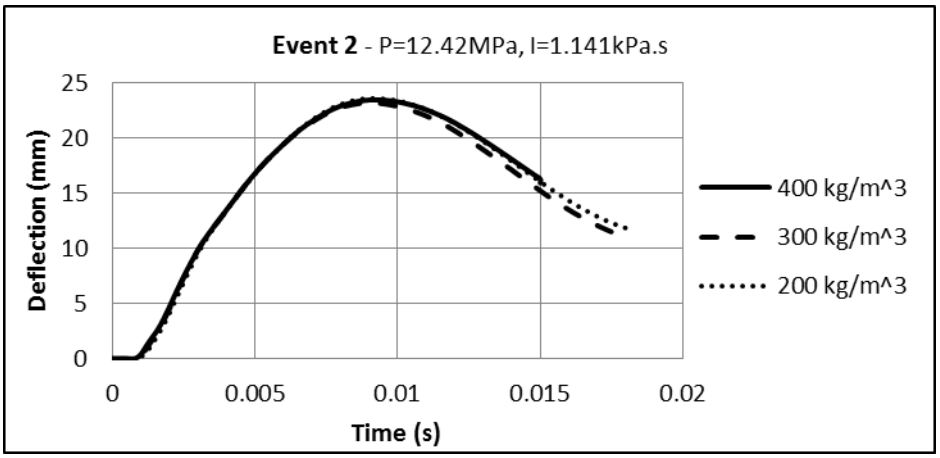

Figure 22. Deflection-time diagrams of RC slabs with different foam density (Event 2)

Table 7. Predicted reactions with different foam density (Event 2)

Event 2 - P=12.42MPa, I=1.141kPa.s			
Foam Density (kg/m^3)	200	300	400
RC Peak Deflection (mm)	23.6	23.6	23.6
Initial Foam Thickness *(mm)*	75	75	75
Final Foam Thickness *(mm)*	27	51	62
Foam Volumetric Strain	0.64	0.32	0.17

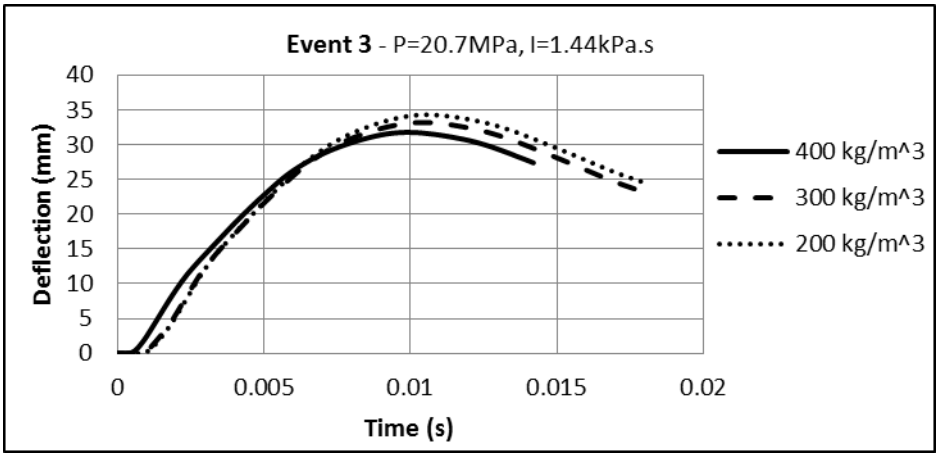

Figure 23. Deflection-time diagrams of RC slabs with different foam density (Event 3)

Table 8. Predicted reactions with different foam density (Event 3)

Event 3 - P=20.7MPa, I=1.44kPa.s

Density (kg/m^3)	200	300	400
Peak Deflection (mm)	34.3	33.2	31.8
Thickness (Before)	75	75	75
Thickness (After)	16	44	56
Volumetric Strain	0.79	0.41	0.25

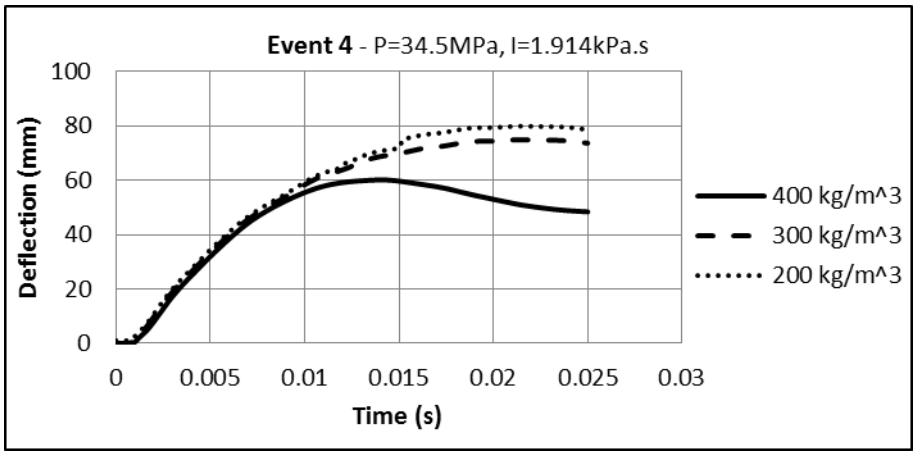

Figure 24. Deflection-time diagrams of RC slabd with different foam density (Event 4)

Table 9. Predicted reactions with different foam density (Event 4)

Event 4 - P=34.5MPa, I=1.914kPa.s			
Density (kg/m^3)	200	300	400
Peak Deflection (mm)	Failed	Failed	60
Thickness (Before)	75	75	75
Thickness (After)	Failed	25	45
Volumetric Strain	-	0.67	0.40

The P-I diagrams for all three 75 mm thick foam layers with different densities were generated and are shown in Figure 25. According to the P-I diagram, the 75 mm thick foam layer with 400 kg/m^3 density resulted in a 31% increase in the impulsive asymptote, while the foam layers with 300 kg/m^3 and 200 kg/m^3 densities increased the impulsive asymptote by 20% and 16.4% respectively. The impulsive asymptote grew 8.5% when foam density was increased from 300 kg/m^3 to 400 kg/m^3. However, the percentage of increase drops to 2.8% if the density is changed from 200 kg/m^3 to 300 kg/m^3. This indicates that the blast resistance of the protected concrete is not directly proportional to the foam density.

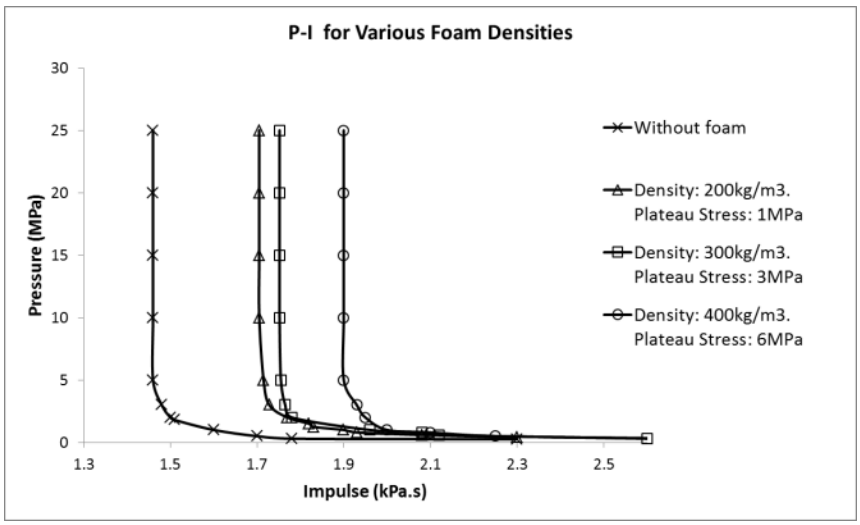

Figure 25: Influence of foam density on P-I diagrams

5.3 Influence of slab thickness

According to Ye and Ma's theory [5], the mitigation of blast effects on foam-protected structures is related to the relationship between the structural resistance and the foam strength. They suggested that if the foam strength were increased blindly without considering the resistance of the protected structure, an adverse effect will occur. In the current research, two identical RC slabs, but with 100 mm and 150 mm thickness respectively, were studied and the P-I diagrams are shown in Figures 26 and 27. The foam thickness was constant at 75 mm.

As discussed previously, for a 100 mm thick slab, the percentage mitigation of blast effect increases with foam density. However, for a 150 mm thick slab, using the 300 kg/m^3 foam as the protective layer is more effective than using the 400 kg/m^3 one. This finding in LS-DYNA agrees well with the discussion of Ye and Ma [5].

When the RC slab is thickened (in other words, the structural resistance is increased), the increase in the impulsive asymptote provided by the 200 kg/m^3 foam is very limited (11%), as the blast load required to cause the slab deflection rises along with the increase in slab thickness. Once the structural resistance is much larger than the strength of the foam, the foam deforms more quickly and more easily than the protected structure.

Compared with the strong RC slab, the energy being absorbed by the relatively weaker foam is very limited.

It is noted that the P-I curves for 150 mm slab protected by different foams (Figure 27) are not smooth. The turning section of the curve for 300 kg/m3 foam seems unreliable as there are two pressure values that correspond to the same impulse. This was caused by the error in the process of manually seeking the failure points. It was assumed that 2% difference in peak deflection was acceptable (Step 2 in Section 4).

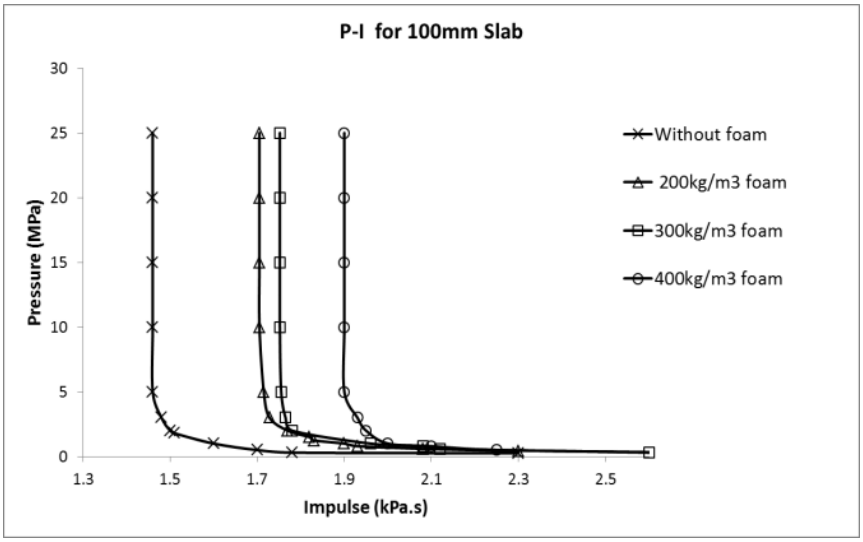

Figure 26: Influence of slab thickness on P-I diagrams (100mm)

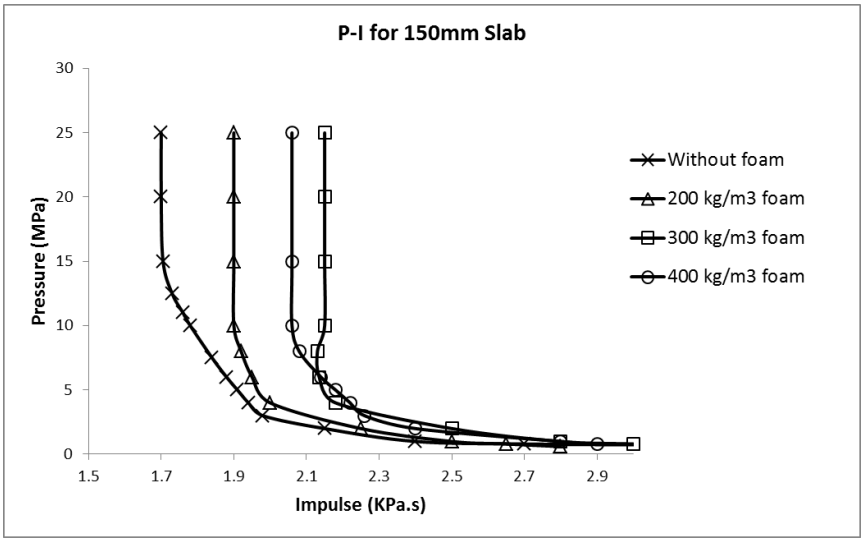

Figure 27: Influence of slab thickness on P-I diagrams (150mm)

5.4 Thicker unprotected slab vs. foam-protected slab

It is evident from the discussion that using the aluminium foam as a sacrificial layer is an effective way of mitigating blast effects. However, the RC slab can also be strengthened by solely increasing its depth and it is difficult to determine which is the better method of strengthening the slab against blast loads. In the current research, the effectiveness of using a 150 mm thick bare slab was compared to the effectiveness of using a 100 mm thick slab with 50 mm foam protection. The results are shown in Figure 28.

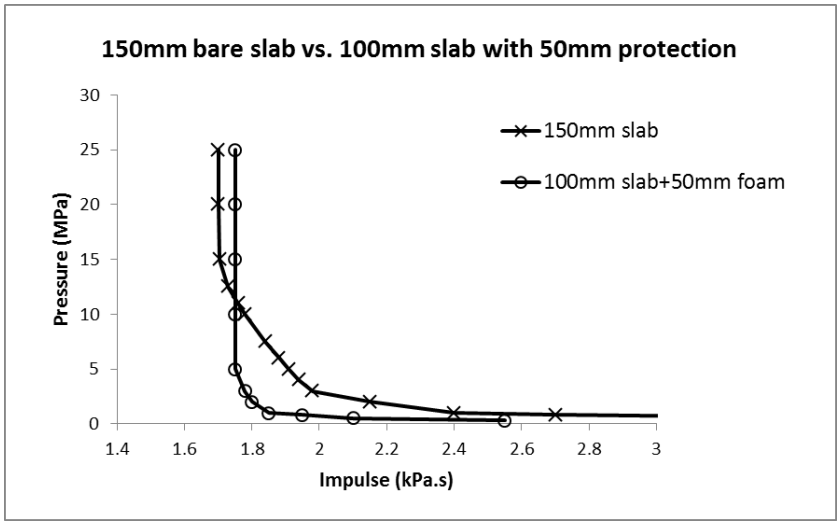

Figure 28: Thicker slab vs. foam protection

It can be seen that when the peak pressure is greater than 10 MPa, the 100 mm thick slab (with 50 mm protection) can withstand larger blast loads. In other words, attaching 50 mm thick foam is more efficient than thickening the slab by 50 mm in an impulsive loading regime. However, once the pressure drops below 10 MPa, much of the foam is redundant because as peak pressure decreases, less foam is required to offer protection.

Thus in this case (dynamic loading regime and quasi-static loading regime), thickening the RC slab by 50 mm leads to a larger blast load bearing capacity than attaching a 50 mm foam layer protection. As the damage from the blast load is mainly caused by the impulsive loading (as seen in Figure 15), the foam layer protection is a better solution to mitigating the blast effect on the RC structures. Nevertheless, there is no absolute answer for whether using foam layer protection is more effective than thickening the RC slab. The design should be carefully chosen according to the required maximum blast load.

6. Conclusion

A numerical model of aluminium foam-protected RC slabs using LS-DYNA was validated. The model is capable of predicting accurate results of the behaviours of both foam and slab. P-I diagrams of the combined system were generated to demonstrate the blast resistance of the foam-protected RC slabs. Sensitivity analysis showed that the thickness and the density of the foam require careful design in accordance with blast loads. Otherwise, over-design can result in the waste of uncompacted foam.

Moreover, the resistance of the RC slab is an important element that needs to be considered during the design of a foam-slab construction. An unbalanced relationship between the aluminium foam and the protected RC slab may not benefit significantly. Meanwhile, the addition of the foam cladding and the increase in the slab's resistance can improve the strength of the system confronted by different forms of blast load. For an impulse dominated blast loading, the attachment of a foam layer calms the shock wave more efficiently.

Acknowledgements

The research presented in this paper jointly supported by the ARC Discovery Grant DP140103025 and the National Science Foundation of China under Grants 51278326 and 51238007 is gratefully acknowledged.

References

[1] Hanssen, A, Enstock, L, and Langseth, M, *Close-range blast loading of aluminium foam panels.* International Journal of Impact Engineering, 2002. **27**(6): p. 593-618.

[2] Reid, S and Peng, C, *Dynamic uniaxial crushing of wood.* International Journal of Impact Engineering, 1997. **19**(5): p. 531-570.

[3] Ma, G and Ye, Z, *Analysis of foam claddings for blast alleviation.* International Journal of Impact Engineering, 2007. **34**(1): p. 60-70.

[4] Ma, G and Ye, Z, *Energy absorption of double-layer foam cladding for blast alleviation.* International Journal of Impact Engineering, 2007. **34**(2): p. 329-347.

[5] Ye, Z and Ma, G, *Effects of foam claddings for structure protection against blast loads.* Journal of Engineering Mechanics, 2007. **133**(1): p. 41-47.

[6] Li, J, Ma, G, Zhou, H, and Du, X, *Blast mitigation of civil structures by using density gradient aluminium foam cladding.* International Journal of Protective Structures, 2011. **2**(3): p. 333-349.

[7] Zhu, F, Zhao, L, Lu, G, and Wang, Z, *Structural response and energy absorption of sandwich panels with an aluminium foam core under blast loading.* Advances in Structural Engineering, 2008. **11**(5): p. 525-536.

[8] Nurick, G, Langdon, G, Chi, Y, and Jacob, N, *Behaviour of sandwich panels subjected to intense air blast–Part 1: Experiments.* Composite Structures, 2009. **91**(4): p. 433-441.

[9] Wu, C, Huang, L, and Oehlers, DJ, *Blast testing of aluminum foam–protected reinforced concrete slabs.* Journal of Performance of Constructed Facilities, 2010. **25**(5): p. 464-474.

[10] Qi, C, Yang, S, Yang, L-J, Wei, Z-Y, and Lu, Z-H, *Blast resistance and multi-objective optimization of aluminum foam-cored sandwich panels.* Composite Structures, 2013. **105**: p. 45-57.

[11] Shen, J, Lu, G, Zhao, L, and Qu, Z, *Response of curved sandwich panels subjected to blast loading.* Journal of Performance of Constructed Facilities, 2011. **25**(5): p. 382-393.

[12] Mullin, MJ and O'Toole, BJ. *Simulation of energy absorbing materials in blast loaded structures*. in *8th International LS-DYNA Users Conference*. 2004.

[13] Hanssen, A, Olovsson, L, Børvik, T, and Langseth, M. *Close-range blast loading of aluminium foam panels: A numerical study*. in *IUTAM Symposium on Mechanical Properties of Cellular Materials*. 2009. Springer.

[14] Schenker, A, Anteby, I, Nizri, E, Ostraich, B, Kivity, Y, Sadot, O, Haham, O, Michaelis, R, Gal, E, and Ben-Dor, G, *Foam-protected reinforced concrete structures under impact: experimental and numerical studies.* Journal of Structural Engineering, 2005. **131**(8): p. 1233-1242.

[15] Shi, Y, Hao, H, and Li, Z-X, *Numerical derivation of pressure–impulse diagrams for prediction of RC column damage to blast loads.* International Journal of Impact Engineering, 2008. **35**(11): p. 1213-1227.

[16] Zhu, F, Zhao, L, Lu, G, and Gad, E, *A numerical simulation of the blast impact of square metallic sandwich panels.* International Journal of Impact Engineering, 2009. **36**(5): p. 687-699.

[17] Karagiozova, D, Nurick, G, and Langdon, G, *Behaviour of sandwich panels subject to intense air blasts–Part 2: Numerical simulation.* Composite Structures, 2009. **91**(4): p. 442-450.

[18] Hu, Y, Wu, C, Lukaszewicz, M, Dragos, J, Ren, J, and Haskett, M, *Characteristics of confined blast loading in unvented structures.* International Journal of Protective Structures, 2011. **2**(1): p. 21-43.

[19] Dragos, J, Visintin, P, Wu, C, and Oehlers, DJ, *A numerically efficient finite element analysis of reinforced concrete members subjected to blasts.* International Journal of Protective Structures, 2014. **5**(1): p. 65-82.

[20] Li, Q and Meng, H, *Pressure-impulse diagram for blast loads based on dimensional analysis and single-degree-of-freedom model.* Journal of Engineering Mechanics, 2002. **128**(1): p. 87-92.

[21] Dragos, J and Wu, C, *A new general approach to derive normalised pressure impulse curves.* International Journal of Impact Engineering, 2013. **62**: p. 1-12.

[22] Zhu, C, Lin, Z.T.L., Chia, Y.F., Chong, K.P., *Protection of reinforced concrete structures against blast loading*, in *School of Civil, Environmental and Mining Engineering*2009, the University of Adelaide.

[23] Wu, C and Zhou, Y, *Simplified analysis of foam cladding protected reinforced concrete slabs against blast loadings.* International Journal of Protective Structures, 2011. **2**(3): p. 351-366.

[24] Wu, C and Sheikh, H, *A finite element modelling to investigate the mitigation of blast effects on reinforced concrete panel using foam cladding.* International Journal of Impact Engineering, 2013. **55**: p. 24-33.

[25] Shkolnikov, M. *Honeycomb modeling for side impact moving deformable barrier (MDB)*. in *7th International LS-DYNA Users Conference*. 2002.

[26] Jackson, K. *Predicting the dynamic crushing response of a composite honeycomb energy absorber using a solid-element-based finite element model*. in *Proceedings of the 11th International LS-DYNA Users Conference, Dearborn, MI*. 2010.

[27] Hallquist, JO, *LS-DYNA KEYWORD USER'S MANUAL VOLUME II: Material Models.* Livermore, California, USA, 2013.

[28] CYMAT, *Techinical Manual for CYMAT*. Vol. 5. 2009: CYMAT Technologies

Ltd.

[29] Ma, G, Ye, Z, and Shao, Z, *Modeling loading rate effect on crushing stress of metallic cellular materials.* International Journal of Impact Engineering, 2009. **36**(6): p. 775-782.

[30] Yu, J, Liu, Y-D, Zheng, Z-J, Li, J-R, and Yu, T. *Influences of inertia and material property on the dynamic behavior of cellular metals*. in *IUTAM Symposium on Mechanical Properties of Cellular Materials*. 2009. Springer.

[31] Murray, YD, Abu-Odeh, AY, and Bligh, RP, *Evaluation of LS-DYNA concrete material model 159*, 2007.

[32] *UFC 3-340-02: Structures to resist the effects of accidental explosions*, 2008, U.S. Department of the Army, Navy, and Air Force: Washington, DC, USA.

[33] Ballantyne, GJ, Whittaker, AS, Dargush, GF, and Aref, AJ, *Air-blast effects on structural shapes of finite width.* Journal of Structural Engineering, 2009. **136**(2): p. 152-159.

[34] Dragos, J, Wu, C, Haskett, M, and Oehlers, D, *Derivation of normalized pressure impulse curves for flexural ultra high performance concrete slabs.* Journal of Structural Engineering, 2012. **139**(6): p. 875-885.

[35] Evans, AG, Hutchinson, JW, Fleck, NA, Ashby, M, and Wadley, H, *The topological design of multifunctional cellular metals.* Progress in Materials Science, 2001. **46**(3): p. 309-327.

Chapter 3 - Optimised Design of Foam Cladding for Protection of Reinforced Concrete Members under Blast Loading

Statement of Authorship

Title of Paper	Optimized Design of Foam Cladding for Protection of Reinforced Concrete Members under Blast Loading
Publication Status	☑ Published ☐ Accepted for Publication ☐ Submitted for Publication ☐ Unpublished and Unsubmitted work written in manuscript style
Publication Details	XIA, Y., WU, C. & LI, Z.-X. 2014. Optimized design of foam cladding for protection of reinforced concrete members under blast loading. *Journal of Structural Engineering,* **141**, 06014010.

Principal Author

Name of Principal Author (Candidate)	Ye Xia		
Contribution to the Paper	Developed the model, conducted parametric studies, analysed and interpreted data, and wrote manuscript.		
Overall percentage (%)	85%		
Certification:	This paper reports on original research I conducted during the period of my Higher Degree by Research candidature and is not subject to any obligations or contractual agreements with a third party that would constrain its inclusion in this thesis. I am the primary author of this paper.		
Signature		Date	

Co-Author Contributions

By signing the Statement of Authorship, each author certifies that:

i. the candidate's stated contribution to the publication is accurate (as detailed above);

ii. permission is granted for the candidate in include the publication in the thesis; and

iii. the sum of all co-author contributions is equal to 100% less the candidate's stated contribution.

Name of Co-Author	Chengqing Wu		
Contribution to the Paper	Supervised development of work, prepared the test, helped in manuscript evaluation, and acted as corresponding author.		
Signature		Date	24/11/2016

Name of Co-Author	Zhong-Xian Li		
Contribution to the Paper	Provided comments for the manuscript.		
Signature		Date	26/11/2016

OPTIMISED DESIGN OF FOAM CLADDING FOR PROTECTION OF REINFORCED CONCRETE MEMBERS UNDER BLAST LOADING

Ye Xia, Chengqing Wu, and Zhong-Xian Li

Abstract

A load-cladding-structure (LCS) model was used to study the mitigating effect provided by metallic foam cladding against blast loading on reinforced concrete (RC) structural members. The model considered the interactions between an external blast load, a protecting foam cladding, and a target RC structural member. The effectiveness of the LCS model was validated by field blast tests conducted in 2009. The validated model was then used to derive pressure impulse diagrams of the foam-protected RC members. Afterwards, two non-dimensional parameters representing the relationship between the foam cladding and the target RC member were characterized. Using the suggested non-dimensional parameters, normalized pressure-impulse (p−i) diagrams for the foam-protected RC members were generated. The effects of the two non-dimensional parameters on the p−i diagrams were investigated by comparing the corresponding asymptotes. Based on the predicted results, an optimized design of the foam cladding for RC structural members was suggested.

1. Introduction

In recent years, terrorist attacks and accidental explosions in urban areas have resulted in catastrophic damage not only to the surrounding structures, but also to the humans occupying the area. Metallic foam has been recognized as one of the most convenient and economical sacrificial claddings to mitigate the impact of explosions, with a great capacity for energy absorption [1-5]. Metallic foams can be manufactured in different densities and configurations with a wide variety of properties by changing the

production recipe. It is essential, however, to design the properties of the metallic foam claddings with care to avoid waste and poor performance. Therefore, to achieve efficient and effective protection, it is vitally important to conduct research on optimizing the design of foam cladding.

Because real blast tests are extremely expensive and time-consuming, numerical models are often substituted for field tests to study blast effects on foam-protected structures, and the single degree of freedom (SDOF) model has proved to be a highly economical method because of its ease of use and low running time. SDOF has therefore been widely used to simulate dynamic reactions and is referenced for standards and guidelines in design manuals, such as Unified Facilities Criteria [6].

Ye and Ma [3] developed a load-cladding-structure (LCS) model based on the SDOF system to evaluate the response of protected structures. Based on the LCS model, non-dimensional pressure and impulse diagrams were drawn to prove the effectiveness of the foam cladding. In Ye and Ma's model [3], only linear stiffness was assessed for the target structure. However, most existing building materials, such as reinforced concrete, behave nonlinearly when moving from an elastic to a plastic state. Therefore, the linear LCS model is limited in terms of evaluating the response of non-linear RC structural members. In order to predict the reaction of cladding-protected RC structural members, a nonlinear LCS model is therefore required.

Recently, Wu and Zhou [7] improved the LCS model to predict the response of foam-protected RC beams under blast loads. The authors compared the predicted deflection of the foam-protected RC slab with an experimental result from Zhu [8], and an error of 19.7% was yielded. Although this error is acceptable in blast simulations, room for improvement, such as using more accurate solving methods and blast load inputs, still exists. In terms of close-range blasting, Slavik [9] found that the variation of the pressure distribution was significant along the member span, rather than being uniformly distributed

as assumed in previous studies [3, 7]. In addition, so far, no parametric studies have been conducted on optimizing the design of foam to be attached to nonlinear RC members.

In the present study, the previous LCS model for RC structural members was further developed. The improved LCS model is able to evaluate the flexural deformation levels of both the foam cladding and the RC structural member under blast loading. It should be noted that shear failure, which is another major failure type of RC members under blast loading, was not considered in the current study and will be investigated specifically in later research. Based on this model, normalized pressure-impulse (p − i) diagrams were generated for different foam-structure configurations. The different foam-RC structure configurations were represented by two non-dimensional parameters, κ and τ. Furthermore, the results of a parametric study were analysed, and ways by which the design of the foam cladding could be optimized were proposed.

2. Load-cladding-structure model

The LCS model employed in the current study largely consists of three components: a linearly decaying external blast load $P(t)$; foam cladding with a cover plate; and a RC structural member represented by its resistance-deflection function $R(y)$. Fig. 1 illustrates the gradual densification of the foam cladding exposed to a blast in terms of the shock front, a fully compacted section, and an uncompacted section of the cladding.

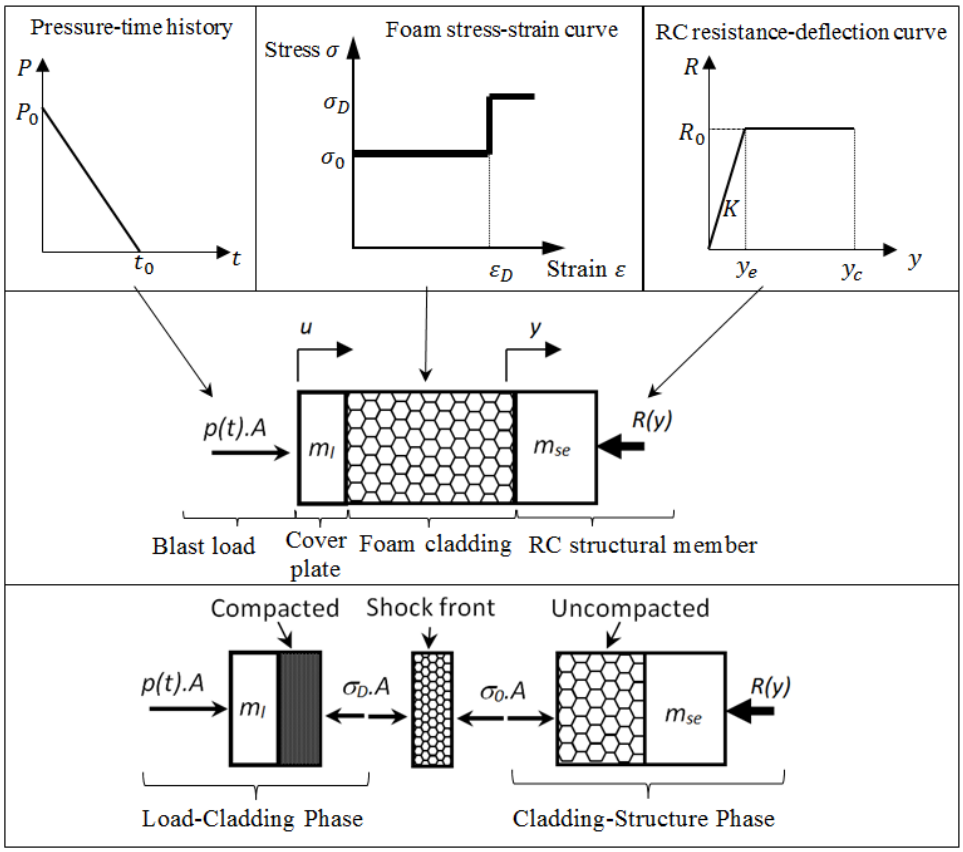

Fig. 1. Load-cladding-structure model for RC structure

As indicated in Fig. 1, the motion equation of the front load- cladding phase can be expressed as [3, 7]:

$$\left[m_l + \frac{\rho A}{\varepsilon_D}(u - y)\right]\ddot{u} + \frac{\rho A}{\varepsilon_D}(\dot{u} - \dot{y})^2 + [\sigma_0 - P(t)]A = 0 \quad (1)$$

where m_l is the mass of the cover plate; u is the displacement of the cladding; y is the displacement of the RC structural member; A is the cross-sectional area; ε_D is the densification strain of the foam; ρ is the foam density.

On the other side of the shock front, the foam is in the undensified phase. This part of the foam moves together with the main structure, which has an equivalent mass of m_{se}. The dynamic equation for the undensified phase is produced and can be expressed as

$$\left[m_f - \frac{\rho A}{\varepsilon_D}(u - y) + m_{se}\right]\ddot{y} + R(y) - \sigma_0 A = 0 \quad (2)$$

where m_f is the mass of the foam cladding and function $\frac{\rho A}{\varepsilon_D}(u - y)$ represents the mass of the densified part of the foam cladding.

Once the foam is fully compacted, all parts of the foam, including the cover plate, move together with the structure at the same velocity. The motion equation for the foam in a fully compacted condition can be written as

$$[m_l + m_f + m_{se}]\ddot{y} + R(y) - P(t)A = 0 \quad (3)$$

when

$$u > \varepsilon_D l \quad (4)$$

where l is the thickness of the foam cladding.

In this study, the fourth-order Runge-Kutta method is used with the equations to solve for the displacement of the foam and the structure from an initial state of zero.

3. Experiments and Validation

The developed LCS model was validated using data obtained from the blast tests on simply supported RC slabs of 2,000 × 400 × 100 mm protected by aluminium foam layers (Figs. 2 and 3). As shown in Fig. 2, the explosive charge used in all four experimental events was spherical (205 mm diameter) and weighed 7.5 kg by composition B (60% RDX and 40% TNT), which was the equivalent of a TNT charge of 8.2 kg. A timber frame supported the charge and a string was used to change the height of the charge from the slab in order to achieve different blast loads. Four blast events at different standoff distances (charge heights) were conducted on RC slabs in blast tests at Pt. Wakefield in 2009 [10]. Fig. 3 shows the configuration of the RC slab employed in the tests and the material properties are listed in Table 1.

The aluminium foam layer was 75 mm thick, with a density of 420 kg/m^3 and was attached to the RC slab by epoxy adhesive for Events 2–4. A 1.15-mm metal cover over the compression face of the aluminium foam was used to prevent the foam from disintegrating

under the large blast loading, and ensure that its energy absorption capacity was fully utilized.

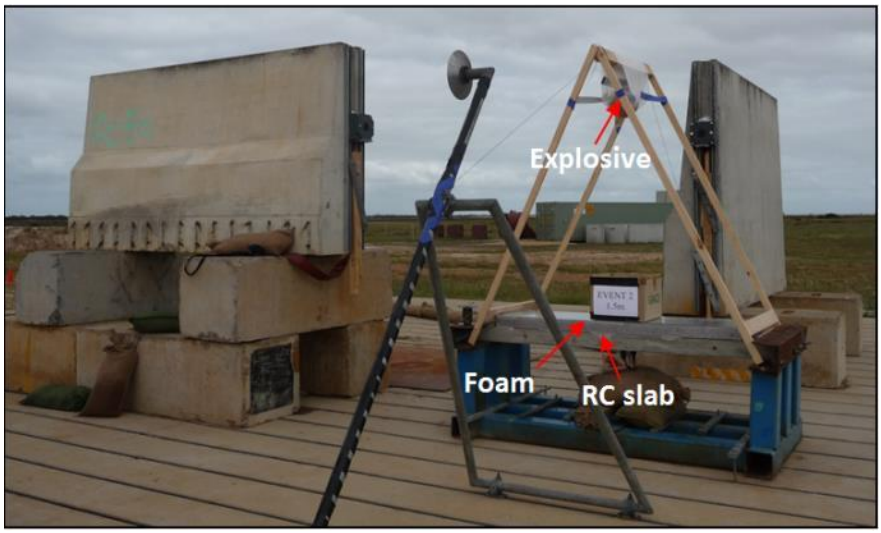

Fig. 2. Experiment setup

Table 1. Basic material properties

Basic Properties of Concrete			
Density (kg/m^3)	Young's Modulus (GPa)	Compressive Strength (MPa)	Crushing Strain
2400	25.7	32	0.004
Basic Properties of Reinforcement			
Diameter (mm)	Young's Modulus (GPa)	Yield Strength (MPa)	Spacing (mm)
12	200	500	89.5
Basic Properties of Aluminium Foam			
Density (kg/m^3)	Plateau Stress (MPa)	Densification Strain	Thickness (mm)
420	5.4	0.54	75
Basic Properties of Cover Plate			
Density (kg/m^3)		Thickness (mm)	
7850		1.15	

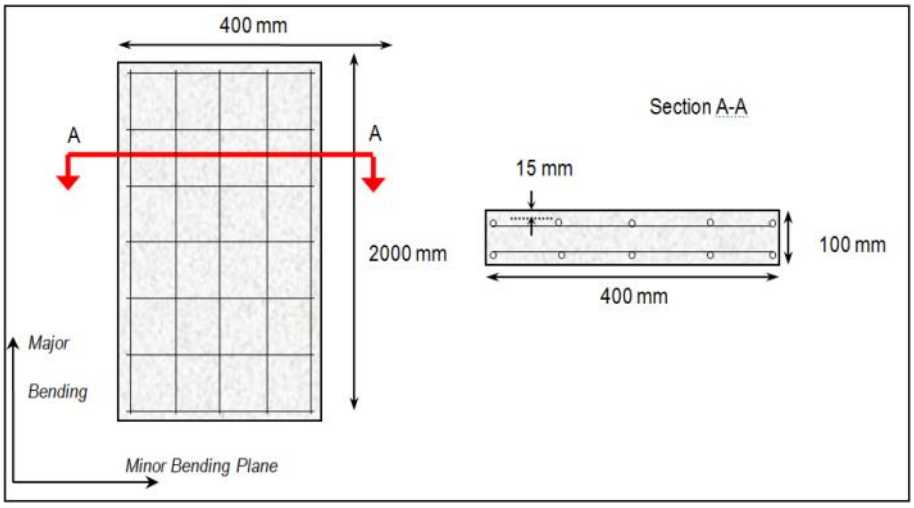

Fig. 3. Slab configuration

Table 2 summarizes the information for all four blast events. The incident pressures were predicted using UFC guidelines [6]. For the reflected impulses, the UFC guidelines over-predicted by more than 30% compared with the test data. An empirical formula based on UFC guidelines and test results was used in predictions [10]:

$$\frac{I}{Q^{\frac{1}{3}}} = 0.78\left(\frac{R}{Q^{\frac{1}{3}}}\right)^{-1.28} \quad (5)$$

where I presents the reflected impulse of the blast; R is the charge distance; and Q is the charge weight.

Table 2. Summary of specimens and blast events

Event	**1**	**2**	**3**	**4**
Foam thickness (mm)	NA	75	75	75
Charge weight (kg)	7.5	7.5	7.5	7.5
Standoff distance (m)	1.50	1.50	1.25	1.00
Incident pressure (MPa)	2.07	2.07	3.45	4.82
Reflected pressure (MPa)	12.4	12.4	20.7	34.5
Reflected impulse (MPa.ms)	1.14	1.14	1.44	1.91
Experimental deflection (mm)	33.6	23.1	31.5	65.2
Model predicted deflection (mm)	36.7	27.8	35.0	65.4
Error (%)	9.2	20.6	10.9	0.29

Close-range blast testing was often carried out in full-scale field tests. Therefore, the significant variations of the blast load along the structural span should be taken into account for model validation. According to Slavik [9], the effective distribution of the blast load at any point along two-dimensional members can be expressed by Eq. (6)

$$P_{eff} = P_{inc}(1 + cos\theta - 2cos^2\theta) + P_{ref}cos^2\theta \quad (6)$$

where the angle of incidence θ is the angle between the central vertical line and the line from the charge centre to the point of interest on the member (Fig. 4); P_{inc} is the incident pressure; and P_{ref} is the reflected pressure.

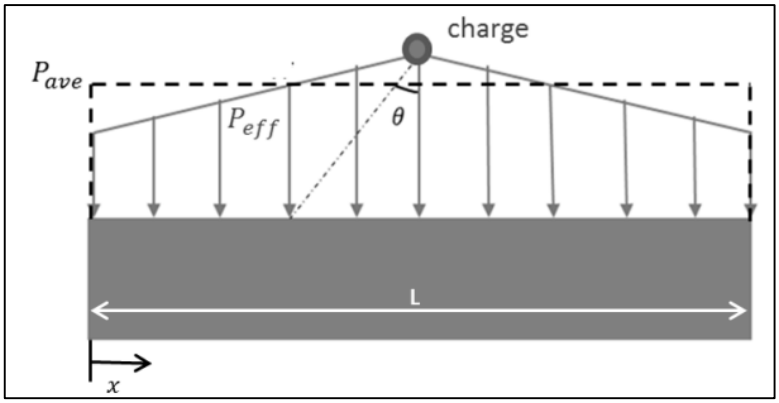

Fig. 4. Blast pressure diagram

Using Eq. (6), the effective pressure acting on the incremental points along the slab can be calculated. The equivalent uniformly distributed average pressure (Fig. 4) of the blast could then be expressed by

$$P_{ave} = \frac{\int_0^L P_{eff}dx}{L} \quad (7)$$

P_{ave} was used as P_0 in Equation (1) for validations and in the generation of pressure-impulse diagrams.

For calculating convenience, the RC structural member was assumed to deform from an elastic state with stiffness K to a perfectly plastic state with maximum resistance R_0 at maximum deflection y_m. Under the elastic response, the structural resistance of a simply supported slab was calculated by 8M=L from structural mechanisms, where M is the section moment along length L. The stiffness K, the slope of the resistance and deflection

curve under the elastic region, is equal to $384EI=5L^3$. The deflection at yield can be calculated by the resistance divided by this stiffness factor. The failure condition was calculated using the moment and rotation model introduced by Haskett et al. [11]. Both concrete crushing and steel bar slip were considered in this model. In the present study, y_m was used to define the structural member damage

$$y_m = y_c \quad (8)$$

where y_c is the critical deflection that indicates a safe scenario at the maximum allowable deflection.

The idealized rigid perfectly plastic-locking (RPPL) model for metallic foam [1] and the bilinear resistance-deflection function for the RC slab were incorporated into the new LCS model for dynamic analysis. The theoretical deflection histories predicted from the above LCS model were validated with the experimental data measured in the blast tests in the current study. The comparisons of the data on the deflection versus time history are shown in Fig. 5 and Table 2.

As seen in Fig. 5, the deflections simulated by the developed LCS model basically followed the shape and period of the results obtained from blast testing. However, the simulations resulted in relatively larger maximum deflections compared to the actual experimental data. This overestimation might be caused by the idealization of the RPPL model for foam cladding and the resistance-deflection relationship of the RC slab.

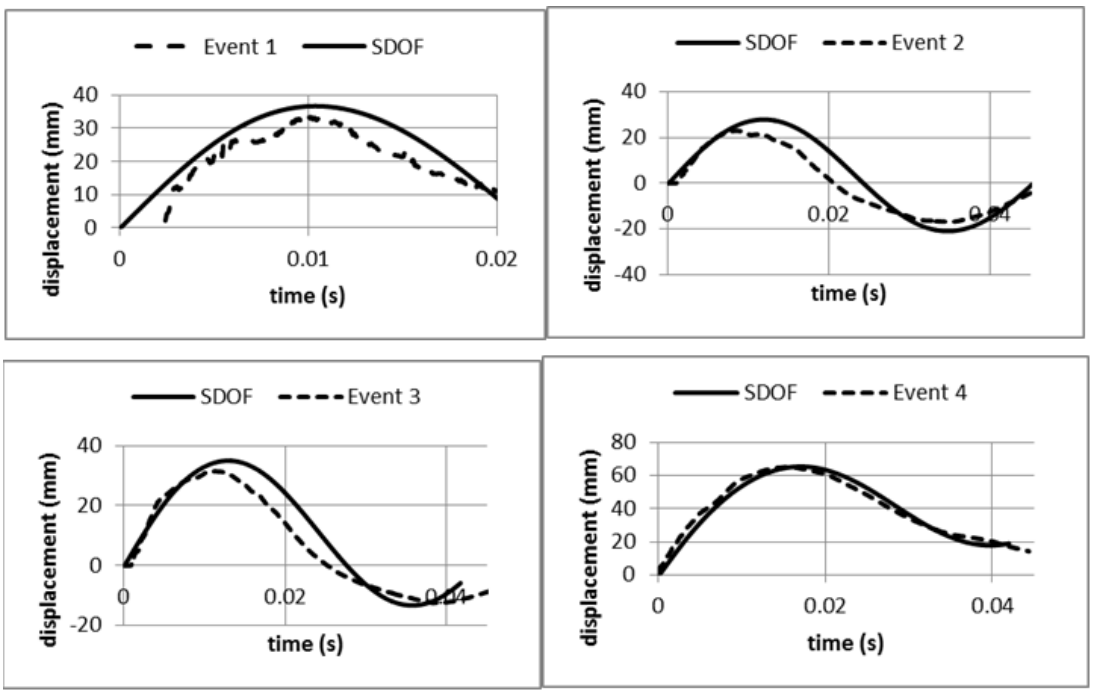

Fig. 5.Validations of load-cladding-structure model against experimental results

4. Optimisation

Optimisation was achieved by the parametric study of different cladding-structure configurations using non-dimensional pressure-impulse (p-i) diagrams. The different foam-structure configurations are presented by two non-dimensional parameters.

4.1 Non-dimensional parameters κ

For the appropriate structural protection, the plateau stress of foam material requires a careful selection corresponding to the resistance of the target structural member. The resistance capacity of a structural member is defined as the maximum allowable constant force that will cause a critical deflection y_c. For an elastic-plastic structure, it can be written as U/y_c, where U is the area beneath the resistance-deflection curve of the protected structural member (shown by the black dashed line in Fig. 6).

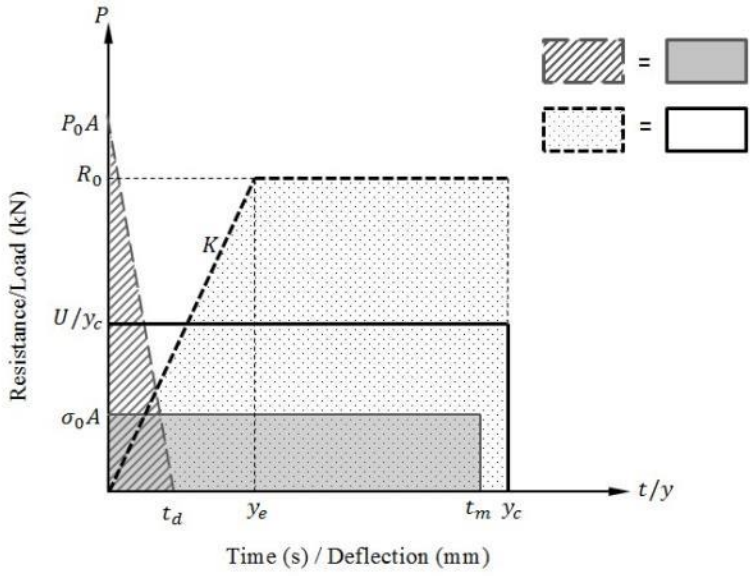

Fig. 6. Loads and resistance diagram

According to Ye and Ma [3], a non-dimensional parameter κ describes the relation between the plateau stress of the foam and the resistance of the structural member. Therefore, the first non-dimensional parameter κ for RC member can be defined as

$$\kappa = \frac{\sigma_0 A}{U/y_c} \tag{9}$$

Fig. 6 illustrates the relationships between the different loads in the system of foam-cladding-protected structural members under blast loading. The grey dashed line represents the linearly decayed blast load acting on the cladding surface. The load $\sigma_0 A$ transmitted through the cladding onto the target structural member is assumed to be a constant and corresponds to the plateau stress of the foam cladding, which is indicated by the grey solid line. The non-dimensional parameter κ represents the ratio between the trans- mitted load and the structural resistance capacity (black solid line in Fig. 6).

4.2 Non-dimensional parameter τ

The other important factor of a safe design is the sufficient thickness of the foam layer. According to Ye and Ma [3], the rectangular pressure ($\sigma_0 A$) transmitted to the target

structural member lasts for a duration of t_m, which can be expressed in terms of the foam thickness (l) and other foam properties as

$$t_m = \sqrt{(m_f + 2m_l)\frac{l\varepsilon_D}{\sigma_0 A}} \quad (10)$$

Ideally, the thickness of the foam layer should be sufficient to be fully compacted at the instant when the structural member experiences the maximum allowable deflection, i.e. $t_m = t_{max}$ shown in Fig. 7.

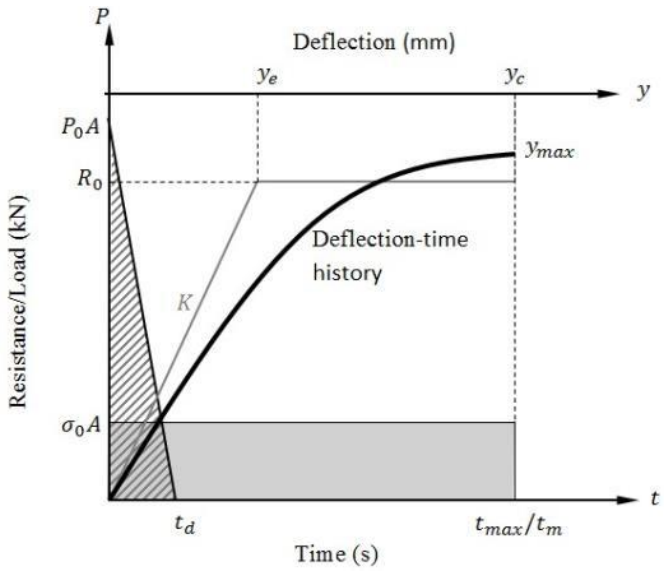

Fig. 7. Foam thickness design

To calculate t_{max}, the time when the maximum deflection y_c occurs, an SDOF model for elastic-plastic structural members subjected to a constant dynamic load of $F = \sigma_0 A$ was considered. This elastic-plastic model was achieved by first developing an elastic model from which the elastic-plastic model could be defined.

4.2.1 Elastic model

Under a low-intensity explosion with low duration, the foam- protected RC structural member deforms under the yield deflection y_e. In this case, the protected RC structural member only responds in an elastic state with a linear stiffness K. This case can be presented in the SDOF model as:

$$m_{se}\ddot{y} + Ky = F \tag{11}$$

From Duhamel's Integral, the deflection time history of the structure is expressed as

$$y(t) = \frac{F}{K}(1 - cos\omega t) \tag{12a}$$

$$\dot{y} = \frac{F}{K\omega} sin(\omega t) \tag{12b}$$

where ω is the natural undamped frequency of the structure, and $\omega = \sqrt{K/m_{se}}$.

Hence, the natural period of the equivalent elastic structure is $T = 2\pi\sqrt{m_{se}/K}$, i.e. $t_{max} = T/2$.

4.2.2 Elastic-plastic model

Once the maximum deflection of the system exceeds the yield deflection y_e, the resistance of the RC structural member experiences the plastic state.

The SDOF model for the pure plastic part is written as

$$m_{se}\ddot{y} + R_0 = F \tag{13}$$

After integrations, it becomes

$$\dot{y}(t) = \left(\frac{F - R_0}{m_{se}}\right) t + C_1 \tag{14a}$$

$$y(t) = \left(\frac{F - R_0}{2m_{se}}\right) t^2 + C_1 t + C_2 \tag{14b}$$

where C_1 and C_2 are constants and can be solved with the initial condition. The initial condition is the intersection point of elastic and plastic parts at the time of $y(t) = R_0/K = y_e$. From Equation (12a), the intersection time t_e can be calculated and then t_e substituted into Equation (12b) to get $\dot{y}_e$. Finally, constants C_1 and C_2 were achieved by substituting $(t_e, \dot{y}_e)$ and (t_e, y_e) into Equation (14a) and Equation (14b) respectively.

Since $y(t)$ is a quadratic equation, the maximum deflection would be reached at

$$t_{max} = \frac{C_1 m_{se}}{R_0 - F} \tag{15}$$

It is then reasonable to suggest that for an optimal design, the foam layer should have such a thickness that the foam is fully compacted at the instant of t_{max} [3]. Therefore, the second non-dimensional parameter for an elastic-plastic structural member is defined as

$$\tau = \frac{t_m}{t_{max}} \tag{16}$$

4.3 Normalised pressure p and impulse i

Pressure-impulse diagrams have been commonly used in the preliminary design to establish a safe response limit for given structural systems [12-15]. For the convenience of comparison and optimization, pressure and impulse were represented as non-dimensional forms in the current study. According to Mays [16], the basic principle of non-dimensional pressure is to equate the work done on the structural member with the strain energy acquired by the structural member as it deforms, while the non-dimensional impulse is expressed by the ratio of the kinetic energy delivered and the strain energy acquired by the structural member. Therefore, the non-dimensional pressure and impulse can be written as Eqs. (17a) and (17b), which would be used in the optimization study

$$p = \frac{P_0 A}{U/y_c} \tag{17a}$$

$$i = \frac{I_0}{\sqrt{2m_{se}U}} \tag{17b}$$

For unprotected RC structural members, both the pressure asymptote and the impulsive asymptote of the normalized p − i curve are 1.0, i.e. $p_0 = 1.0 \ and \ i_0 = 1.0$ [16], shown as the solid line in Fig. 8. The points on the $p - i$ curve indicate the $p - i$ combinations that result in the structure just reaching the critical deflection y_c.

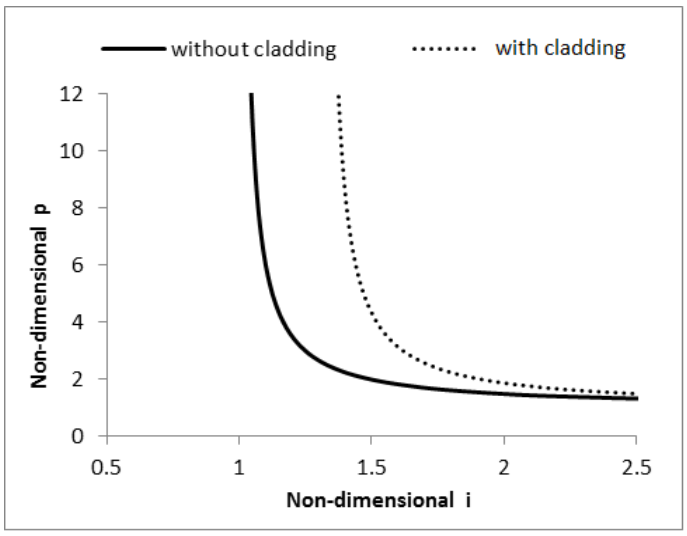

Fig. 8. Non-dimensional $p-i$ diagrams of the structure ($\kappa = 1, \tau = 1$)

The dashed curve in Fig. 8 is the non-dimensional p − i diagram after attaching a foam cladding that satisfies κ =1, τ =1. It was observed that the impulsive asymptote (i_0 =1.33) of the p − i diagram of the cladding-protected RC member increased compared with the unprotected RC member. This indicates that the RC structural member with the foam cladding was capable of withstanding a 33% higher impulse under a very high peak pressure load. On the other hand, the pressure asymptote of the non-dimensional p − i curve for the protected RC member remained the same (p_0 = 1.0). This result means that under a very low peak pressure, the protective effect becomes insignificant.

5. Parametric study

To investigate the optimal relationship between the foam cladding and the protected RC structural member, a parametric study was carried out by changing the two non-dimensional parameters. The influence of each non-dimensional parameter on the normalized $p-i$ diagrams was examined.

Because the addition of the foam cladding has no influence on the pressure asymptotes, only impulse asymptotes were considered in this section. A protection effective factor of the foam cladding was employed to express the protection effectiveness of the given $p-i$ diagram [3]

$$n = \frac{i_{with} - i_{without}}{i_{without}} \quad (2$$

where i_{with} and $i_{without}$ = normalised impulse asymptotes for the RC structural member with and without the foam cladding.

Fig. 9 displays the influence of the non-dimensional parameter κ on the protection effective factor n. For a constant τ, the protective effect of the foam cladding varies with κ. It was noticed that $\kappa = 0.8$ was a turning point in the protective tendency of the foam claddings acting on RC structural members. When κ was smaller than 0.8, n increased with the increase of κ until it reached a peak protective effect at $\kappa = 0.8$. This rising trend also increased with the increase in τ. Between $\kappa = 0.8$ to $\kappa = 1.0$, there appeared to be a relatively stable range where the protective effect was maintained at a high level. After κ became larger than 1.0, n started decreasing until reaching $\kappa = 2.0$. For further increases of κ, the protection effective factor n remained at a relatively steady state. Hence, the cladding that satisfied $\kappa = 0.8$ can provide the optimal protective effect for the RC structural member for a certain τ.

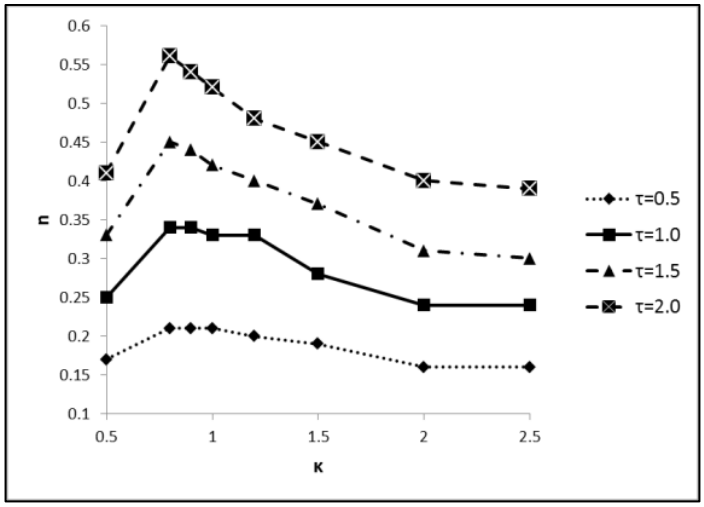

Fig. 9. Influence of τ on the protective effect of the foam cladding

The influence of the other non-dimensional parameter, τ , is presented in Fig. 10. For a fixed κ, the protective effect improved almost linearly with the increase of τ. This

indicates that thicker foam is capable of absorbing more blast energy, especially when the foam cladding is slightly weaker than the target RC member, i.e. $\kappa \approx 0.8$.

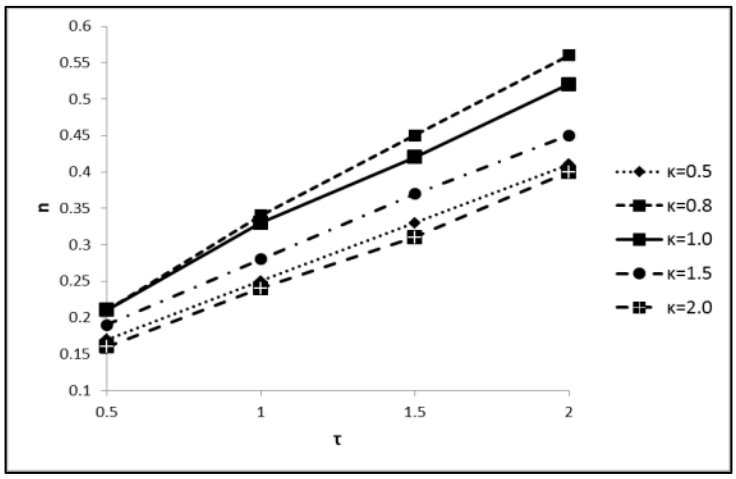

Fig. 10. Influence of κ on the protective effect of the foam cladding

6. Conclusion

This study developed a nonlinear LCS model to simulate the protective effectiveness of foam cladding on RC structural members. To validate the model, the predictions of the LCS model were compared with experimental results of four blast tests and an average error of 10% was yielded. Two non-dimensional parameters – κ and τ – have also been generated to account for the relationships between the cladding properties and the elastic-plastic behaviour in structural members. A parametric study was carried out to deter- mine the optimal design of the metallic cladding foam for RC members using the normalized p-i diagrams. According to the optimizing study, maximum protection is achieved when both the properties of the foam and the structural resistance are considered in conjunction with one another. For a certain RC structural member and a specified design blast load, the optimal design can be achieved with $\kappa \approx 0.8$ and a relative large τ ($\tau \geq 1$) based on budget and availability.

References

[1] Ma, G and Ye, Z, *Analysis of foam claddings for blast alleviation.* International

Journal of Impact Engineering, 2007. **34**(1): p. 60-70.

[2] Ma, G and Ye, Z, *Energy absorption of double-layer foam cladding for blast alleviation.* International Journal of Impact Engineering, 2007. **34**(2): p. 329-347.

[3] Ye, Z and Ma, G, *Effects of foam claddings for structure protection against blast loads.* Journal of Engineering Mechanics, 2007. **133**(1): p. 41-47.

[4] Ma, G, Ye, Z, and Shao, Z, *Modeling loading rate effect on crushing stress of metallic cellular materials.* International Journal of Impact Engineering, 2009. **36**(6): p. 775-782.

[5] Li, J, Ma, G, Zhou, H, and Du, X, *Blast mitigation of civil structures by using density gradient aluminium foam cladding.* International Journal of Protective Structures, 2011. **2**(3): p. 333-349.

[6] *UFC 3-340-02: Structures to resist the effects of accidental explosions*, 2008, U.S. Department of the Army, Navy, and Air Force: Washington, DC, USA.

[7] Wu, C and Zhou, Y, *Simplified analysis of foam cladding protected reinforced concrete slabs against blast loadings.* International Journal of Protective Structures, 2011. **2**(3): p. 351-366.

[8] Zhu, C, Lin, Z.T.L., Chia, Y.F., Chong, K.P., *Protection of reinforced concrete structures against blast loading*, in *School of Civil, Environmental and Mining Engineering*2009, the University of Adelaide.

[9] Slavik, TP. *A coupling of empirical explosive blast loads to ALE air domains in LS-DYNA®.* in *IOP Conference Series: Materials Science and Engineering*. 2010. IOP Publishing.

[10] Wu, C and Sheikh, H, *A finite element modelling to investigate the mitigation of blast effects on reinforced concrete panel using foam cladding.* International Journal of Impact Engineering, 2013. **55**: p. 24-33.

[11] Haskett, M, Oehlers, DJ, Ali, MM, and Wu, C, *Rigid body moment–rotation mechanism for reinforced concrete beam hinges.* Engineering Structures, 2009. **31**(5): p. 1032-1041.

[12] Shi, Y, Hao, H, and Li, Z-X, *Numerical derivation of pressure–impulse diagrams for prediction of RC column damage to blast loads.* International Journal of Impact Engineering, 2008. **35**(11): p. 1213-1227.

[13] Li, Q and Meng, H, *Pressure-impulse diagram for blast loads based on dimensional analysis and single-degree-of-freedom model.* Journal of Engineering Mechanics, 2002. **128**(1): p. 87-92.

[14] Dragos, J, Wu, C, Haskett, M, and Oehlers, D, *Derivation of normalized pressure impulse curves for flexural ultra high performance concrete slabs.* Journal of Structural Engineering, 2012. **139**(6): p. 875-885.

[15] Dragos, J and Wu, C, *A new general approach to derive normalised pressure impulse curves.* International Journal of Impact Engineering, 2013. **62**: p. 1-12.

[16] Mays, G, *Blast effects on buildings: design of buildings to optimize resistance to blast loading*. 1995: Thomas Telford.

Chapter 4 – Protective Effect of Graded Density Aluminium Foam on RC Slab under Blast Loading – An Experimental Study

Statement of Authorship

Title of Paper	Protective effect of graded density aluminium foam on RC slab under blast loading – An experimental study
Publication Status	☑ Published ☐ Accepted for Publication ☐ Submitted for Publication ☐ Unpublished and Unsubmitted work written in manuscript style
Publication Details	XIA, Y., WU, C., LIU, Z.-X. & YUAN, Y. 2016. Protective effect of graded density aluminium foam on RC slab under blast loading–An experimental study. *Construction and Building Materials*, 111, 209-222.

Principal Author

Name of Principal Author (Candidate)	Ye Xia		
Contribution to the Paper	Design the experiment, analysed and interpreted data, and wrote manuscript.		
Overall percentage (%)	85%		
Certification:	This paper reports on original research I conducted during the period of my Higher Degree by Research candidature and is not subject to any obligations or contractual agreements with a third party that would constrain its inclusion in this thesis. I am the primary author of this paper.		
Signature		Date	

Co-Author Contributions

By signing the Statement of Authorship, each author certifies that:

i. the candidate's stated contribution to the publication is accurate (as detailed above);

ii. permission is granted for the candidate in include the publication in the thesis; and

iii. the sum of all co-author contributions is equal to 100% less the candidate's stated contribution.

Name of Co-Author	Chengqing Wu		
Contribution to the Paper	Supervised development of work, helped conduct the experiment, provided critical manuscript evaluation, and acted as corresponding author.		
Signature		Date	24/11/2016

Name of Co-Author	Zhong-Xian Liu		
Contribution to the Paper	Helped design and conduct the test.		
Signature		Date	2016.11.25

Name of Co-Author	Yuemin Yuan		
Contribution to the Paper	Helped design and conduct the test.		
Signature		Date	2016. 12. 9

PROTECTIVE EFFECT OF GRADED DENSITY ALUMINIUM FOAM ON RC SLAB UNDER BLAST LOADING – AN EXPERIMENTAL STUDY

Ye Xia, Chengqing Wu, Zhong-Xian Liu, Yuemin Yuan

Abstract

In recent decades, bomb incidents have significantly increased due to various blast accidents and growing terrorist threats. Therefore, the protection of important infrastructures against blast loading has never been more important. Aluminium foam, which is often used as a protective layer to absorb impact energy, has demonstrated its ability to mitigate blast effect in several studies. The outstanding energy absorption capacity of aluminium foam is mainly resulted from its long-lasting plateau stress region which allows it to only transmit a small stress (which is equal to the plateau stress) to the protected structure while absorbing the rest by self-compaction. For aluminium foam that is manufactured by the same method, the overall energy absorbing capacity per unit volume increases proportionally with mass density; however, the plateau stress also increases with density which means a larger stress would be transmitted to the protected structure. Therefore, there is a trade-off between the mass density and the transmitted stress. In order to increase the overall energy absorbing capacity of aluminium foam while keeping the transmitted stress at a reasonably low magnitude, the idea of density-graded foam has been proposed which is simply a foam structure with various densities along its thickness. In this paper, the effectiveness of density-graded foams has been investigated. A number of static compressive tests are conducted on different types of aluminium foams including aluminium foams with uniform density, density-graded aluminium foams with linear gradient as well as density-graded aluminium foams with unordered gradient. In addition, a blast test program is also carried out to investigate the blast mitigation effect of graded density foams on reinforced concrete (RC) slabs

1. Introduction

Aluminium foam is a cellular aluminium structure with gas-filled pores. The volume fraction of gas-filled pores determines the density of aluminium foam which also directly affects its strength. As a lightweight, low-cost, recyclable and energy absorptive material, aluminium foam has been widely used as a buffer material in areas such as airplanes, ships, cars, packaging and so on. In recent years, a number of studies have shown that using aluminium foam as a sacrificial cladding is an cost-effective means to mitigate blast effect as it does not require any renovation on the existing structures [1-10]. However, some studies also reported that, under some circumstances, aluminium foams along with other metallic foams can also lead to an adverse effect which amplifies the damage caused to the protected structure [11-14].

Layered structure with different densities is one of the most effective ways to increase the performance of aluminium foam against blast loading [15-18]. Ma and Ye [19] introduced a double-layered structure to improve the energy absorption capacity of foam cladding. It was found that the layered foam structure increased the maximum blast impulses that the claddings can withstand. In addition, their study also showed that foam clad- dings were able to absorb much more energy when they were subjected to high strain rate dynamic loading than quasi-static loading. Li et al. [20] numerically investigated aluminium foams with three different densities along its thickness under various impact velocities. The results indicated that, by increasing the impact velocity, the initial stress acting on the top of foam was increased; however, the stress transmitted to the protected structure still remained small which was solely determined by the plateau stress of foam at the bottom which was in direct contact with the protected structure. Further to the research conducted by Li [20], aluminium foams with four different densities along its thickness were also numerically studied [21]. It was reported that different density arrangements would result in different mitigation effect: the foam with linearly decreasing density from

top to bot- tom (the foam layer at the bottom is stuck with the protected structure) yielded the most reduction in deflection while the foam with the opposite density arrangement resulted in the least reduction.

In this paper, a series of field tests were carried out to investigate the effectiveness of using aluminium foam with graded density to protect RC slabs against blast loading. The results obtained by using density-graded foams are compared to those obtained by using foams with uniform density. In addition, different density arrangements of density-graded foams are also investigated in the test. The results of the blast testing are valuable for the study of graded density foam and for validations of the numerical models.

2. Quasi-Static Compressive Test of Aluminium Foams

It is well known that the overall energy absorption capacity of a sacrificial cladding is predominantly determined by the area enclosed by its stress–strain curve as shown in Fig.1. As aluminium foams normally have a very long region of plateau stress, the energy absorption capacity is thus mainly determined by the magnitude of the plateau stress. On the other hand, prior to an aluminium foam being fully compacted, the pressure transmitted through the foam to the protected structure is also determined by the magnitude of the plateau stress[22]. Therefore, the stress–strain curve of an aluminium foam cladding is the most significant and the most relevant to its effectiveness against blast loading.

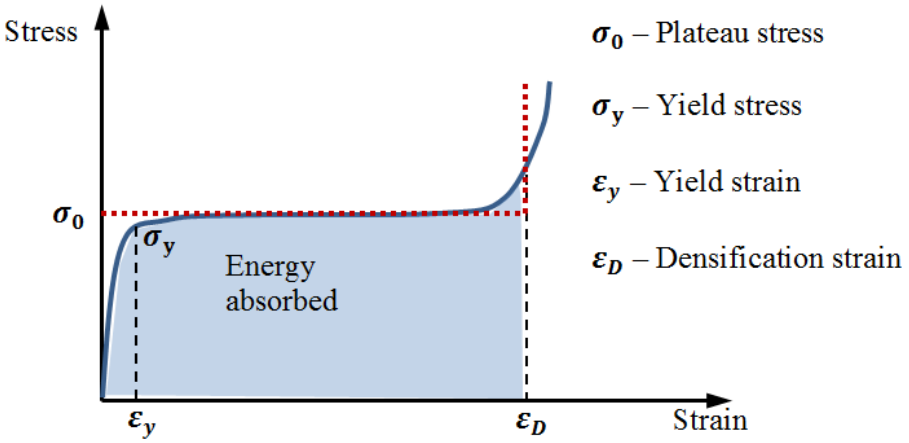

Figure 1. Typical stress-strain curve of an aluminium foam

To investigate the performance of density-graded aluminium foams, a variety of aluminium foams with different density arrangements were tested under static compressive tests. A number of 100 mm x 100 mm x 80 mm closed-cell aluminium foam specimens were compressed under a quasi-static condition at the speed of 10 mm/min (as shown in Fig. 2). Three types of aluminium foam specimens were studied including foams with uniform density, density-graded foams with linear density gradient, and density-graded foams with unordered density gradient. Apart from the foam specimens with uniform density, all other graded density foam specimens were made with four different aluminium foam layers attached by using epoxy, as shown in Fig. 3.

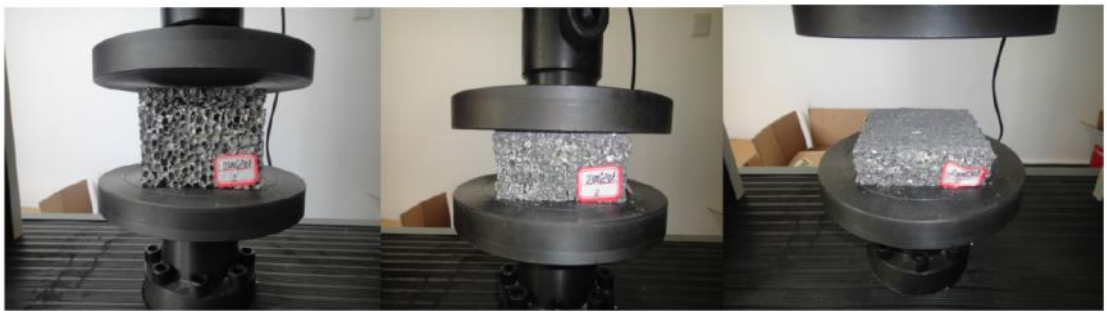

Figure 2. Static compressive test of aluminium foam specimens

Uniform density foam specimen

Graded density foam specimen

Figure 3. Cross-section of aluminium foam specimens

2.1 Uniform Density Foams

Five aluminium foam specimens with uniform density were tested in the static compressive test and the density of these specimens were ranged from 200 kg/m^3 to 500 kg/m^3. Table 1 summarises the material properties of all specimens. It should be mentioned

that, as a result of the manufacturing procedure, the density of these foam specimens inevitably had small variations along the thickness despite the manufacturers specifies that each foam layer has uniform density.

Table 1. Uniform density (UD) foam specimens

Type	UD200	UD250	UD300	UD400	UD500
Actual Density (kg/m^3)	196	257	330	398	526
Densification strain	0.59	0.56	0.56	0.58	0.50
Plateau Stress (MPa)	1.65	2.24	4.98	7.72	10.1

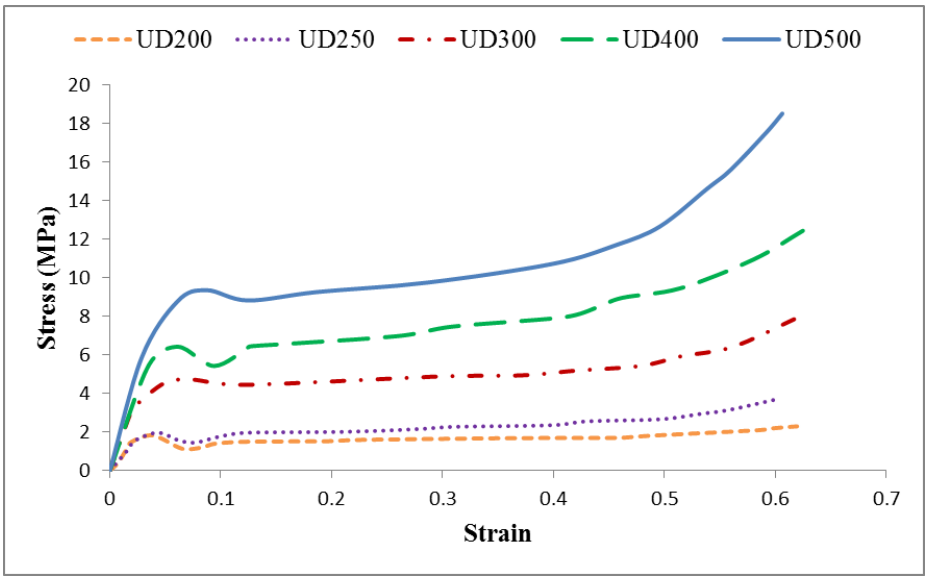

Figure 4. Stress-strain relationships of uniform density foam samples

Fig. 4 presents the stress–strain relationships of the aluminium foam specimens. It is evident that the plateau stress increases with density. Each foam specimen has an upper yield stress (σ_y) followed by its plateau stress (σ_0) region before reaching the densification strain (ε_D). Densification strain is determined from efficiency-strain curve according to the energy absorption efficiency equation from Li et al. [23]:

$$\eta(\varepsilon) = \frac{1}{\sigma(\varepsilon)} \int_{\varepsilon_y}^{\varepsilon} \sigma(\varepsilon) d\varepsilon \quad (1)$$

where η is energy absorption efficiency and ε_y is yield strain at the beginning of the plateau regime. The densification strain is the point where the energy absorption efficiency reaches the maximum on the efficiency-strain curve as illustrated in Fig. 5.

Please note that the starting point of efficiency in Fig. 5 starts from yield strain ε_y, hence, the curve does not start at the origin.

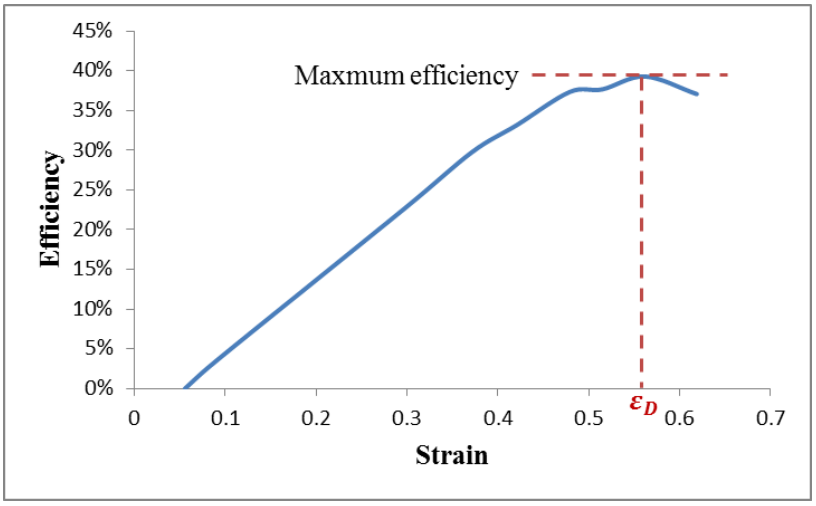

Figure 5. Efficiency-strain curve of foam sample UD300

Plateau stress not only indicates the strength of an aluminium foam, it also determines the pressure transmitted from the foam to the protected structure [2]. For aluminium foams with uniform density, the plateau stress can be calculated by the following equation [23]:

$$\sigma_0 = \frac{\int_{\varepsilon_y}^{\varepsilon_D} \sigma(\varepsilon) d\varepsilon}{\varepsilon_D - \varepsilon_y} \quad (2)$$

2.2 Linear Density Foams

As mentioned in the previous section, density-graded aluminium foam specimens with linear density gradient were manufactured by sticking four foam layers with different densities together as shown in Fig. 6. The details of each foam specimen are summarised in Table 2. The average density of each foam specimen was calculated so that they can be directly compared to their counterparts with uniform density. For example, foam specimen GD300G2.50A indicates that the average density of this foam is 300 kg/m^3 and the density gradient is 2.50 kg/m^3/mm along its thickness.It should be noted that, due to the complexity of the manufacturing process, it is difficult to keep every layer of the foam to

have the exact designed density gradient (i.e. GD300G2.5 and GD400G2.5). For easy comparison, approximate density gradients were listed in Table 2.

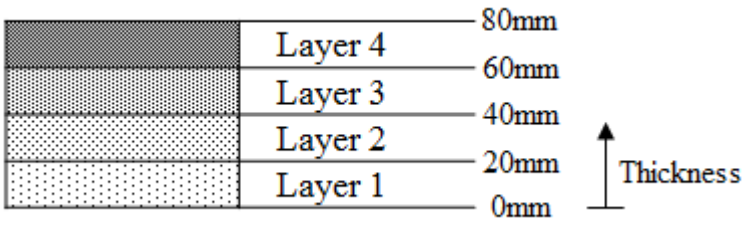

Figure 6. Configuration of graded foam specimens

Table 2. Density distributions of linear density foam samples

Type	Layer Density （kg/m3）				Approximate Average Density (kg/m3)	Approximate Density Gradient (kg/m3/mm)
	1	2	3	4		
GD300G2.50A	204	269	333	360	300	2.50
GD400G2.50A	327	355	431	463	400	2.50
GD300G1.25A	264	281	318	330	300	1.25
GD250G1.25A	215	230	261	293	250	1.25

Foam specimens with the same average density but different density gradients are compared in Figs. 7–9. Unlike the foams with uniform density, the foams with linear density gradient do not exhibit a very clear plateau region as the stress increased after yielding at a relatively steady rate. At the beginning of the compression process, the initial yield stress of the density-graded foam with linear gradient was significantly smaller than the uniform- density foam with the same average density. As the process continued, at a certain strain, the compressive stress of the density-graded foam exceeded that of the corresponding foam of uniform density. This phenomenon indicates that the density-graded foam with linear gradient was compacted from bottom to top, or in other words, from the layer of smaller density to the layer of higher density.

When the applied load is insignificant, only the layer of smaller density is compacted so that the transmitted pressure can remain small until the layer is fully compacted. On the contrary, if a more severe load is expected, the applied load can result in all layers of the foam being compacted so that the transmitted pressure is close to the plateau stress of the

foam layer with the highest density. In this way, the density-graded foam can adapt to more situations thanks to its variable plateau stress as opposed to the foam with uniform density which is only applicable to a certain situation due to the invariable plateau stress.

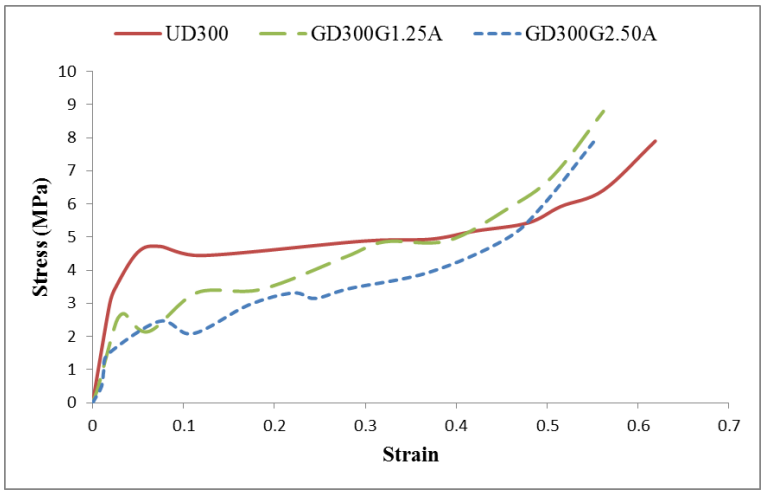

Figure 7. Stress-strain curves of foams with average density 300 kg/m^3 but different density gradients

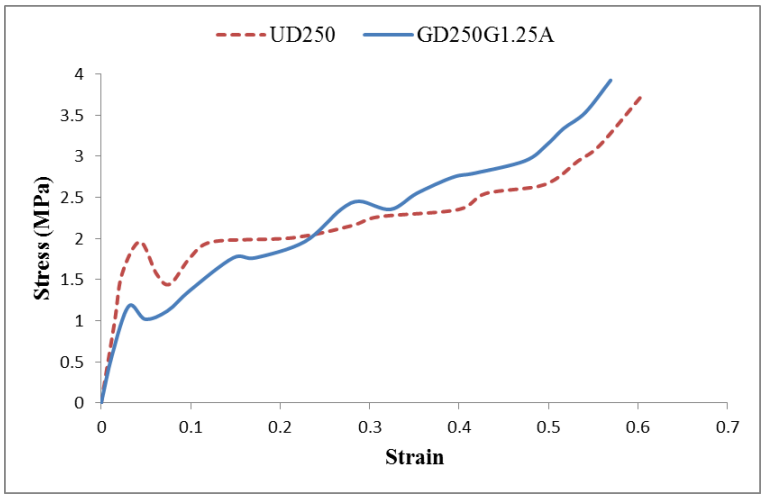

Figure 8. Stress-strain curves of foams with average density 250 kg/m^3 but different density gradients

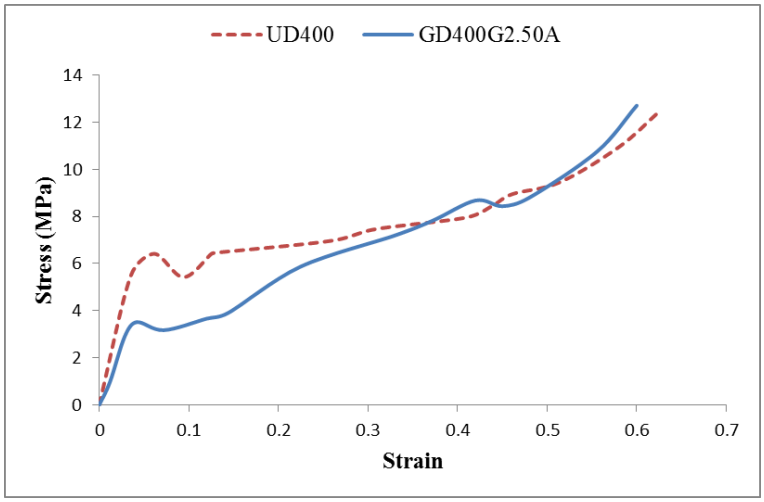

Figure 9. Stress-strain curves of foams with average density 400 kg/m^3 but different density gradients

In addition, foam specimens with the same initial density but different density gradients were also studied as shown in Figs. 10 and 11. It was found that the same initial density (layer 1) resulted in similar stress–strain curves from the beginning until the first yield point. After the initial layer (layer 1) was fully compacted, the graded-density foam exhibited a continuously growing stress, rather than a plateau region as in the foam with uniform density. In this case, the advantage of the density-graded foam is that its overall energy absorption capacity is larger than the foam with uniform density. Meanwhile, its transmitted pressure varies according to the applied load acting on the protected structure. Furthermore, Fig. 11 suggests that higher density gradient can enhance the energy absorption capacity as the slope of the stress–strain curve of the foam with higher density gradient was larger. However, it was also noticed that all density-graded foam specimens resulted in multiple crests in the stress–strain curves. This was because each foam specimen was manufactured by gluing four layers of foam together, which resulted in them yielding separately during static compressive tests. Therefore, in order to eliminate the influence of multiple crests, the density-graded foams with linear gradient used in the blast tests (discussed later in the paper) were directly manufactured as one whole piece, instead of four separate ones being glued together. The density-graded aluminium foam was manufactured by using titanium oxide as the foaming agent. Through chemical reaction, the titanium oxide can release hydrogen which was controlled by the temperature: higher the temperature, slower the rate of releasing hydrogen, thus smaller the density gradient.

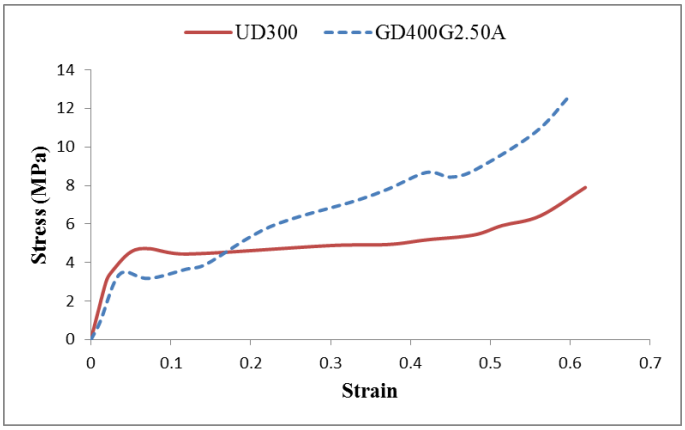

Figure 10. Stress-strain curves of foams with initial density 300 kg/m^3 but different density gradients

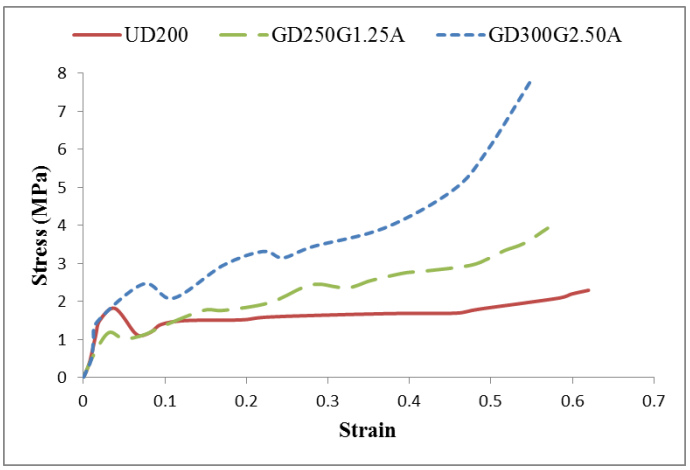

Figure 11. Stress-strain curves of foams with initial density 200 kg/m^3 but different density gradients

2.3 Unordered Density Foams

It has been mentioned in several studies that the order of density layers may affect the performance of density-graded foams [20, 21, 24]. To investigate the influence of density arrangement, the order of density layers in foam specimen GD300G2.50A (or GD300A) was altered into foams GD300B–GD300E as listed in Table 3. Due to the complexity of the manufacturing process, the average density of each specimen cannot be made exactly300 kg/m^3. However, since the density variation was very minimal, it is therefore assumed to have no influence on the results.

Table 3. Density distributions of unordered density foam samples

Type	Density (kg/m^3)				Average Density (kg/m^3)	
	Layer 1	Layer 2	Layer 3	Layer 4	Real	Idealised
GD300A	204	269	333	360	292	300
GD300B	280	225	328	350	296	300
GD300C	330	270	208	253	265	300
GD300D	366	207	326	266	291	300
GD300E	368	320	290	246	306	300

Figure 12 demonstrates the stress-strain curves of foam specimens GD300B – GD300E together with foam specimen UD300 and GD300A for comparison purpose. It is observed that all foam specimens with unordered density gradient yielded similar stress from original point until the strain reached around 0.3. Within this range, the stress of all

density-graded foams was lower than the plateau stress of UD300, which meant all density-graded foams were compacted from the layer with smaller density regardless of what density order was. However, according to Li [24], the impact speed can change the static mechanism of density-graded foams. In addition, Chang [21] suggested that the optimal structure of aluminium foam against blast loading should have a unordered density distribution based on the numerical model. Therefore, unordered foam GD300C and GD300E were also used in the blast experiment.

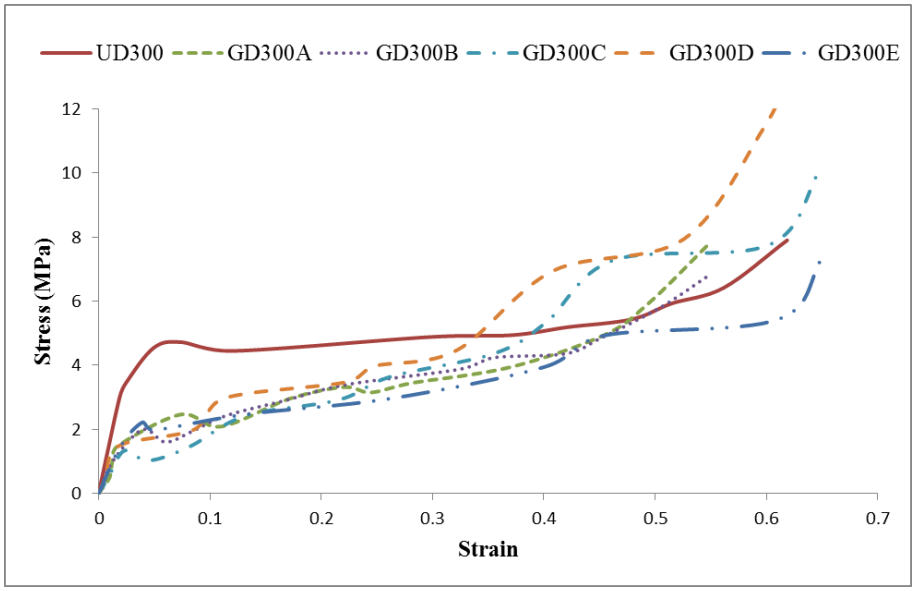

Figure 12. Stress-strain curves of unordered density foam samples

3. Blast Test of Foam-Protected RC Slabs

A blast test program was conducted to investigate the effectiveness of density-graded aluminium cladding against blast loading. The reinforced concrete (RC) slabs were made by the same formulae and mixing procedures for all events in the blast tests. The unconfined compressive strength of the concrete was 35 MPa while the yield strength of all reinforcing steel bars was 350 MPa. As demonstrated in Fig. 13, the dimension of the RC slab was 2000 mm long, 800 mm wide and 120 mm thick. Nine 12 mm steel bars were placed in the longitudinal direction and eleven 10 mm steel bars were placed in the transverse direction. Four strain gauges were attached to the longitudinal reinforcing bar as labelled by the cross markers in Fig. 13. A LVDT (square marker in Fig. 13) was located in

the centre of slabs to measure the displacement–time histories of all RC slabs. One pressure transducer (circular marker in Fig. 13) was placed on the RC slab of Event 1 to measure the blast pressure acting on the slab.

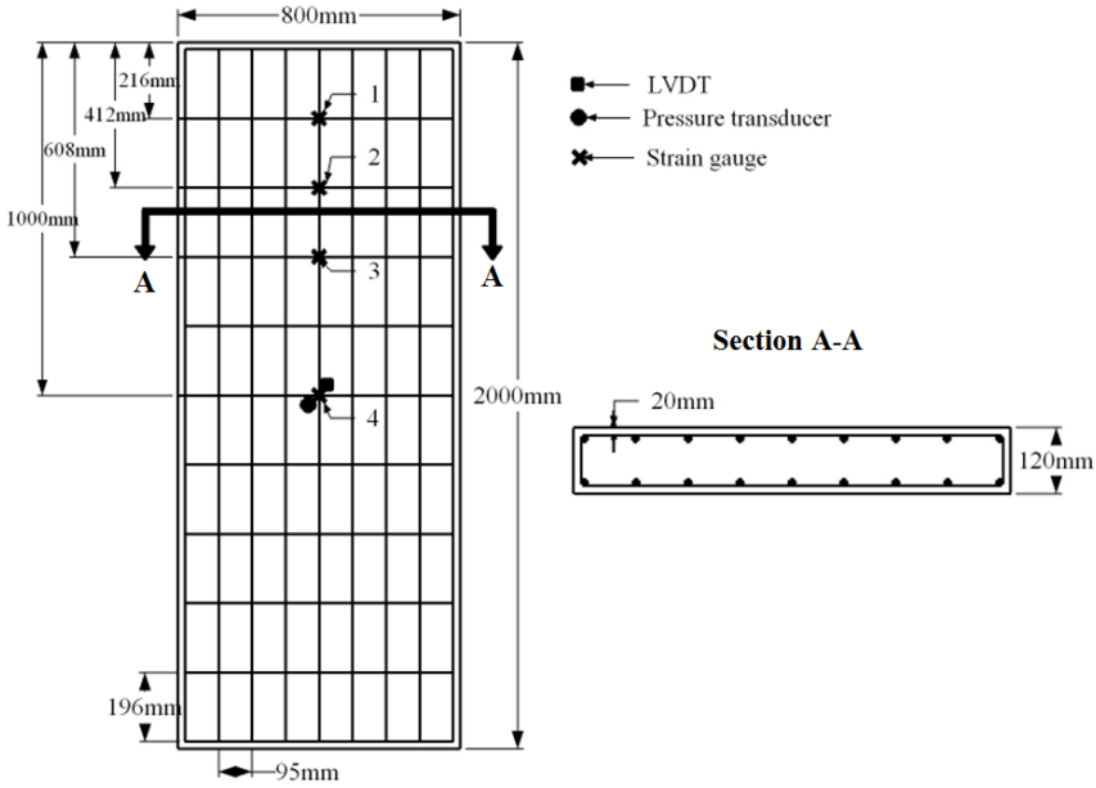

Figure 13. Configuration of RC slab

The experimental setup is presented in Fig. 14. An 8 kg cylindrical TNT charge was placed above the centre of the slab at a standoff distance of 1.5 m. The cylindrical charge was 225 mm in diameter and 120 mm in height. It should be mentioned that the cylindrical charge was placed vertically to the slab which resulted in a much larger blast load than if the charge was placed horizontally [25]. The steel support clamped both foam and RC slab at both ends.

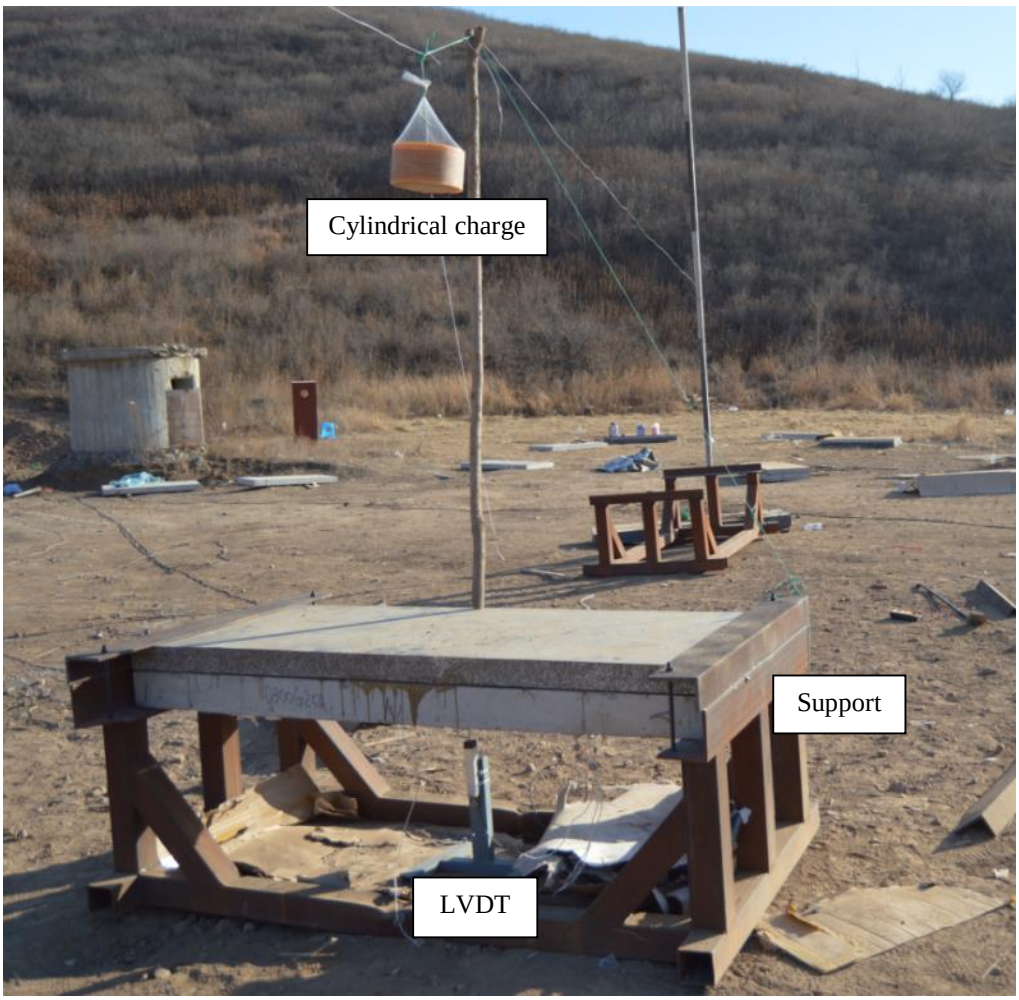

Figure 14. Setup of blast test

Table 4 summarises six blast events in the test program. As mentioned previously, the RC slabs and charges were made into the same dimensions in all events. The only difference was the aluminium foam cladding. Five 2000 mm x 800 mm x 80 mm aluminium foam panels with different density distributions were tested in Events 2–6. The detailed density distributions of the foam panels can be referred to Tables 1–3. The foam panels were attached to the RC slabs by epoxy. A steel cover plate was attached to each foam panel as shown in Fig. 15. According to Langdon et al. [26], the cover plate thickness could greatly influence the response of the aluminium foam cladding. On one hand, a thicker cover plate is able to result in the foam cladding being more uniformly compressed, thus unveiling the full potential of the energy absorbing capacity of the aluminium foam. However, on the other hand, a thicker cover plate greatly increase the total mass and stiffness of the structure which makes the structure naturally more resistant to blast loading

even without using any foam claddings. Since the current research mainly investigates the effectiveness of different aluminium foams under blast loading, a thin steel cover plate of 1.13 mm was used to eliminate the possible influence of the cover plate.

Table 4. Details of blast events

Event No.	Blast Properties			Foam Panel	
	Charge Weight (kg in TNT)	Standoff Distance (m)	Scaled Distance ($m/kg^{1/3}$)	Type	Thickness (mm)
1	8	1.5	0.75	-	-
2	8	1.5	0.75	UD300	80
3	8	1.5	0.75	GD300G2.50A	80
4	8	1.5	0.75	GD300G2.50C	80
5	8	1.5	0.75	GD300G2.50E	80
6	8	1.5	0.75	GD400G2.50A	80

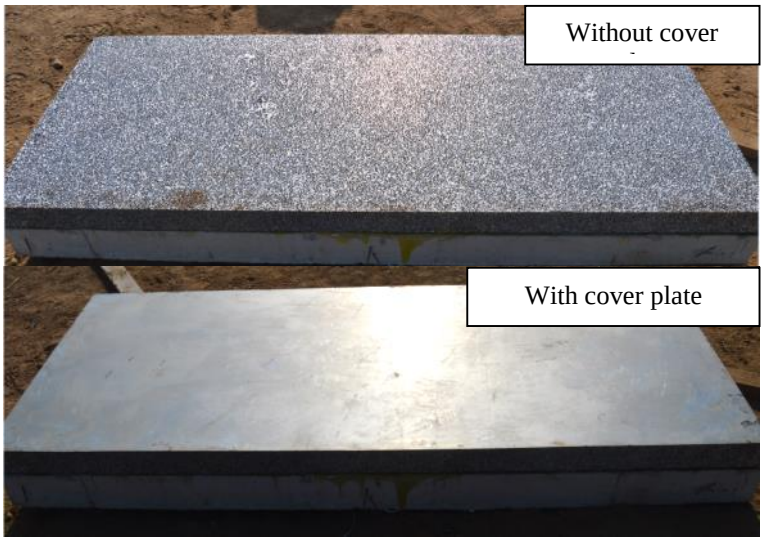

Figure 15. Foam panel without and with cover plate

3.1 Event 1

Event 1 served as a control event, the RC slab was not protected. A pressure transducer (as shown in Fig. 16(a)) was placed at the centre of the slab in Event 1 to measure the blast pressure. However, as mentioned previously, the charge was placed vertical to the slab, resulting in the blast pressure significantly exceeding the capacity of the pressure transducer as shown in Fig. 17. There- fore, this paper did not discuss the

pressure–time history in great details. Fig. 16(b) shows that the RC slab in Event 1 completely failed with a permanent deflection of 19 cm which as manually measured after the test. The deflection-time history from LVDT is depicted in Fig. 18 and the peak deflection of the RC slab was 25.1cm.

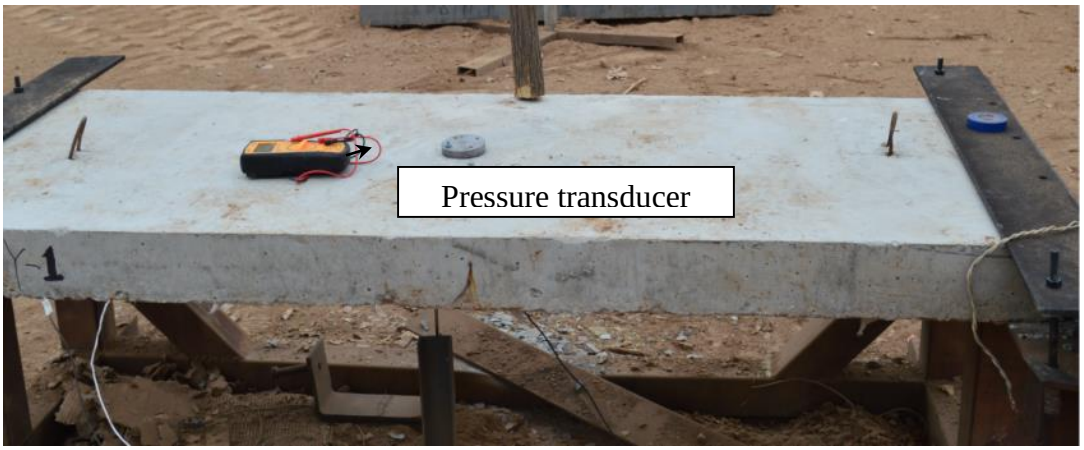

(a). RC slab before explosion

b). RC slab after explosion

Figure 16. Event 1 – Unprotected RC slab

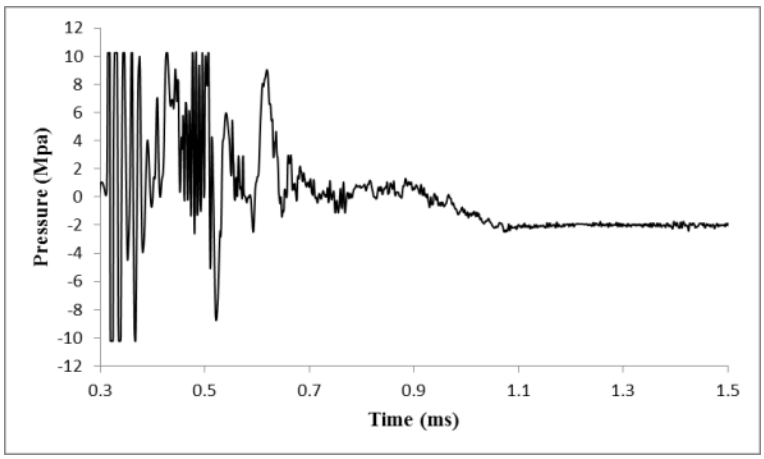

Figure 17. Pressure-time diagram of the blast test

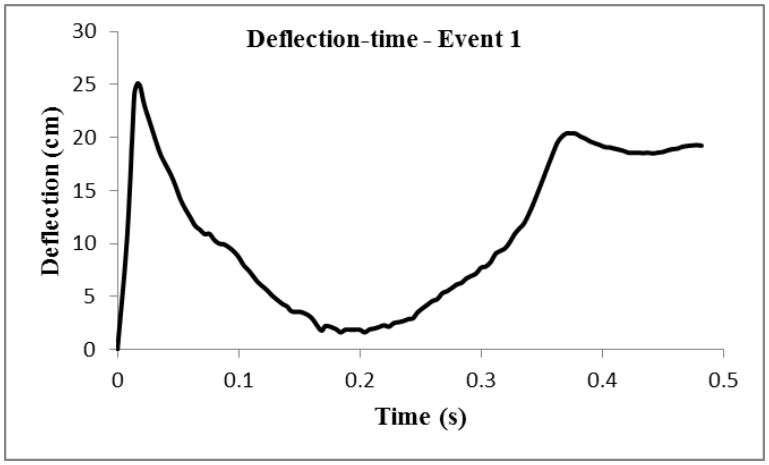

Figure 18. Deflection-time history of RC slab in Event 1

3.2 Event 2-6

RC slabs used in Events 2–6 were all protected by aluminium foams of different types, the details of each event can be referred to Tables 3 and 5. Fig. 19 depicts the deflection–time histories of Events 2–6 and Fig. 20 compares the deflection–time histories for all 6 events. The LVDTs of Events 3, 5 and 6 failed to get the permanent displacements. For Events 1, 2 and 4, the deflection–time histories are extended to show the permanent displacements. It can be seen that the LVDT readings are very close to the manual measurements.

Table 5. Summary of the results for blast test

Event No.	Foam type	Peak deflection		Permanent deflection	
		Result (cm)	Reduction	Result (cm)	Reduction
1	N.A.	25	-	19	-
2	UD300	19	24%	14	26%
3	GD300G2.50A	19	24%	12	37%
4	GD300C	20	20%	15	21%
5	GD300E	23	8%	17	11%
6	GD400G2.50A	22	12%	11	42%

With regard to the peak deflections at mid-span, the uniform- density foam UD300 and the density-graded foam GD300G2.50A were most effective in reducing the peak deflection. This is because the total energy absorption capacity of UD300 and GD300G2.50A were similar (the area enclosed by the stress–strain relationship were similar). In addition, apart from GD300E, all foams with an average density of 300 kg/m^3 were able to reduce more peak deflection than D400G2.50A which was with an average density of 400 kg/m^3. This might be due to the foams with smaller density having a lower stress–strain curve, thus transmitting a smaller pressure to the RC slab.

As for permanent deflection, it was found that foam GD400G2.50A yielded the best result with a 42% reduction. The higher foam density results in a higher overall energy absorption capacity which, in return, provides a larger reduction in the permanent deflection. At the same time, the higher density foam also results in a larger pressure transmitted to the RC slab which may be the reason why the peak deflection in Event 6 was not the lowest. Moreover, the graded-density foam GD300G2.50A yielded better results than the uniform-density foam UD300 in regards to permanent deflections. This might be because the continuously ascending stress ensured that the transmitted pressure on the slab was gradually increased until the foam is fully compacted, as a result, the final permanent deflection in Event 3 was a bit smaller than that in Event 2. Furthermore, foam GD300E had the worst protection based on both peak and permanent deflections. The decreasing density from the bottom of the top has an adverse effect on the aluminium foam as a protective cladding, which agrees well with the findings in Li [24] and Chang [21].

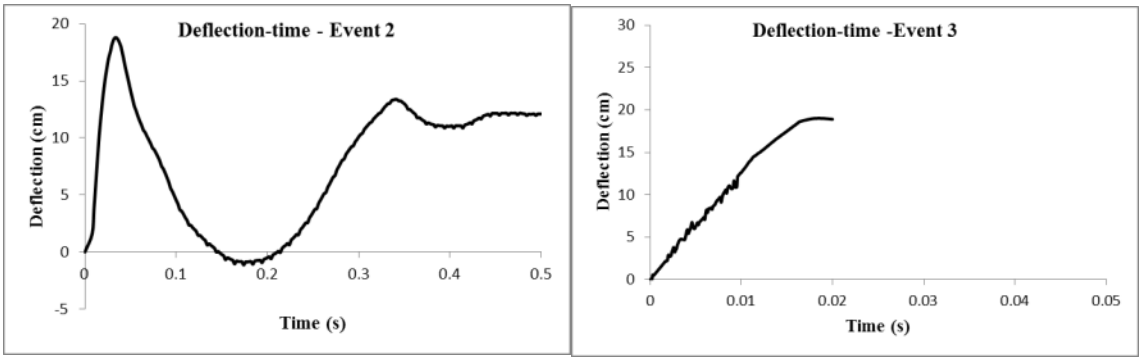

(a) (b)

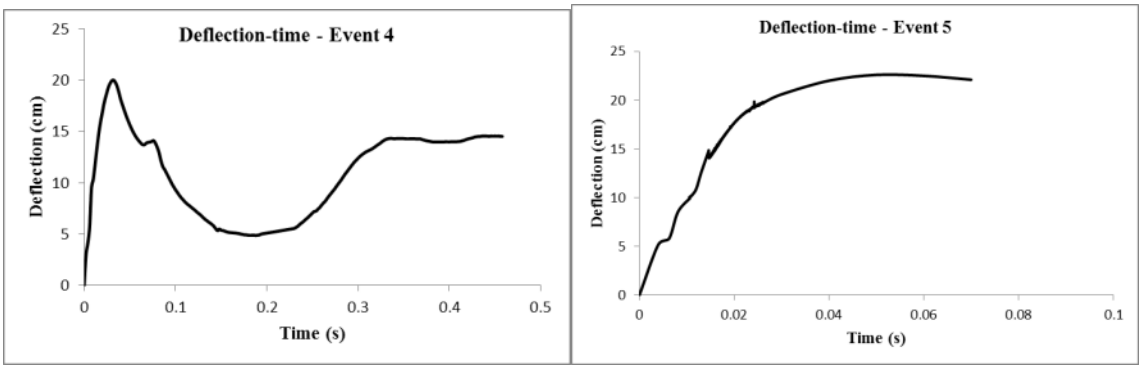

(c) (d)

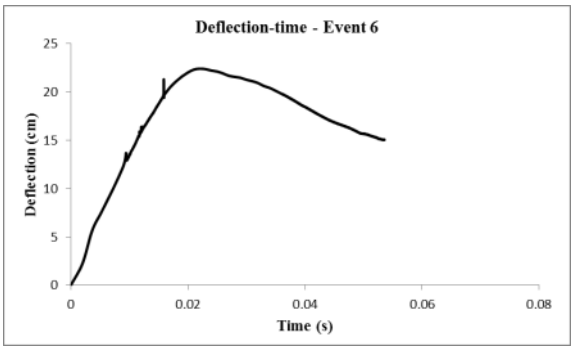

(e)

Figure 19. Deflection-time history of RC slab in Events 2-6

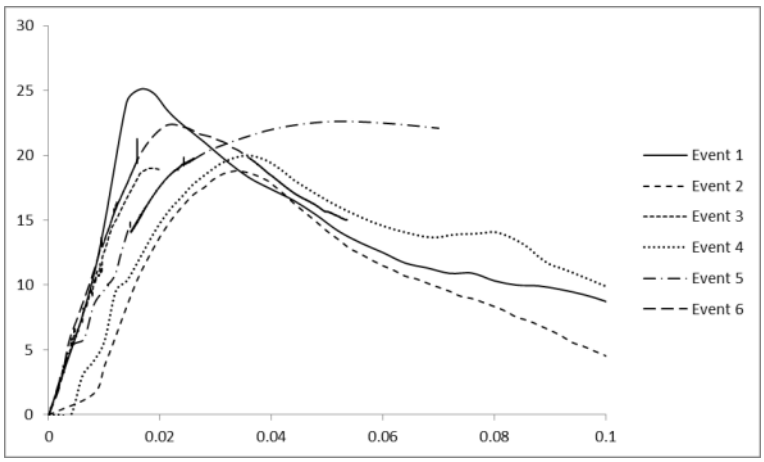

Figure 20. Comparison of deflection-time histories

Fig. 21 shows the failure modes of RC slabs in Events 2–6. The damage on the steel plate indicated only a circular area around the centre of the slab was severely damaged.

This suggests that the blast load resulted from a close range detonation, was more concentrated on a small area rather than being uniformly distributed over the slab. It may have significantly compromised the effectiveness of using aluminium foam as sacrificial cladding whose sole means of mitigating blast energy is through self-compression; however, in this case, a large part of it remained uncompressed. Although the tests may have not yet unveiled the full energy absorbing potential of aluminium foam, some evident improvements over the unprotected slab in Event 1 can be still observed. In addition to the reduction in peak and permanent deflection as discussed previously, the aluminium foam protected slab experienced less spalling damage under blast loads compared to the unprotected one. For instance, for Events 2, 3 and 6 where good mitigation effect was achieved, the RC slabs were still intact after the explosion with only a few major cracks forming near the mid-span whereas, for Event 1, the concrete at the same location spalled completely.

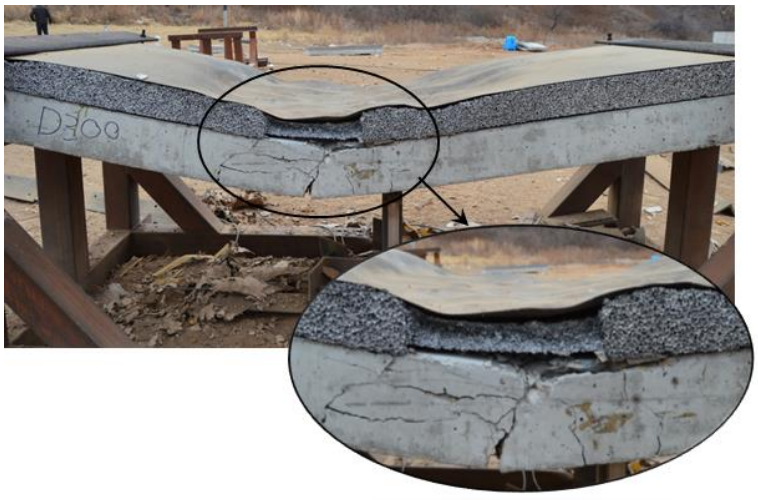

(a) Event 2

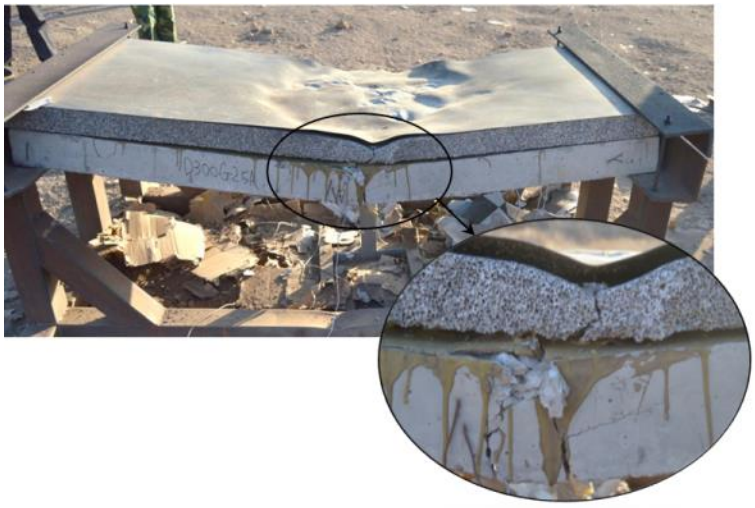

(b) Event 3

(c) Event 4

(a). Foam-protected RC slab after explosion

(b). Fractured foam

(c). Fractured cover plate and concrete

(d) Event 5

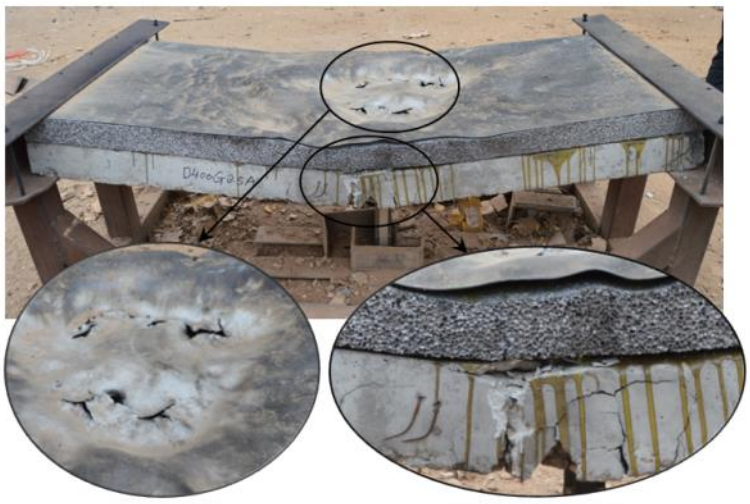

(e) Event 6

Figure 21: Failure modes of events 2-6

3.3 Strain-time histories

The strain–time histories were recorded by strain gauges with an effective length of 5 mm. The strain gauges were placed on the reinforcement bars so that the longitudinal strain can be measured. The data was collected by a high-speed data collecting system with a sampling interval of 0.001 ms.

As shown in Figure 22 that the oscillation period of strain-time histories of all test specimens was significantly smaller than the corresponding oscillation period of structural response as depicted in Figure 20. This suggests that the measured strain-time histories were mainly caused by the shock wave of blast loads long before the structure began to deform. The shock wave travelled through and bounced back to the slab so fast that there was no time to develop global response initially. The strain rate of each event can be derived by simply differentiate the strain-time history. It was found that the strain rates of all events were beyond 15000/s which also suggests that it was caused by the shock wave rather than the structural response.

Since the initial peak strains of all strain-time histories exceeded the measurement range, for comparison purpose, Table 6 lists the second peak strains of strain gauge 4 of all events. It is evident that for foam-protected slab were significantly smaller than the

unprotected slab. This confirms that the foam cladding can effectively absorb the incoming blast energy.

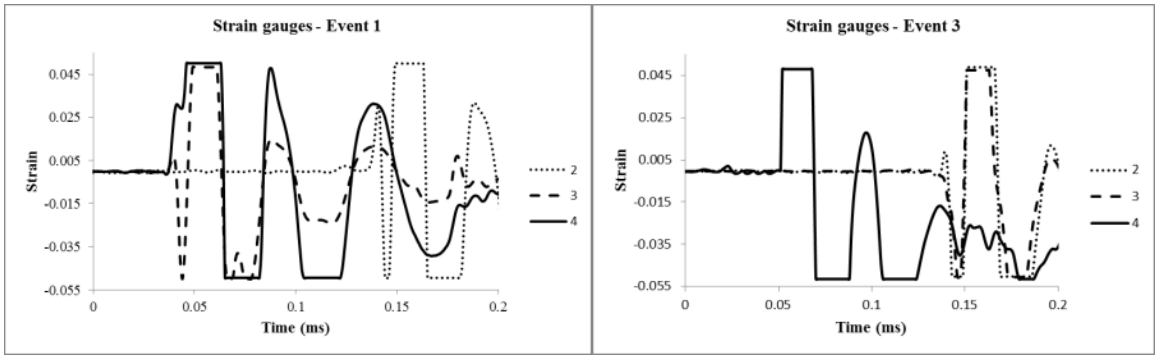

(a) Event 1

(b) Event 3

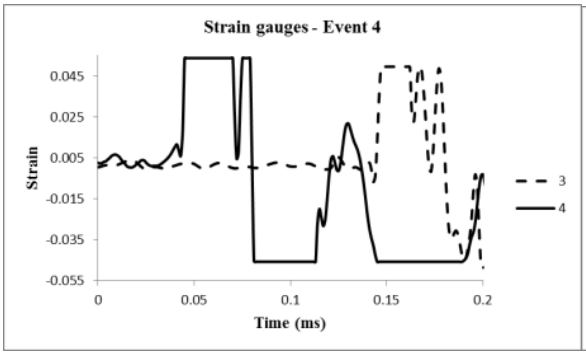

(c) Event 4

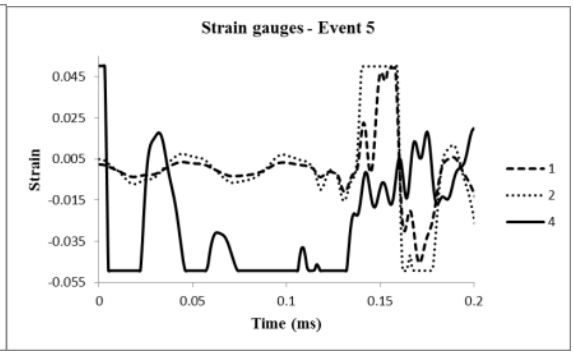

(d) Event 5

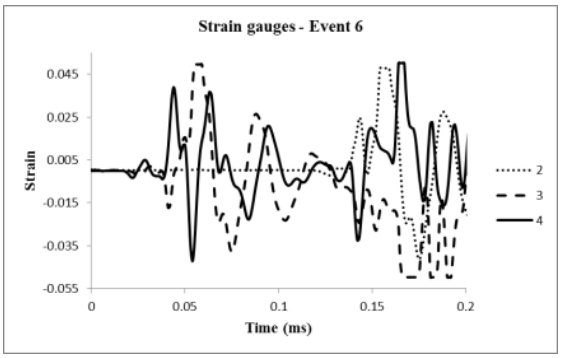

(e) Event 6

Figure 22. Strain-time histories for test specimens

Table 6: Comparison of strain values

Event	**Second positive peak**	
	Strain	Reduction
1	0.0475	-
3	0.0172	64%
4	0.0212	55%
5	0.0173	64%
6	0.0367	23%

4. Conclusion

This paper aims to investigate the protective effectiveness of density-graded foams. A series of aluminium foams with different density distributions were tested under static compression as well as blast loading. It was found that the linear density gradient offers an increasing stress–strain curve, rather than a plateau region as found in foams with uniform density. Although foams of the same average density, regardless of their density arrangements, have similar energy absorption capacity, the lower initial stress of density-graded foams can guarantee a smaller blast pressure transmitted to the protected structure under moderate blast loading. The blast test results indicate that aluminium foam is capable of mitigating blast effects on the protected RC slabs and the density gradient can significantly affect its effectiveness. It was found in the blast tests that the ascending density from bottom to top can improve the blast resistance of the foam compared to the foam with uniform density. In contrast, the descending density can decrease the effectiveness of the foam.

Acknowledgements

The research presented in this paper jointly supported by the ARC Discovery Grant DP140103025, the National Natural Science Foundation of China under Grants 51278326 and 51238007 are gratefully acknowledged.

References

[1] Schenker, A, Anteby, I, Nizri, E, Ostraich, B, Kivity, Y, Sadot, O, Haham, O, Michaelis, R, Gal, E, and Ben-Dor, G, *Foam-protected reinforced concrete structures under impact: Experimental and numerical studies.* Journal of Structural Engineering, 2005. **131**(8): p. 1233-1242.

[2] Ye, Z and Ma, G, *Effects of foam claddings for structure protection against blast loads.* Journal of Engineering Mechanics, 2007. **133**(1): p. 41-47.

[3] Su, Y, Wu, C, and Griffith, M, *Mitigation of blast effects on aluminum foam*

protected masonry walls. Transactions of Tianjin University, 2008. **14**(1): p. 558-562.

[4] Schenker, A, Anteby, I, Gal, E, Kivity, Y, Nizri, E, Sadot, O, Michaelis, R, Levintant, O, and Ben-Dor, G, *Full-scale field tests of concrete slabs subjected to blast loads.* International Journal of Impact Engineering, 2008. **35**(3): p. 184-198.

[5] Zhu, F, Zhao, L, Lu, G, and Wang, Z, *Structural response and energy absorption of sandwich panels with an aluminium foam core under blast loading.* Advances in Structural Engineering, 2008. **11**(5): p. 525-536.

[6] Wu, C, Huang, L, and Oehlers, DJ, *Blast testing of aluminum foam–protected reinforced concrete slabs.* Journal of Performance of Constructed Facilities, 2010. **25**(5): p. 464-474.

[7] Wu, C and Zhou, Y, *Simplified analysis of foam cladding protected reinforced concrete slabs against blast loadings.* International Journal of Protective Structures, 2011. **2**(3): p. 351-366.

[8] Merrett, R, Langdon, G, and Theobald, M, *The blast and impact loading of aluminium foam.* Materials & Design, 2013. **44**: p. 311-319.

[9] Wu, C and Sheikh, H, *A finite element modelling to investigate the mitigation of blast effects on reinforced concrete panel using foam cladding.* International Journal of Impact Engineering, 2013. **55**: p. 24-33.

[10] Xia, Y, Wu, C, and Li, Z-X, *Optimized design of foam cladding for protection of reinforced concrete members under blast loading.* Journal of Structural Engineering, 2014.

[11] Hanssen, A, Enstock, L, and Langseth, M, *Close-range blast loading of aluminium foam panels.* International Journal of Impact Engineering, 2002. **27**(6): p. 593-618.

[12] Li, Q and Meng, H, *Attenuation or enhancement—a one-dimensional analysis on shock transmission in the solid phase of a cellular material.* International Journal of Impact Engineering, 2002. **27**(10): p. 1049-1065.

[13] Hohe, J, Hardenacke, V, Fascio, V, Girard, Y, Baumeister, J, Stöbener, K, Weise, J, Lehmhus, D, Pattofatto, S, and Zeng, H, *Numerical and experimental design of graded cellular sandwich cores for multi-functional aerospace applications.* Materials & Design, 2012. **39**: p. 20-32.

[14] Xia, Y, Wu, C, Zhang, F, Li, Z-X, and Bennett, T, *Numerical analysis of foam-protected RC members under blast loads.* International Journal of

Protective Structures, 2014. **5**(4): p. 367-390.

[15] Beals, J and Thompson, M, *Density gradient effects on aluminium foam compression behaviour.* Journal of Materials Science, 1997. **32**(13): p. 3595-3600.

[16] Brothers, AH and Dunand, DC, *Mechanical properties of a density-graded replicated aluminum foam.* Materials Science and Engineering: A, 2008. **489**(1): p. 439-443.

[17] Cui, L, Kiernan, S, and Gilchrist, MD, *Designing the energy absorption capacity of functionally graded foam materials.* Materials Science and Engineering: A, 2009. **507**(1): p. 215-225.

[18] Zhang, X and Zhang, H, *Optimal design of functionally graded foam material under impact loading.* International Journal of Mechanical Sciences, 2013. **68**: p. 199-211.

[19] Ma, G and Ye, Z, *Energy absorption of double-layer foam cladding for blast alleviation.* International Journal of Impact Engineering, 2007. **34**(2): p. 329-347.

[20] Li, J, Ma, G, Zhou, H, and Du, X, *Energy absorption analysis of density graded aluminium foam.* International Journal of Protective Structures, 2011. **2**(3): p. 333-350.

[21] Chang, Q, Li-jun, Y, and Shu, Y, *Simulation and optimization of blast-resistant performance of graded aluminum foam sandwich structures.* Journal of Vibration and Shock, 2013. **32**(13): p. 70-75.

[22] Mazor, G, Ben-Dor, G, Igra, O, and Sorek, S, *Shock wave interaction with cellular materials.* Shock Waves, 1994. **3**(3): p. 159-165.

[23] Li, Q, Magkiriadis, I, and Harrigan, J, *Compressive strain at the onset of densification of cellular solids.* Journal of Cellular Plastics, 2006. **42**(5): p. 371-392.

[24] Li, JD, Zhou, HY, and Ma, GW, *Numerical simulation of blast mitigation cladding with gradient metallic foam core.* Applied Mechanics and Materials, 2011. **82**: p. 461-466.

[25] Wu, C, Fattori, G, Whittaker, A, and Oehlers, DJ, *Investigation of air-blast effects from spherical-and cylindrical-shaped charges.* International Journal of Protective Structures, 2010. **1**(3): p. 345-362.

[26] Langdon, G, Karagiozova, D, Theobald, M, Nurick, G, Lu, G, and Merrett, R, *Fracture of aluminium foam core sacrificial cladding subjected to air-blast*

loading. International Journal of Impact Engineering, 2010. **37**(6): p. 638-651.

Chapter 5 - An Analytical Model of Linear Density Foam Protected Structure under Blast Loading

Statement of Authorship

Title of Paper	An Analytical Model of Linear Density Foam Protected Structure under Blast Loading
Publication Status	☐ Published ☐ Accepted for Publication ☐ Submitted for Publication ☑ Unpublished and Unsubmitted work written in manuscript style
Publication Details	N.A.

Principal Author

Name of Principal Author (Candidate)	Ye Xia		
Contribution to the Paper	Developed the model, processed and analysed the data, and wrote the manuscript.		
Overall percentage (%)	85%		
Certification:	This paper reports on original research I conducted during the period of my Higher Degree by Research candidature and is not subject to any obligations or contractual agreements with a third party that would constrain its inclusion in this thesis. I am the primary author of this paper.		
Signature		Date	

Co-Author Contributions

By signing the Statement of Authorship, each author certifies that:

i. the candidate's stated contribution to the publication is accurate (as detailed above);

ii. permission is granted for the candidate in include the publication in the thesis; and

iii. the sum of all co-author contributions is equal to 100% less the candidate's stated contribution.

Name of Co-Author	Chengqing Wu		
Contribution to the Paper	Supervised development of the work and helped in manuscript evaluation.		
Signature		Date	24/11/2016

Name of Co-Author	Terry Bennett		
Contribution to the Paper	Helped to evaluate and edit the manuscript.		
Signature		Date	19/12/2016

AN ANALYTICAL MODEL OF LINEARLY GRADED FOAM PROTECTED STRUCTURE UNDER BLAST LOADING

Ye Xia, Chengqing Wu, and Terry Bennett

Abstract

Aluminium foam is widely known as an energy absorptive material which can be used as a protective cladding on structures to enhance the blast resistance of the protective structure. Previous studies show that higher density gives larger energy absorption capacity of aluminium foam, but results in a larger transmitted pressure to the protected structure. To lower the transmitted pressure without sacrificing the maximum energy absorption, graded density foam has been examined in this study. An analytical model is developed in this paper to investigate the protective effect of linearly graded foam on the response of a structure under blast loading. The model is able to simulate structural deformation with reasonable accuracy compared with experimental data. The sensitivity of density gradient of foam cladding on RC structure is tested in the paper.

1. Introduction

As a protective material, aluminium foam claddings are able to mitigate blast effect on the protected structures by absorbing a significant amount of kinematic energy [1-4]. The outstanding energy absorption capacity of aluminium foams is contributed by the cellular structure with gas-filled pores which provides a plateau of stress after deformation. The volume proportion determines the density and strength of aluminium foams which directly affect the protective performance. When blast load is applied, the foam cladding will absorb a significant amount of energy and transfer the intensive load into a much lower pressure with a longer duration onto the protected structure. Theoretically, the plateau stress of the foam is equal to the pressure transmitted from the foam onto the target structure [5]. Since the plateau stress exhibits a power law function with density [1, 6], the

density of the aluminium foam is one of the key properties when designing protective cladding.

As demonstrated by the natural density-graded bone and wood, grading the density of foam cladding may be an effective method to increase the protective effectiveness and efficiency. According to several numerical studies in regard to double, triple and quadruple layers of aluminium foams [7-9], it appeared that under dynamic loading, density-graded foams with decreasing density from loaded end to protected end outperform homogeneous foams with the same average density. When dynamic loading is applied, the low-density layer at the bottom, which is in direct contact with the protected structure, will transmit a relatively lower pressure to the structure compared with homogenous foam with same average density. As a result, the deformation of the protected structure against blast loading can be smaller.

Techniques have been developed to manufacture continuously graded density aluminium foams [10-13], which allows experiments to be undertaken. Similar to the findings from the aforementioned numerical studies, experimental results showed that the density gradient increases the slope of the plateau stress range of the foam [14-16]. This means that the transmitted pressure onto the protected structure will depend on how the graded density foam deforms, rather than a constant plateau stress of homogenous foam. For example, if the blast load is relatively small and only the lower-density part of the foam is compacted, the transmitted pressure will be the strength of the lower-density foam, which is smaller than the plateau stress of the homogeneous foam with the same average density. On the other hand, when the blast load is high enough to fully compact the entire graded density foam, the transmitted pressure will depend on the foam density which is densified at last. Researchers have found that graded density foam will always deform from the loaded end gradually through the thickness regardless the density distribution if the loading velocity is large enough [8, 17, 18]. Hence, theoretically, decreasing the foam

density from loaded end to protected end will improve the protective effectiveness of foam cladding. Furthermore, a series of blast tests conducted by Xia [16] also indicates that the foam with decreasing density from loaded end protects the reinforced concrete (RC) slab better than uniform density foam.

Using analytical model is a convenient and economical method in investigating the protective effect of aluminium foam against blast loading. The one-dimensional shock wave theory has been verified numerically and experimentally in the analysis of aluminium foam under blast loading [1, 5, 19, 20]. Based on the shock wave theory and single degree of freedom theory, loading-cladding-structure models have been developed to predict the response of structural members with homogeneous foam cladding [3, 20]. Recently, a theoretical model of continuous graded density foam under blast loading was established by Zhou et al. [21]. In this model, the foam density was designed as a decreasing exponential function and the study concludes that the density gradient makes foam densify slower [21]. However, no foam-structure interaction was considered in this theoretical model.

In the current research, an analytical model is developed to investigate the protective effect of linearly graded foam on the structure under blast loading. The model is verified by blast experimental results conducted by Xia [16]. Additionally, a case study is carried out to test the influence of linear density gradient on reducing the peak deflection of protected RC slab.

2. Derivation of analytical model

The blast pressure considered in the model is simplified as a triangular pulse and uniformly acts on the cover plate of the foam cladding, which is expressed by equation (1):

$$P(t) = \begin{cases} P_0\left(1 - \frac{t}{t_d}\right) & t \le t_d \\ 0 & t > t_d \end{cases}$$

where P_0 is the initial peak pressure of the blast and t_d is the duration of the blast load.

For linearly graded foam, the density can be calculated with the distance x along the thickness:

$$\rho(x) = \rho_0 - \left(\frac{\rho_0 - \rho_L}{L}\right) x$$

where ρ_0 is the initial density contacted with cover plate; ρ_L is the final density attached on the structure; and L is the thickness of the foam cladding.

The analytical model in this paper is developed based on shock wave theory [19] which assumes that the foam deforms gradually from the loaded end through the cross-sectional direction under blast load as illustrated in Figure 1. The foam is idealised as a rigid-perfectly plastic-locking (RPPL) material with a plateau stress σ_{pl} and a densification stress σ_D as shown by Figure 1. The plateau stress and densification stress of graded density foam are written as functions of foam density which is calculated by the location of shock front:

$$\sigma_{pl} = C_1 \left(\frac{\rho}{\rho_s}\right)^{2/3} \sigma_{ys}$$

$$\sigma_D = \sigma_{pl} + \frac{\rho}{\varepsilon_D}(\dot{u} - \dot{y})^2$$

where ρ_s is the density of the base material of the foam; C_1 is a material constant; σ_{ys} is the compressive yield strength of the base material; $\dot{u}$ is the velocity of cover plate which moves together with the loaded face of the foam cladding. Cover plate is commonly used in the applications of protective foam cladding to distribute the blast pressure uniformly on the foam and avoid disintegrating; $\dot{y}$ is the velocity of the protected structure; the densification strain of the foam ε_D is expressed as:

$$\varepsilon_D = 1 - \lambda\frac{\rho}{\rho_s}$$

where λ is a material constant.

The mass of the densified part of the foam cladding can be calculated by the product of densified foam mass and densified foam volume:

$$\Delta m = \rho_* A(s - u + y)$$

where A is the loading area of the foam cladding which is equal to the loading area of the RC structure; s is the progressive location of the shock front in the foam from the loaded end; u is the displacement of the cover plate which is the same as the displacement of the densified foam; y is the displacement of protected structure; and the density of the fully densified foam ρ_* is written as:

$$\rho_* = \frac{\rho}{1-\varepsilon_D}$$

$$= \frac{\rho_s}{\lambda}$$

When considering the density of the originally undeformed foam $\rho(x)$ and the location of shock front s, the mass of the densified part of the foam cladding also can be calculated by the following equation due to the mass conservation:

$$\Delta m = A\int_0^s \rho(x)dx$$

$$= \rho_0 As$$

$$-\left(\frac{\rho_0-\rho_L}{2L}\right)As^2 \qquad (8)$$

Equating Equations (6) and (8), the displacement of the cover plate, can be ascertained in a function of the shock front location:

u

$$= \mathrm{s} + \mathrm{y} - \frac{\lambda\rho_0}{\rho_s}s$$

$$+\frac{\lambda}{\rho_s}\left(\frac{\rho_0-\rho_L}{2L}\right)s^2 \qquad (9)$$

With initial conditions $u_0 = 0$ and $\dot{u}_0 = 0$, the velocity and acceleration of the cover plate, can be obtained by differentiating Equation (9):

$\dot{u}$

$$= \dot{s} + \dot{y} - \frac{\lambda\rho_0}{\rho_s}$$

$$+\frac{\lambda(\rho_0-\rho_L)}{\rho_s L}s \qquad (10)$$

$\ddot{u}$

$$= \ddot{s} + \ddot{y}$$

$$+\frac{\lambda(\rho_0-\rho_L)}{\rho_s L}$$

The system of the densified foam with the cover plate in Figure 1 is considered as a single degree of freedom system where damping is ignored. The dynamic equation of motion is written as:

$$(m_l + \Delta m)\ddot{u} + [\sigma_D - P(t)]A = 0 \quad (12)$$

where m_l is the mass of cover plate. Substituting Equations (2)-(4) and (8)-(11), into Equation (12), the dynamic equation of equilibrium can be written as:

$$\left[m_l - \left(\frac{\rho_0 - \rho_L}{2L}\right)As^2 + \rho_0 As\right]\left[\ddot{s} + \ddot{y} + \frac{\lambda(\rho_0 - \rho_L)}{\rho_s L}\right] + \left[C_1\left(\frac{\rho(s)}{\rho_s}\right)^{\frac{2}{3}}\sigma_{ys} + \frac{\rho(s)}{1 - \lambda\frac{\rho(s)}{\rho_s}}\left(\dot{s} + \frac{\lambda(\rho_0 - \rho_L)}{\rho_s L}s - \frac{\lambda\rho_0}{\rho_s}\right)^2 - P(t)\right]A = 0$$

The motion equation of the system of the undeformed foam with protected structure (as shown in Figure 1) can be expressed as:

$$\left(m_f - \Delta m + m_{se}\right)\ddot{y} + R(y) - \sigma_{pl}A = 0 \quad (14)$$

where m_f is the mass of foam cladding; m_{se} is the equivalent mass of the protected structure; and $R(y)$ is the resistance function of the structure. Taking the Equations (3) and (8) into account, Equation (14) can be rewritten as:

$$\left[m_f + \left(\frac{\rho_0 - \rho_L}{2L}\right)As^2 - \rho_0 As + m_{se}\right]\ddot{y} + R(y) - C_1\left(\frac{\rho}{\rho_s}\right)^{\frac{2}{3}}\sigma_{ys}A = 0 \quad (15)$$

From the simultaneous nonlinear differential Equations (13) and (15), the deflection of the protected structure y can be solved by using the fourth-order Runge-Kutta method with initial conditions $s_0 = 0,\ y_0 = 0,\ \dot{s}_0 = 0, \dot{y}_0 = 0$.

The current analytical model is only applicable when satisfying the Shock Wave Theory. Researchers have proved that sufficient impact velocity will make the graded density foam densifies progressively from the loaded end (denser end) while keeping the other part of foam undeformed [8, 17, 18]. Therefore, an important assumption of the analytical model in the present paper is that it is assumed the blast load is large enough to deform the foam from the loaded end progressively towards the structure.

When the foam cladding is totally densified along the thickness, the densified foam will move in unison with the protected structure. Therefore, the covered foam and the protected structure can now be seen as a single degree of freedom system:

$$\left(m_l + m_f + m_{se}\right)\ddot{y} + R(y) - P(t)A = 0 \qquad (16)$$

Equations (13), (15) and (16) form an analytical model which can theoretically calculate the deformations of linearly graded foam cladding and protected structure. The running cost of this model is low and suitable for the huge amount of parametric studies on the protective effect of linearly graded foams. This proposed analytical model is applicable for different types of foams and different target structures with different resistance functions $R(y)$. In the following sections of this paper, RC will be considered as the protected structure to investigate the protective effect of linearly graded aluminium foam on RC slab under blast loading. The material constants of aluminium foam are taken as $C_1 = 0.3$ and $\lambda = 1.5$ [6].

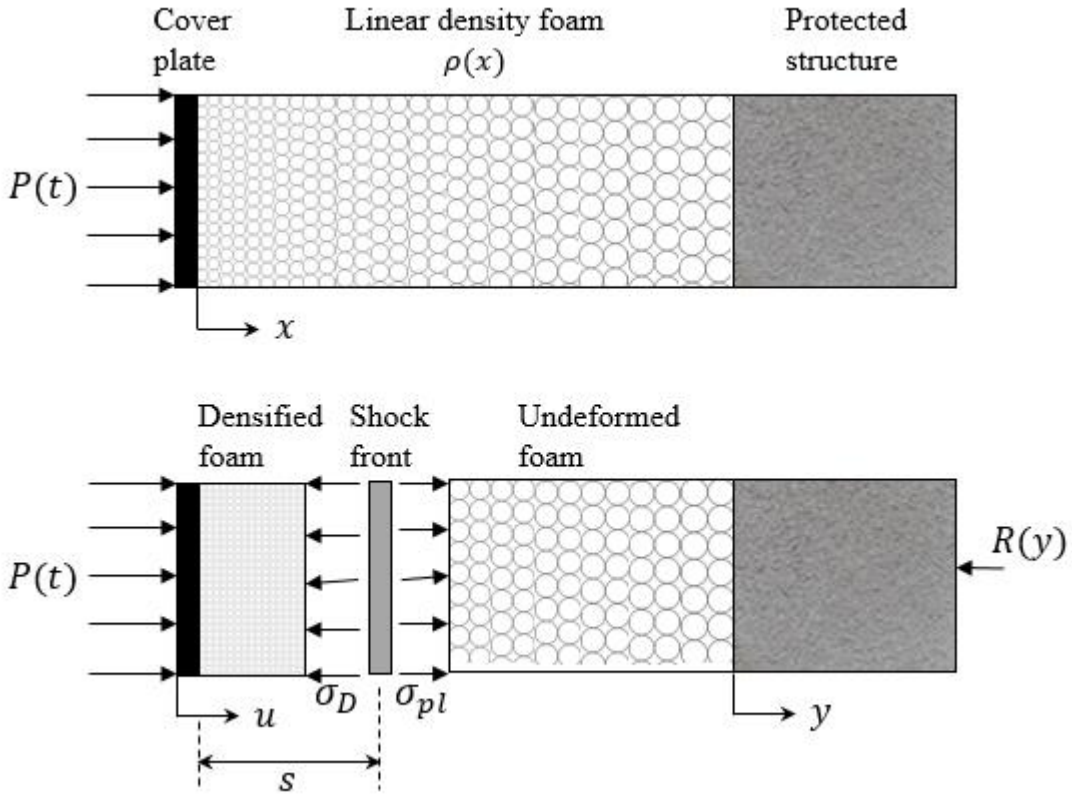

Figure 1. Graded density foam protected RC model under blast loading

3. Verification of analytical model

The analytical model is verified by the full-scale blast test conducted by Xia et al. (2016). In the blast test, the blast loads and the protected RC slabs in all events are the same. The 8 kg TNT charges used in the test are cylindrical with a diameter of 225 mm and a height of 120 mm. All charges were placed vertically on the top of the RC slabs as shown in Figure 2. The standoff distance from the charge to the centre of the RC slab is 1.5 m. All the protected RC slab is 2000 mm long, 800 mm wide and 120 mm thick and more details can be referred in Xia et al. (2016). All aluminium foams tested in the experiment were covered by a 1.13 mm thick steel cover plate and were glued on the RC slabs by epoxy. Three major elements are required by the analytical model to verify its predictions: 1) pressure-time history of the blast load; 2) resistance-deflection function of the protected RC slab; 3) density distribution of the aluminium foams.

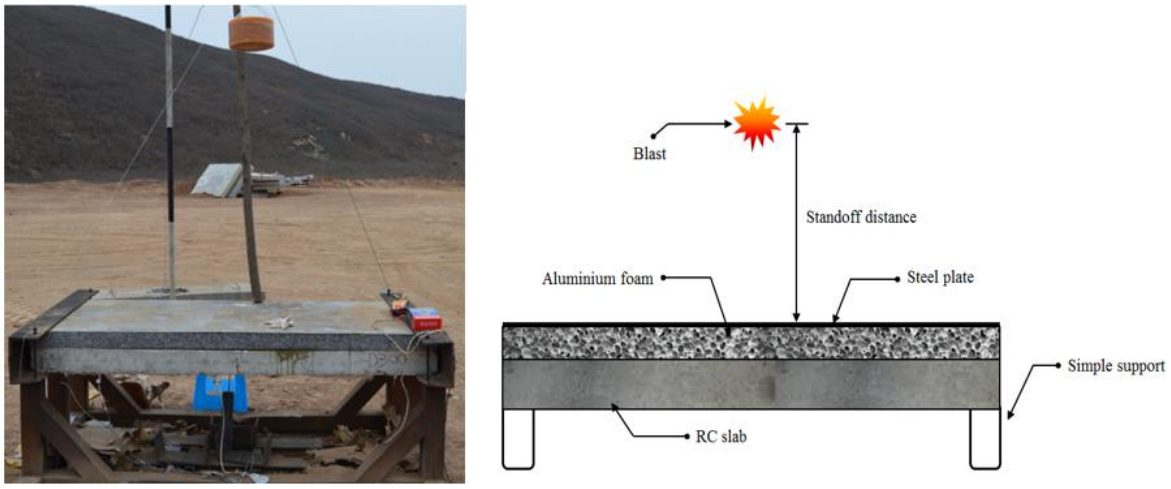

Figure 2. Setup of the blast test

3.1 Simulation of the blast load

Due to the fact that the pressure-time history during the blast event [16] was not successfully recorded, the pressure-time history applied on the analytical model was therefore calculated by using LS-DYNA.

In LS-DYNA, the Arbitrary-Lagrangian-Eulerian (ALE) Method was used in order to accurately model the wave-structure interaction. It was previously mentioned that a cylindrical explosive was used during the experiment; however, the current built-in ConWep functions in LS-DYNA are only able to account for spherical or hemispherical explosive. Therefore, the TNT explosive and the surrounding air domain are both explicitly modelled in the subsequent numerical simulation.

As shown in Figure 3, hexahedral elements were used for all numerical components to achieve the best computational stability and accuracy. The air mesh extended approximately 10 centimetres beyond the slab's edges and bottom. To maximise the efficiency, an eighth-symmetric model was used by imposing appropriate boundary conditions to the nodes lying on the x-y, y-z and x-z planes which intersect at the explosive centre while non-reflecting boundary conditions were forced on the remaining exterior surfaces of the air domain. To output the pressure-time history, a pressure transducer was placed at the centre of the slab.

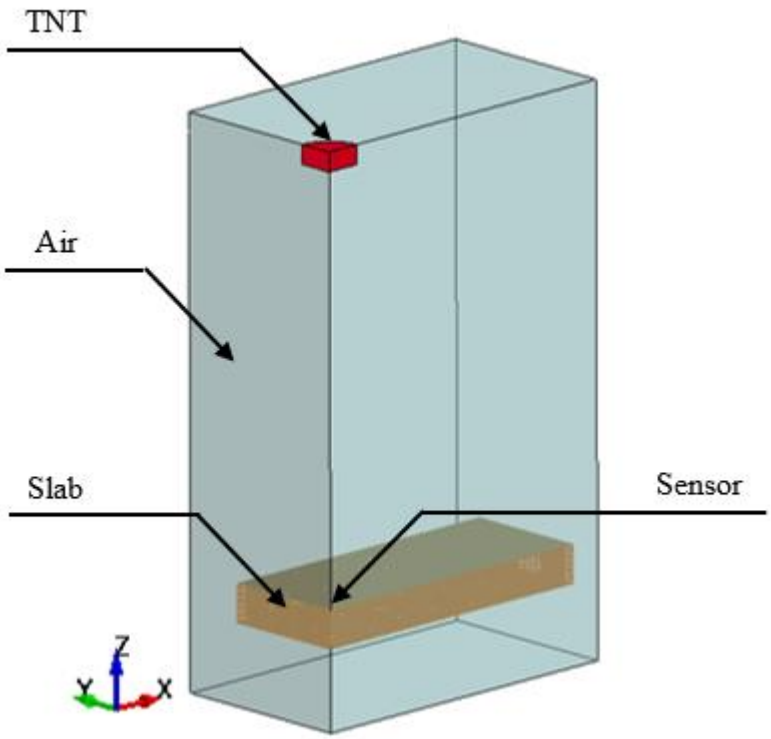

Figure 3. ALE model employed for determination of blast pressure

The constitutive model *MAT_HIGH_EXPLOSIVE_BURN was used to model TNT explosive and the equation of state was *EOS_JWL. Standard input parameters [22] for the constitutive model and equation of state were used and the detonation point was assumed at the centroid of the explosive.

The ambient air domain was modelled by *MAT_NULL with the density of air being the sole material input. The equation of state was *EOS_LINEAR_POLYNOMIAL.

In the current study, the only purpose of the numerical simulation is to obtain the reflected pressure-time history for the proposed analytical model, and the response/behaviour of the structure itself in LS-DYNA is not of interest. Therefore, the slab was modelled as a rigid body with *MAT_RIGID to minimise the computational effort.

The simulated pressure-time history on the central point of the slab is presented in Figure 4. To apply to the analytical model, the pressure-time history is idealised into a triangular load as shown by the dashed line in Figure 4. The idealised pressure has a peak reflected pressure of 18 MPa to match the simulated peak pressure. A duration of 0.6 ms is

adopted to match the impulse neglecting the low-pressure tail. In the idealisation, the extensive low-pressure range after 0.001 s was ignored so that the idealised impulse is slightly smaller than the simulated pressure. The idealised pressure will be uniformly applied on the slab in the analytical model whereas the actual pressure will experience clearing, therefore, the influence of the neglecting the low-pressure tail will compensate the overestimated pressure on the sides of the slab.

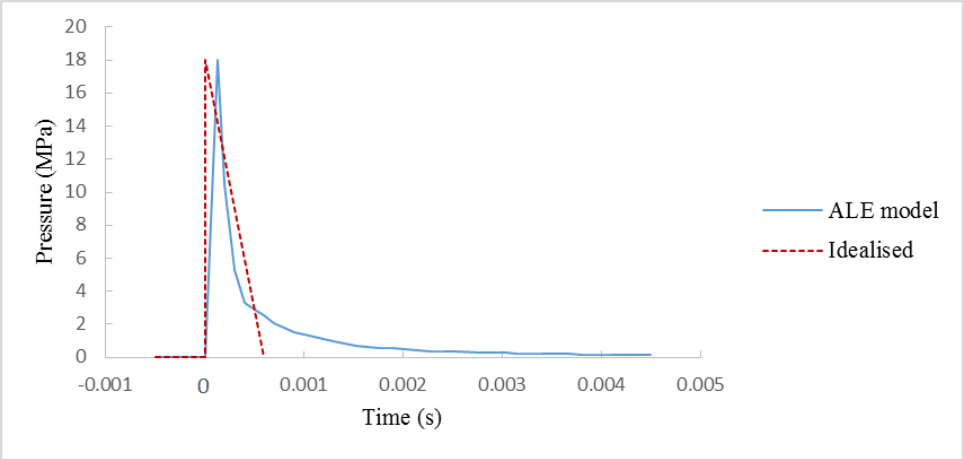

Figure 4. Pressure-time history in the blast test

3.2 Resistance function of the RC slab

According to Xia [16], the bilinear resistance-deflection diagram (Figure 5) of the RC slabs used in the blast test is calculated by:

$$R_{yield} = \frac{8M_{yield}}{L_{slab}}$$

$$R_{ult} = \frac{8M_{ult}}{L_{slab}}$$

$$y_{yield} = \frac{R_{yield}}{K}$$

$$y_{ult} = \frac{\theta L_{slab}}{2}$$

where M_{yield} and M_{ult} are the yield and ultimate moment of the RC slab and dynamic increase factors are considered in the calculations based on ASCE guidelines [23]; L_{slab} is the length of the RC slab; K is the stiffness of the RC slab calculated by $K =$

$384EI/5L_{slab}^3$; θ is the ultimate rotation of the RC slab taken as 2 degrees in the present study.

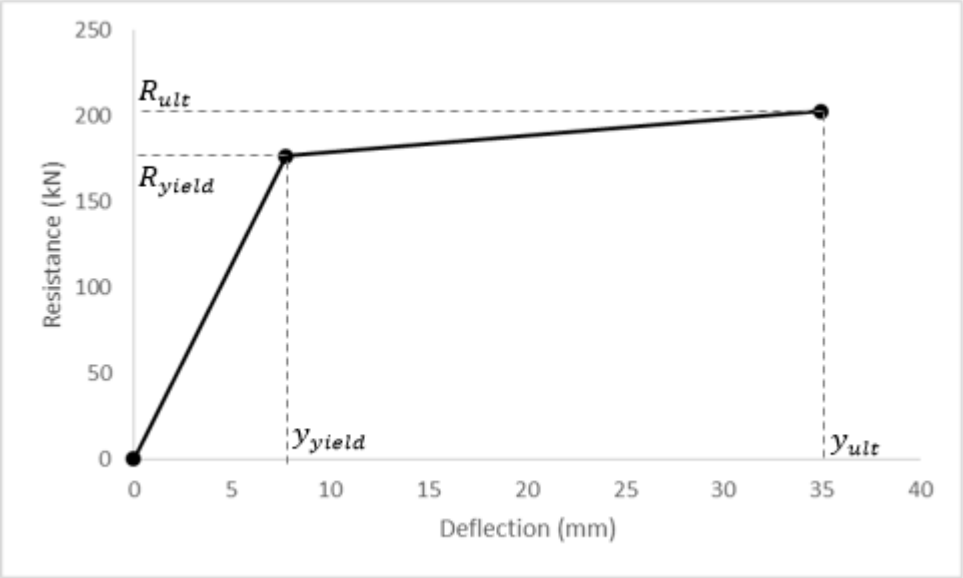

Figure 5. Resistance-deflection diagram of RC slabs in the blast test

3.3 Aluminium foams in the blast test

Three aluminium foam cladding in the blast test [16] are referred in the current study: one uniform density foam UD300 and two graded foams LD300 and LD400. Due to the manufacturing process, the density cannot be perfectly controlled as per the designed values. For a clear comparison, the approximate density distribution introduced in Xia [16] will be used in the analytical model as listed in Table 1.

Table 1. Density distributions of aluminium foams

Foam type	Initial density ρ_0 kg/m^3	Final density ρ_L kg/m^3	Average density kg/m^3	Density gradient kg/m^3/mm
UD300	300	300	300	0
LD300	400	200	300	2.5
LD400	500	300	300	2.5

3.4 Result comparisons

Four events of the blast test [16] are simulated by the analytical model. Table 2 summarises the results achieved from the experiment and the analytical model.

Table 2. Experimental and simulated results of peak deflection

Foam type	Peak deflection of RC slab (cm)		Difference %
	Experiment	Model	
N.A.	25.1	26.5	5.7
UD300	18.8	20.4	8.3
LD300	19.0	20.7	8.9
LD400	22.4	21.0	6.3

The first event in the blast test is an unprotected RC slab under the explosive. The deflection-time history is calculated by a basic SDOF model with the resistance function shown in Figure 5. The comparison with experimental result in Figure 6 shows a good agreement until the peak deflection is reached. This indicates that the idealised pressure-time history is reasonable. After the peak deflection, the predicted curve keeps at the high level because the damping effect is not considered in the model.

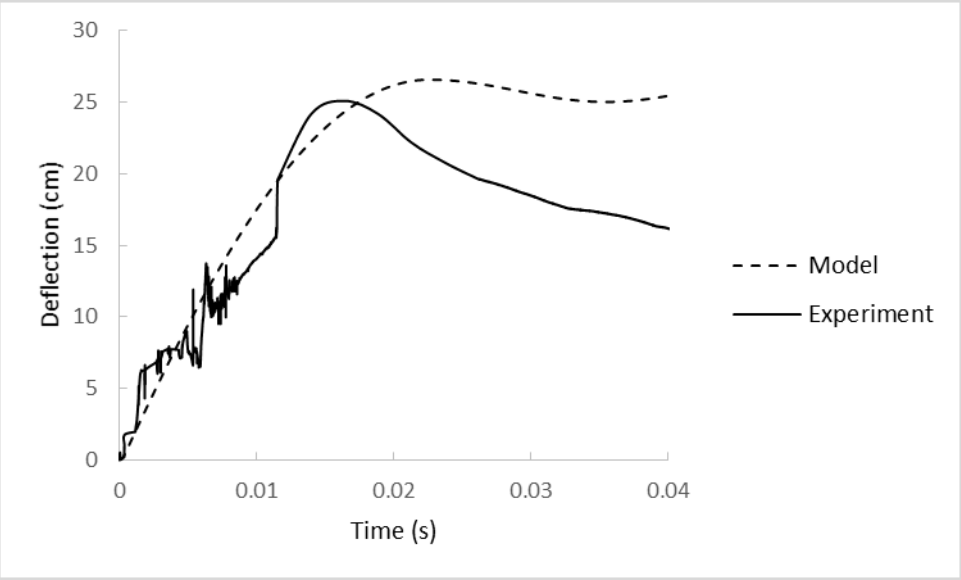

Figure 6. Deflection-time diagrams of the unprotected RC slab

The analytical model introduced in this paper is verified by comparing the deflection-time diagrams of RC slabs with experimental results where foams UD300, LD300 and LD400 were employed respectively in the tests [16]. The uniform density foam UD300 is modelled by setting the initial density equal to the final density of the foam. The

model yields an error of 8.3% on peak deflection (Figure 7) which is acceptable in blast analysis. For graded foams LD300 and LD400, the predicted results are shown in Figures 8 and 9. The simulated peak deflections and periods of the protected slabs are matched, however, the simulated deflections after peaks are not reliable due to ignoring the damping effect. Therefore, the current model is only applicable in the calculations of peak deflection. It was observed that the graded foam did not show any advantage in the experiment [16]. This is because the blast load was too intensive and caused all of the RC slabs to fail with significant deformations so that the actual foam effectiveness is hard to display. Therefore, in the next section, a lower blast load is applied to this verified model to investigate the protective improvement of linearly graded foam.

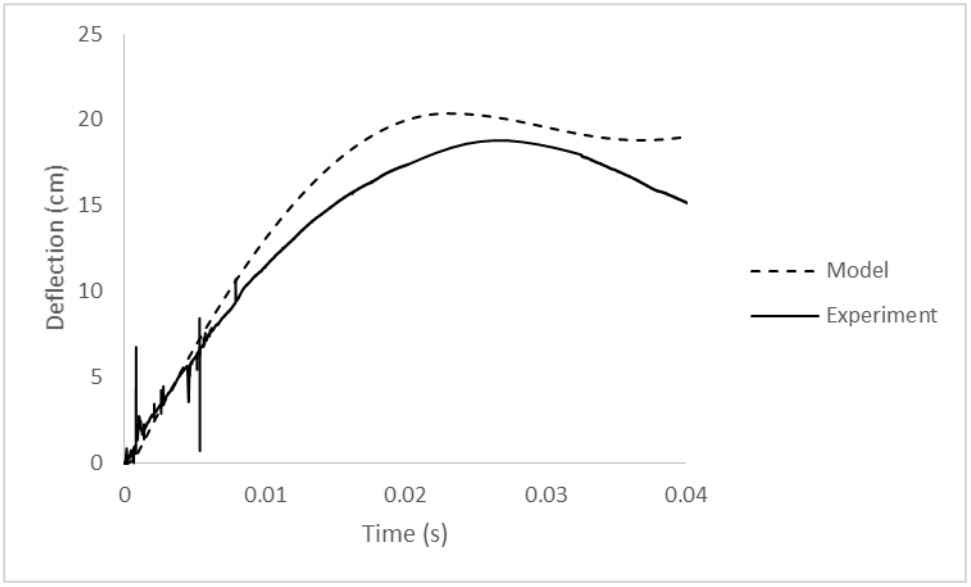

Figure 7. Deflection-time diagrams of the UD300 protected RC slab

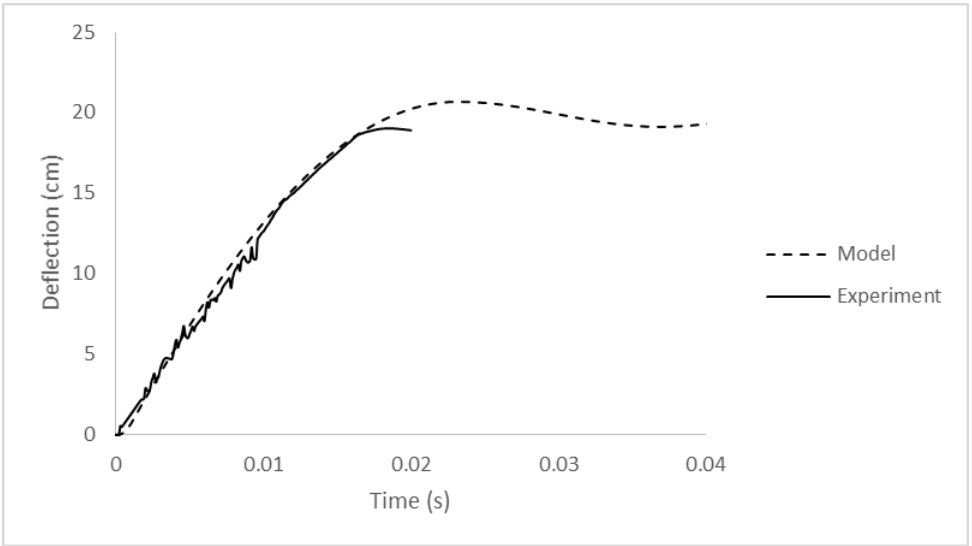

Figure 8. Deflection-time diagrams of the LD300 protected RC slab

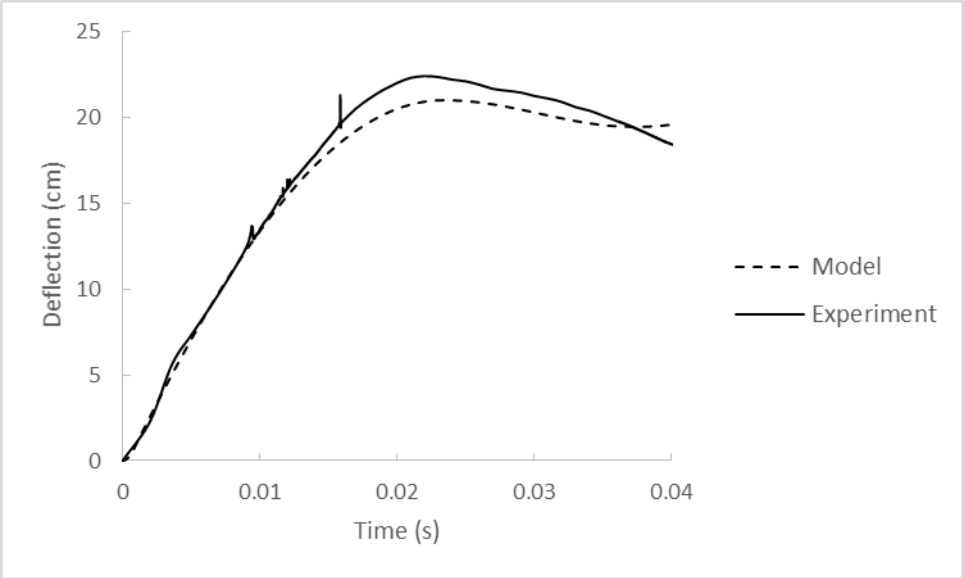

Figure 9. Deflection-time diagrams of the LD400 protected RC slab

4. Case Study

A blast load with a peak pressure of 12 MPa and duration of 0.3 ms is applied to the same RC slab used in the experiment to test the influence of various linearly graded foams shown in Table 3. The results predicted by the analytical model are presented in Figures 10 and 11. As shown, the homogeneous foam reduced the peak deflection of RC slab by 59% while the graded foam LD300G2.5 mitigated a further 11.7% on peak deflection. With an increase of density gradient, graded foam LD300G5.0 protected even better with a total decrease of 75% on peak deflection.

Despite the simplifying assumptions made in formulating the model, the improvement in the protective effect of using a density gradient foam is evident when the blast load is large enough to compact the foam from loading end.

Table 3. Details of case study

Foam type	Initial density kg/m^3	Final density kg/m^3	Density gradient kg/m^3/mm
No foam	-	-	-
UD300	300	300	0
LD300G2.5	400	200	2.5
LD300G5.0	500	100	5.0

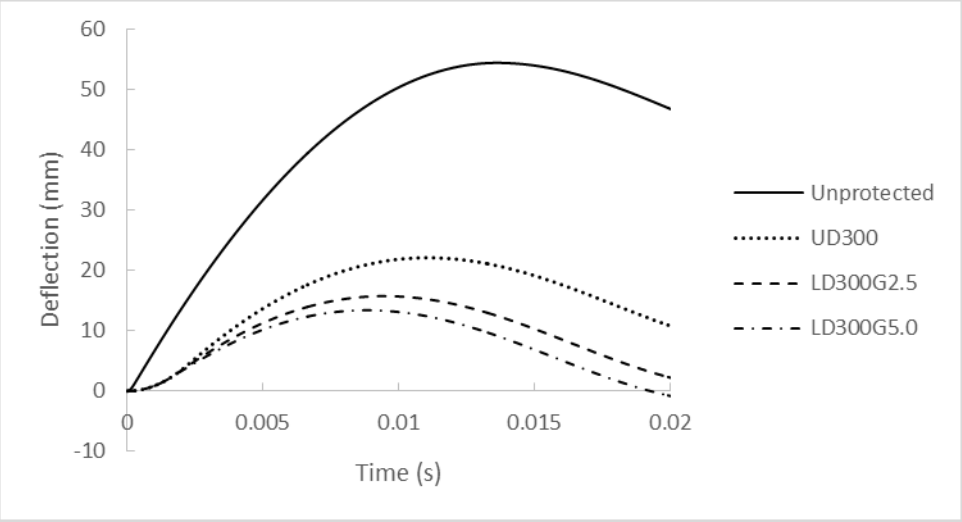

Figure 10. Deflection-time diagrams of RC slabs in case study

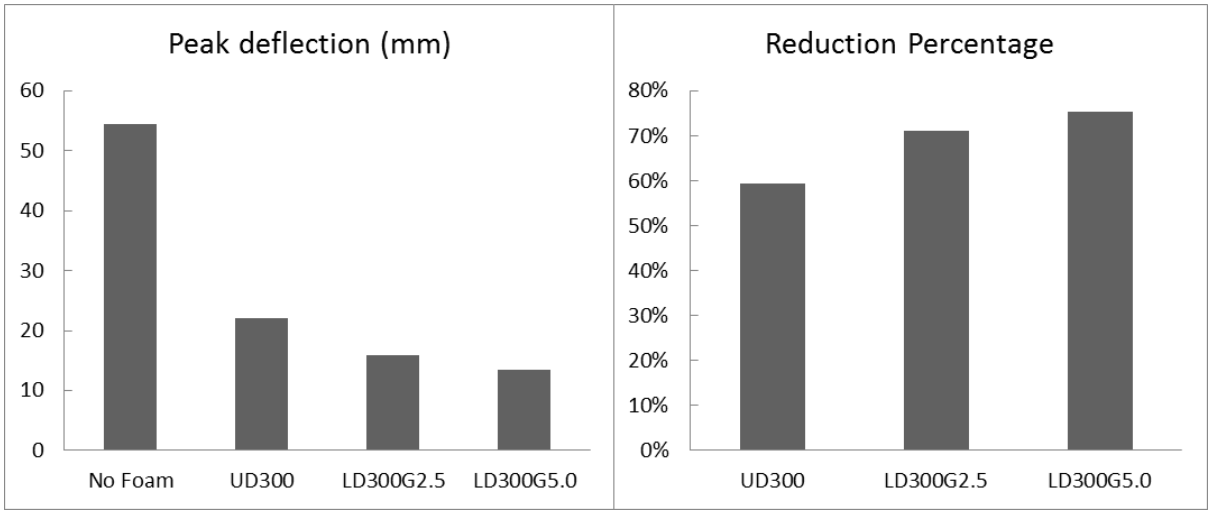

Figure 11. Peak deflections of RC slabs and percentages of reduction with different foam protections in the case study

5. Conclusion

An analytical model is developed to calculate the protective effect of linearly graded foam on the structure under blast loading. The model is verified by experimental results and yields an acceptable error. A case study is carried out to evaluate the effect of density gradient of the foam cladding. Outcomes display an improved protective ability of linearly graded foam with respect to uniform density, which means graded foam is capable of mitigating the response of the RC structural member more effectively under stronger explosions. In addition, for a given average density, the increase of density gradient further improves the performance on mitigating the peak deflection of the protected structure.

References

[1] Hanssen, A, Enstock, L, and Langseth, M, *Close-range blast loading of aluminium foam panels.* International Journal of Impact Engineering, 2002. **27**(6): p. 593-618.

[2] Schenker, A, Anteby, I, Nizri, E, Ostraich, B, Kivity, Y, Sadot, O, Haham, O, Michaelis, R, Gal, E, and Ben-Dor, G, *Foam-protected reinforced concrete structures under impact: experimental and numerical studies.* Journal of Structural Engineering, 2005. **131**(8): p. 1233-1242.

[3] Ye, Z and Ma, G, *Effects of foam claddings for structure protection against blast loads.* Journal of Engineering Mechanics, 2007. **133**(1): p. 41-47.

[4] Wu, C, Huang, L, and Oehlers, DJ, *Blast testing of aluminum foam–protected reinforced concrete slabs.* Journal of Performance of Constructed Facilities, 2010. **25**(5): p. 464-474.

[5] Li, Q and Meng, H, *Attenuation or enhancement—a one-dimensional analysis on shock transmission in the solid phase of a cellular material.* International Journal of Impact Engineering, 2002. **27**(10): p. 1049-1065.

[6] Ashby, MF, Evans, T, Fleck, NA, Hutchinson, J, Wadley, H, and Gibson, L, *Metal foams: a design guide*. 2000, Woburn, USA: Butterworth-Heinmann.

[7] Ma, G and Ye, Z, *Energy absorption of double-layer foam cladding for blast alleviation.* International Journal of Impact Engineering, 2007. **34**(2): p. 329-347.

[8] Li, J, Ma, G, Zhou, H, and Du, X, *Energy absorption analysis of density graded aluminium foam.* International Journal of Protective Structures, 2011. **2**(3): p. 333-349.

[9] Chang, Q, Li-jun, Y., Shu,Y., *Simulation and optimization of blast-resistant performance of graded aluminum foam sandwich structures.* Journal of Vibration and Shock, 2013. **32**(13): p. 70-75.

[10] Brothers, AH and Dunand, DC, *Density‐graded cellular aluminum.* Advanced Engineering Materials, 2006. **8**(9): p. 805-809.

[11] Hassani, A, Habibolahzadeh, A, and Bafti, H, *Production of graded aluminum foams via powder space holder technique.* Materials & Design, 2012. **40**: p. 510-515.

[12] Higuchi, M, Adachi, T, Yokochi, Y, and Fujimoto, K. *Controlling of*

distribution of mechanical properties in functionally-graded syntactic foams for impact energy absorption. in *Materials Science Forum*. 2012. Trans Tech Publ.

[13] He, S-Y, Zhang, Y, Dai, G, and Jiang, J-Q, *Preparation of density-graded aluminum foam.* Materials Science and Engineering: A, 2014. **618**: p. 496-499.

[14] Beals, J and Thompson, M, *Density gradient effects on aluminium foam compression behaviour.* Journal of Materials Science, 1997. **32**(13): p. 3595-3600.

[15] Brothers, AH and Dunand, DC, *Mechanical properties of a density-graded replicated aluminum foam.* Materials Science and Engineering: A, 2008. **489**(1): p. 439-443.

[16] Xia, Y, Wu, C, Liu, Z-X, and Yuan, Y, *Protective effect of graded density aluminium foam on RC slab under blast loading–An experimental study.* Construction and Building Materials, 2016. **111**: p. 209-222.

[17] Liu, Y, Wu, H-X, and Wang, B, *Gradient design of metal hollow sphere (MHS) foams with density gradients.* Composites Part B: Engineering, 2012. **43**(3): p. 1346-1352.

[18] Shen, C, Lu, G, and Yu, T, *Dynamic behavior of graded honeycombs–a finite element study.* Composite Structures, 2013. **98**: p. 282-293.

[19] Reid, S and Peng, C, *Dynamic uniaxial crushing of wood.* International Journal of Impact Engineering, 1997. **19**(5): p. 531-570.

[20] Xia, Y, Wu, C, and Li, Z-X, *Optimized design of foam cladding for protection of reinforced concrete members under blast loading.* Journal of Structural Engineering, 2014. **141**(9): p. 06014010.

[21] Zhou, H, Wang, Y, Wang, X, Zhao, Z, and Ma, G, *Energy absorption of graded foam subjected to blast: A theoretical approach.* Materials & Design, 2015. **84**: p. 351-358.

[22] Kingery, C and Bulmash, G, *Technical Report ARBRL-TR-02555: Air Blast Parameters from TNT Spherical Air Burst and Hemispherical Burst.* AD-B082, 1984. **713**.

[23] *TM5-1300: Structures to resist the effects of accidental explosions*, 1990, US Army, US Navy, US Air Force.

Chapter 6 – Concluding Remarks and Recommendation for Future Work

Conclusion

This thesis studied the protective effects against blast loading on RC structures of two types of aluminium foams: uniform density foams and graded density foams. Three approaches were involved: finite element modelling, analytical modelling and a physical experimental program.

For the uniform density foams, a finite element model and an analytical model were conducted to investigate the protective performance on RC slabs. Both models were validated against experimental data and received reasonable agreements. Pressure-impulse diagrams were generated to clearly show the mitigation performance of homogeneous foams under different loading conditions. To find the optimised design of foam on different RC slabs, two non-dimensional parameters were introduced to show the relationship between the foam and protected structure. Through a series of parametric studies of non-dimensional pressure-impulse diagrams, an optimised design for uniform density foam cladding on RC structural member was concluded.

For the graded density foam, numerous experiments were carried out to test its static and dynamic properties. Static stress-stain diagrams of layered foams with different density distributions were drawn from a number of compression experiments. Furthermore, the graded density foams which show good potential in the compression experiments were tested in blast experiments on the response of RC slabs. All the experimental results collected are valuable for later numerical and theoretical analysis.

Following the experimental program, an analytical model was developed for linearly graded foams which showed the best protection on RC slab in the experiment. This analytical model was verified against the test data and showed reasonable agreement. In addition, the influence of density gradient of foam cladding is evaluated when average density is constant.

The major findings and contributions arise from this research are summarised below:

1. Thickness and density/plateau stress of homogeneous aluminium foam determine its protective ability against blast loading. Thicker or denser the foam can improve the energy absorption capacity so that the foam can mitigate more deformation of the protected structure. The performance of different foams on a given RC slab is dependent not only on the foam thickness and density, but also the value of blast load. A thicker or stronger foam could protect from a relatively lower blast load, but would be inefficient as a thinner or weaker foam which is sufficient to absorb all the blast energy. Hence, proper design is needed to just meet the requirement of absorbing all the design blast energy.

2. According to the finite element model, homogeneous foams with different densities yielded different protections on different RC slabs. Every RC slab has its own optimised foam density/plateau stress.

3. From the simulations of the proposed analytical model for uniform density foam, the optimisation of foam design on RC slab is suggested as: the plateau stress of foam is slightly weaker than the structural resistance of RC slab with a strength ratio of 0.8. Thicker foam is always able to absorb more blast energy. For a specified design blast load, the optimised foam thickness should absorb all the blast energy before it is fully densified based on budget and availability.

4. A range of quasi-static compressive experiments on graded density foams were conducted and results can be concluded that 1) the graded density foam is compacted from smaller density to higher density under quasi-static condition; 2) when the average density is constant, foam with graded density has an increasing stress curve after yield, rather than a plateau stress for homogeneous foam; 3) the stress curve after yield of a graded foam with bigger density gradient is steeper; 4)

if the initial density is kept the same, larger density gradient of graded foam gives a higher energy absorption capacity while the yielding condition remains the same; 5) unordered density layers of foams did not show any advantage in the stress-strain diagrams.

5. The blast test of graded density foam protected RC slab showed that the density gradient of foam cladding affected its protection effectiveness. The increasing density of foam from loaded end to the structural end can improve the blast resistance compared to the homogeneous foam with the same average density.

6. An analytical model to predict the dynamic response of a structure with the protection of linearly graded foam was developed. This model was validated against the blast test results with a good agreement. Therefore, this analytical framework can be used in future research.

Recommendations for future work

Directions for future research endeavours that have emerged in the conduct of this thesis include:

1. Based on the proposed analytical model, future parametric studies could be carried out on properties of linearly graded foam and protected structures. The influence of density gradient on different protected structures could be concluded.

2. As the analytical model for linearly graded foam is limited by the assumption of requiring adequate loading range, the actual performance of graded foam under low loading rate cannot be accurately predicted. Hence, future work could develop a model for graded density foam to calculate the structural response under lower loading rate which causes the foam deforms from lower density to higher density.

3. More study could be conducted to find the transition loading rate at which the graded density foam would change its deforming mechanism.

4. Two graded foams were tested in the blast experiments in this research. From the experimental results, unordered density foam and ascending density foam have shown their weakness in the protection of RC slab. Therefore, future experimental studies could focus on changing the density gradient of foam.

5. Another important variable of the study on graded density foam-protected RC structures in future experiments or numerical models could be scaled distance. The influence of density gradient may vary when the blast load changes.